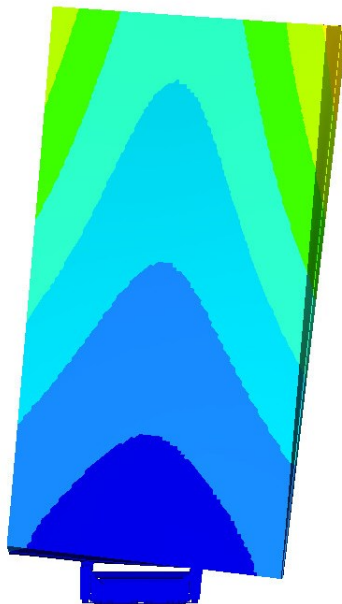
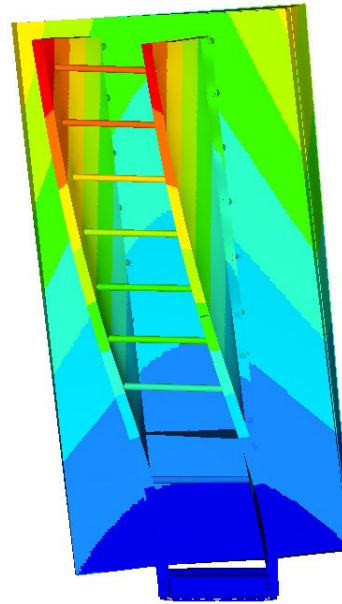




Analysis system
1.721E+00
1.529E+00
1.338E+00
1.147E+00
9.559E-01
7.647E-01
5.735E-01
3.823E-01
1.912E-01
0.000E+00
■ No result
Max = 1.721E+00
Node 976512
Min = 0.000E+00
Node 749684



Analysis system
1.721E+00
1.529E+00
1.338E+00
1.147E+00
9.559E-01
7.647E-01
5.735E-01
3.823E-01
1.912E-01
0.000E+00
■ No result
Max = 1.721E+00
Node 976512
Min = 0.000E+00
Node 749684



Engineering design of a radar structure using Design of Experiments and Structural Optimization

Master's thesis in Applied Mechanics

VILMA ANDERSSON

MASTER'S THESIS IN APPLIED MECHANICS

Engineering design of a radar structure using Design of Experiments and
Structural Optimization

VILMA ANDERSSON

Department of Mechanics and Maritime Sciences
Division of Dynamics
CHALMERS UNIVERSITY OF TECHNOLOGY
Gothenburg, Sweden 2019

Engineering design of a radar structure using Design of Experiments and Structural Optimization
VILMA ANDERSSON

© VILMA ANDERSSON, 2019

Master's thesis 2019:38
Department of Mechanics and Maritime Sciences
Division of Dynamics
Chalmers University of Technology
SE-412 96 Gothenburg
Sweden
Telephone: +46 (0)31-772 1000

Cover:
Cover shows the first eigenmode of a part of a ground based radar.

Chalmers Reproservice
Gothenburg, Sweden 2019

Engineering design of a radar structure using Design of Experiments and Structural Optimization
Master's thesis in Applied Mechanics
VILMA ANDERSSON
Department of Mechanics and Maritime Sciences
Division of Dynamics
Chalmers University of Technology

ABSTRACT

Models of complex systems contain a large amount of different parameters and several constraints, which make structural optimization very time consuming. Therefore, Saab AB wanted to develop a method based on Design of Experiments to use for optimization within structural analysis and concept generation. Consequently, the purpose of the project was to develop a method that efficiently evaluates concepts and new products with regard to structural analysis in product development. The method was used to ease the evaluation of different concepts, as well as the understanding of the impact that the parameters had on the system. The method was developed by using three different trial cases in order to learn to use the different software, as well as developing and fine tuning the method. Thereafter, a simplified version of an authentic, complex problem from Saab was evaluated using the developed method.

Different Design of Experiments methods were investigated while executing the first sample cases. Thereafter, only one of the Design of Experiments method, called Hammersley, was used in order to make the simulations equivalent. The second and third cases were created in order to learn how to, for example, model and parameterize the concepts. The advanced case consisted of a simplified version of an existing analysis model from Saab's product portfolio. The original existing analysis and simplified models were both evaluated and the results obtained from the two cases were compared to each other. This was done in order to be certain that the behaviour of the simplified model resembled the behaviour of the original model. When the simplified model was assumed to be sufficiently accurate, a new concept based on the simplified model was created and analyzed using the developed method. The method used structural optimization and informed about which parameters that influenced the specified objective function and which parameters that could be neglected. The advanced case had six different design variables and the number of values each parameter had ranged from 2 to 11. In the software HyperStudy, the Design of Experiments method Hammersley calculated that 105 concepts had to be created in order to get a sufficient optimization. Thus, 105 evaluations were executed, since one concept needs one evaluation. By using this method, the number of parameters was, in the advanced case, reduced from six to two, which saves both computational and optimization time.

Keywords: DOE, Structural optimization, FEM, Military radar, HyperStudy, Parameterization, Structural analysis, Hammersley

Teknisk design av en radarstruktur genom användning av Försöksplanering och Strukturoptimering
Examensarbete i Tillämpad Mekanik
VILMA ANDERSSON
Institutionen för Mekanik och Maritima Vetenskaper
Avdelningen för Dynamik
Chalmers tekniska högskola

SAMMANFATTNING

Modeller av komplexa system innehåller många olika parametrar och randvillkor, vilket gör strukturoptimering väldigt tidskrävande. Med grund i det ville Saab AB utveckla en metod som baseras på försöksplanering (DOE på svenska) med syftet att användas för optimering inom strukturanalys och konceptgenerering. Följaktligen, syftet med projektet var att fastställa en metod som utvecklar och optimerar koncept och nya produkter med hänsyn till strukturanalys och produktutveckling. Metoden underlättar utvärdering av olika koncept och förståelse av parameters inverkan på konceptet. Metoden utvecklades stegvis genom att börja med tre fall som blev svårare efter hand. Detta gjordes för att ha tid att lära sig programvarorna samt för att utveckla metoden under projektets gång. Efter de tre första fallen var färdiga och metoden var utvecklad undersöktes ett fjärde, mer verklighetstroget koncept. Det berörde en avancerad produkt från Saab som utvärderades med hjälp av metoden.

Olika metoder av försöksplanering undersöktes i det första fallet, därefter användes bara en av metoderna för att göra de olika simuleringarna jämförbara med varandra. Det andra och tredje fallet gjordes med syftet att lära, bland annat, hur man modellerar och parametriserar koncept och produkter. I det fjärde fallet modellerades en förenklad version av en existerande analysmodell av en produkt från Saabs produktportfölj. Analysmodellen från Saab och den förenklade modellen var båda utvärderade med samma randvillkor och krafter, därefter jämfördes resultaten från båda simuleringarna med varandra. Detta gjordes för att undersöka om den förenklade modellen hade ett likvärdigt beteende som den existerande analysmodellen. Ytterligare ett koncept skapades när modellernas beteende antogs ha tillräckligt lika beteende. Antennen gjordes dubbelt så hög och konceptet utvärderades därefter med den framtagna metoden. Metoden använde sig av strukturoptimering och informerade om vilka parameterar som hade en stor påverkan på systemet och vilka som kan bortses ifrån. Det avancerade fallet hade sex olika designvariabler, varav de innehöll mellan 2 och 11 värden var. Försöksplaneringsmetoden Hammersley i HyperStudy angav att 105 koncept behövde skapas. Eftersom varje koncept motsvarar en simulering så utfördes även 105 simuleringar. Genom användning av den framtagna metoden hittades information kring vilka parametrar som påverkar modellen och därmed minskade antalet parametrar som behövde undersökas, vilket i sig kapade både simulerings- och utvecklingstid.

Nyckelord: Försöksplanering, Strukturoptimering, FEM, Militärradar, HyperStudy, Parameterisering, Strukturanalys, Hammersley

PREFACE

This master's thesis was completed as part of the master's programme Applied Mechanics at Chalmers University of Technology. The thesis was executed at Saab AB's *Business Area Surveillance* in Gothenburg during the spring of 2019. The supervisors at Saab were M.Sc. Madeleine Andersson and PhD Ruoshan Luo and the supervisor and examiner from Chalmers was Professor Mikael Enelund.

ACKNOWLEDGEMENTS

I would like to send my largest gratitude to my two supervisors at Saab AB, Madeleine Andersson and Ruoshan Luo. I am very grateful for all the hours of supervision and guidance that you have provided me during the thesis work. The project would not have developed as good as it did without your support. I would also like to thank the rest of the members of the analysis team which all have been a huge help by answering questions at all times. I would also like to acknowledge and thank my supervisor and examiner at Chalmers, Mikael Enelund, for helping and guiding me, not only in this project but throughout the years I've studied at Chalmers. It has been a huge support and I am so grateful. Last, but definitely not least, I would like to say thank you to my family and Mattias who always supports me, no matter what.

Gothenburg, May 2019

Vilma Andersson

ABBREVIATIONS

.bdf	Glyph Bitmap Distribution Format (file format)
.blk	Bulk (file format)
DOE	Design Of Experiments
DOF	Degree Of Freedom
FE	Finite Element
FEM	Finite Element Method
MELS	Modified Extensible Lattice Sequence
.tpl	Template (file format)
.txt	Text (file format)

NOMENCLATURE

Roman upper case letters

A_c	Area of core
A_s	Area of skin
E	Young's modulus
F	Force
G	Shear modulus
I	Moment of inertia
L	Length of beam

Roman lower case letters

b	Width of beam
h	Height of beam
c	Thickness of core
s	Thickness of skin

Greek lower case letters

δ	Displacement
δ_H	Displacement with Honeycomb as core material
δ_R	Displacement with Rohacell as core material

LIST OF FIGURES

List of Figures

1.1	A ground-based radar from Saab AB. [2]	1
2.1	Evaluation plot, the vertical axis shows the displacement in mm and the horizontal shows all evaluations. The plot shows the displacement in z -direction and the arrow points at the evaluation that obtained the largest displacement. The value of the largest displacement is $\delta = 1.203$ mm.	6
2.2	Histogram plot visualizes how often the simulations end up in with a certain solution when varying different parameters in the model. The horizontal axis shows the range of the output, the left vertical axis shows the frequency of the results and the right vertical axis shows the probability of the solution to obtain the result.	7
2.3	A Pareto plot visualizing which parameters that are influencing the magnitude of the displacement. The horizontal axis shows the different parameters which are displayed, the parameter with the largest influence is to the left. The vertical axis shows the value of the displacement in the z -direction in mm.	8
2.4	Sandwich structure	8
3.1	Flow chart of the process	11
3.2	The different steps of a setup and a Hammersley DOE in HyperStudy	13
3.3	Figure shows how the resource, solver input file and solver execution script were defined in the “Define Models” step. The Resource tab includes the .tpl-file with complete file path, the Solver input file contains the .bdf-file and which solver to use was defined under Solver execution script.	13
3.4	Defining a real parameter with Lower Bound, Nominal and Upper Bound values.	14
3.5	A string is parameterized. The name of the .blk-files that are parameterized are listed in the “List” box.	14
3.6	Define Input Variables, this case contains one string and one real parameter, but only the parameter called “Case” is active.	15
3.7	Define Input Variables, this case contains two string, two real and two discrete parameters.	15
3.8	Choose between different approaches.	16
3.9	The different DOE methods to choose between in HyperStudy.	16
4.1	Plate with applied force and constraints	17
4.2	Definition of the PSHELL property in MSC. Nastran. [24]	18
4.3	The parameterization in HyperStudy. The values marked in blue were parameterized. According to the definition in Figure 4.2, thickness = T and the material ID = MID1, MID2 and MID3 were parameterized.	18
4.4	The parameterization of the first case. When opening the .tpl-file in a text editor, the parameterization is shown.	18
4.5	The displacement of the plate. The scale ranges from the blue = 0 to the red = $1.342 \cdot 10^{-2}$ mm.	19
4.6	Evaluation plot. The left plot shows midpoint displacement and the right plot shows mass.	19
4.7	Histogram plot. The left plot shows the displacement and the right shows the mass.	20
4.8	Pareto plot shows the parameters’ influence on the solution. The plot to the left displays displacement and the plot to the right displays the mass.	20
4.9	Evaluation plot displaying midpoint displacement to the left and natural frequencies to the right.	21
4.10	Histogram plot midpoint displaying displacement to the left and natural frequencies to the right.	21
4.11	Pareto plot shows how much the parameters influence the solution.	22
4.12	Sandwich plate with perpendicular force and constraints.	22
4.13	Definition of the PCOMP property in Nastran. [24]	23
4.14	The parameterization in the HyperStudy editor.	23
4.15	The parameterization when opening the .tpl-file in a text editor.	23
4.16	Evaluation plot. The midpoint displacement is plotted to the left and the mass to the right.	24
4.17	Histogram plot. The left plot visualizes the midpoint displacement and the right shows the mass. The displacement obtained four different values in the simulations and the mass obtained two.	25

4.18	Pareto plot. The left plot shows the parameters' influence on the midpoint displacement and the right plot shows the parameters influence on the mass. The thickness had a larger influence than the material had for both cases.	25
4.19	Evaluation plot. The left plot displays the natural frequencies and the right displays the midpoint displacement.	26
4.20	Histogram plot. The left displays the natural frequencies and the right displays the midpoint displacement.	26
4.21	Pareto plot. The left plot displays which parameters that influenced the natural frequencies and the right displays which parameters that influenced the midpoint displacement. The design variable <code>mat_core</code> regards the core material and <code>t_skin</code> regards the thickness of the skins.	27
4.22	Sandwich structure with a split core	27
4.23	The core divided into panels. Figure shows the case in which the core is split into 50 parts in the x -direction and 4 parts in the y -direction.	28
4.24	The entire model with skins, core, force and constraints. The skins were one pieces while the core was split in parts.	29
4.25	The name of the <code>.blk</code> -files which were to be run in the parameter. The used format means that the parameter is a string.	29
4.26	The parameterized <code>.tpl</code> -file, the name of the file is the parameter.	29
4.27	Parameterization of the upper and lower skins.	30
4.28	Evaluation plot for magnitude of midpoint displacement.	31
4.29	Histogram plot for magnitude of midpoint displacement.	31
4.30	Pareto plot for magnitude of midpoint displacement.	32
4.31	The percentage change of the magnitude of midpoint displacement.	32
5.1	Simplified G4 model. The yellow parts are the antenna, the green and pink parts are the back structure and the red part is the bottom.	34
5.2	The antenna and back structure were tilted 5°	34
5.3	The first mode shape of the simplified model. The scale regards normalized displacement and ranges from the blue = 0 to red = 2.325.	35
5.4	The second mode shape of the simplified model. The scale regards normalized displacement magnitude and ranges from the blue = 0 to the red = 1.849.	35
5.5	The third mode shape of the simplified model. The scale regards normalized displacement magnitude and ranges from the blue = 0 to red = 2.127.	36
5.6	G8 model from the front and back.	36
5.7	The parameters regarding the back structure. The blue panels were the support structure height and support structure width parameters. The red box was the bottom structure and the gray parts are constant for the two different cases.	38
5.8	Back of the antenna. The yellow part represents the sandwich plate which is where the equally distributed nonstructural mass was applied and where the core material was changed. The red part was the bottom structure which did not change from the simple case.	39
5.9	G8 model. The black circle shows where Figures 5.10a and 5.10b are zoomed.	39
5.11	The marked area in Figure 5.9 was zoomed in the HyperMesh model for visualization. The Support Structure in the front was removed in order to see the parameter Thickness BackHeight. Thickness BackHeight is marked with green arrows and Thickness BackWidth is marked with black arrows.	40
5.12	Evaluation plot presenting maximum displacement in the x -direction. Figure shows that the maximum displacement in x -direction is smallest at evaluation 15.	41
5.13	Histogram plot presenting maximum displacement in x -direction. Figure shows that the range that the maximum displacement has is between 3.90 mm and 10.52 mm. Most simulations end up with a maximum displacement between 4.45 mm and 6.11 mm, with a majority at 6.11 mm.	42
5.14	Pareto plot displays which parameter that influences the solution regarding the maximum displacement in x -direction the most. In this case, it is clear that the parameter "Case" influences the most with around 48%. Consequently, the sandwich material and nonstructural mass affect second and third most with 18% and 16%, respectively.	42
5.15	Displacement in x -direction. The scale ranges from blue = -0.0122 mm to red = 3.625 mm.	43
5.16	The displacement in x -direction is scaled with a scale factor of 200 for visualization. The scale ranges from blue = -0.0122 mm to red = 3.625 mm.	43

5.17	Evaluation plot presenting the natural frequencies for the first mode. It shows that the three largest frequencies were obtained from evaluation 36, 35 and 56.	44
5.18	Histogram plot presenting the natural frequencies in the first mode. It shows that the range of the frequencies in the first mode was between 1.78 Hz and 9.03 Hz. Most simulations end up at a frequency between 7.22 Hz and 8.43 Hz, with a majority at 7.82 Hz.	44
5.19	Pareto plot displaying which parameter that influences the solution regarding the natural frequencies at the first mode the most. In this case, it is clear that the parameter “Case” influences the most with around 58%. Consequently, the sandwich material and nonstructural mass affects second and third most with 26% and 8%, respectively.	45
5.20	Mode 1, with frequency = 8.949 Hz. The scale ranges from blue = 0 to red = 1.721.	46
5.21	Mode 2, with frequency = 9.315 Hz. The scale ranges from blue = 0 to red = 1.271.	46
5.22	Mode 3, with frequency = 14.07 Hz. The scale ranges from blue = 0 to red = 1.739.	47
5.23	Mode 4, with frequency = 20.78 Hz. The scale ranges from blue = 0 to red = 4.094.	47
5.24	Mode 5, with frequency = 22.79 Hz. The scale ranges from blue = 0 to red = 10.86.	48
A.1	The plots regarding displacement in x for the linear static case.	III
A.2	The plots regarding displacement in y for the linear static case.	IV
A.3	The plots regarding displacement in z for the linear static case.	V
A.4	The plots regarding axial forces in screws in the x -direction for the linear static case.	VI
A.5	The plots regarding axial forces in screws in the y -direction for the linear static case.	VII
A.6	The plots regarding axial forces in screws in the z -direction for the linear static case.	VIII
A.7	The plots regarding shear in x -direction for the linear static case.	IX
A.8	The plots regarding shear in y -direction for the linear static case.	X
A.9	The plots regarding shear in z -direction for the linear static case.	XI
A.10	The plots regarding composite stress (von Mises) in x -direction in ply 1 for the linear static case.	XII
A.11	The plots regarding composite stress (von Mises) in x -direction in ply 2 for the linear static case.	XIII
A.12	The plots regarding composite stress (von Mises) in x -direction in ply 3 for the linear static case.	XIV
A.13	The plots regarding composite stress (von Mises) in y -direction in ply 1 for the linear static case.	XV
A.14	The plots regarding composite stress (von Mises) in y -direction in ply 2 for the linear static case.	XVI
A.15	The plots regarding composite stress (von Mises) in y -direction in ply 3 for the linear static case.	XVII
A.16	The plots regarding composite stress (von Mises) in z -direction in ply 1 for the linear static case.	XVIII
A.17	The plots regarding composite stress (von Mises) in z -direction in ply 2 for the linear static case.	XIX
A.18	The plots regarding composite stress (von Mises) in z -direction in ply 3 for the linear static case.	XX
A.19	The plots regarding stress von Mises in x -direction for z_1 for the linear static case.	XXI
A.20	The plots regarding stress von Mises in x -direction for z_2 for the linear static case.	XXII
A.21	The plots regarding stress von Mises in y -direction for z_1 for the linear static case.	XXIII
A.22	The plots regarding stress von Mises in y -direction for z_2 for the linear static case.	XXIV
A.23	The plots regarding stress von Mises in z -direction for z_1 for the linear static case.	XXV
A.24	The plots regarding stress von Mises in z -direction for z_2 for the linear static case.	XXVI
A.25	Evaluation 36, mode 1. Frequency = 9.336 Hz	XXVII
A.26	Evaluation 36, mode 2. Frequency = 9.396 Hz	XXVIII
A.27	Evaluation 36, mode 3. Frequency = 14.14 Hz	XXVIII
A.28	Evaluation 36, mode 4. Frequency = 19.77 Hz	XXIX
A.29	Evaluation 36, mode 5. Frequency = 22.73 Hz	XXIX
A.30	Evaluation 35, mode 1. Frequency = 9.283 Hz	XXX
A.31	Evaluation 35, mode 2. Frequency = 9.409 Hz	XXXI
A.32	Evaluation 35, mode 3. Frequency = 14.22 Hz	XXXI
A.33	Evaluation 35, mode 4. Frequency = 22.75 Hz	XXXII
A.34	Evaluation 35, mode 5. Frequency = 27.50 Hz	XXXII

LIST OF TABLES

List of Tables

2.1	The anisotropic material properties used in the composite honeycomb [25], defined as a MAT8 [24].	9
2.2	The isotropic material properties used for aluminium honeycomb, defined as a MAT1 [24].	9
2.3	The anisotropic material properties used in Rohacell [27], defined as a MAT8 [24].	9
4.1	Young's modulus of the skin and core materials.	24
4.2	The MAT9 card for Honeycomb used in the core [24]. The matrix is symmetrical.	28
5.1	Percentage change of natural frequencies between the original and simplified model.	35
5.2	The parameters which were parameterized in the G8 model.	38
5.3	The design variables and the used values for evaluation 15, which obtained the smallest displacement.	41
5.4	The parameters and the obtained values at the 56 th simulation.	45
5.5	The five first natural frequencies obtained from the 56 th simulation.	45
A.1	Natural frequencies for the 10 first modes for evaluation 36.	XXVII
A.2	Natural frequencies for the 10 first modes for evaluation 35.	XXX

CONTENTS

Abstract	i
Sammanfattning	ii
Preface	iii
Acknowledgements	iii
Abbreviations	v
Nomenclature	v
List of Figures	vi
List of Tables	ix
Contents	xi
1 Introduction	1
1.1 Background	1
1.2 Purpose	1
1.3 Objective	1
1.4 Limitations	2
1.5 Expected outcomes	2
2 Theory	3
2.1 Finite Element Method	3
2.2 Structural Optimization	3
2.3 Design of Experiments	4
2.3.1 Full Factorial	4
2.3.2 Fractional Factorial	4
2.3.3 Plackett-Burman	4
2.3.4 Modified Extensible Lattice Sequence (MELS)	5
2.3.5 Hammersley	5
2.4 Plots	5
2.4.1 Evaluation plot	5
2.4.2 Histogram plot	6
2.4.3 Pareto plot	7
2.5 Sandwich structure	8
2.5.1 Core material	8
2.6 Bending	9
2.6.1 Bending of a beam	10
2.6.2 Bending of beam with Sandwich structure	10
3 Methodology	11
3.1 Software	12
3.1.1 HyperMesh	12
3.1.2 MSC. Nastran	12
3.1.3 HyperView	12
3.1.4 HyperStudy	12
3.2 Parameterization	12

4 Results - Sample cases	17
4.1 Plate	17
4.1.1 Methodology	17
4.1.2 Linear static simulation	18
4.1.3 Natural Frequency simulation	20
4.2 Sandwich Structure	22
4.2.1 Methodology	22
4.2.2 Linear static simulation	23
4.2.3 Natural Frequency simulation	25
4.3 Divided sandwich structure	27
4.3.1 Methodology	27
4.3.2 Linear static analysis	30
5 Results - Authentic case	33
5.1 Methodology	33
5.1.1 Build FE-model	33
5.1.2 Parameterization	37
5.2 Linear static analysis	40
5.3 Natural Frequency analysis	43
6 Discussion and Future Work	49
6.1 Method	49
6.2 Model	50
7 Concluding remarks	52
References	53
Appendices	I
A G8 model	II
A.1 Linear static analysis	II
A.2 Natural Frequency analysis	XXVII
A.2.1 Evaluation 36	XXVII
A.2.2 Evaluation 35	XXX

1 Introduction

The project's background, purpose, objective, limitations and expected outcomes are explained below.

1.1 Background

Structural optimization of a complex system is very time consuming due to a large amount of parameters, several constraints and, possible, several conflicting objectives. Therefore, Saab AB wants to develop a method based on Design of Experiments (DOE) to limit the number of design variables and tests. It will be used for optimization within structural analysis and concept generation. The method will consequently ease the evaluation of the concepts and the understanding of the impact that each parameter has on the system. The method will be developed and tested through application on an appropriate product from Saab's portfolio. Thereafter it can be used as a parameter screening tool to determine which parameters that are most influential to the design objective when generating a new concept. Through the initial screening, parameters which have minor or no influence on the system will be omitted. Thereby, the number of parameters which need to be studied will be reduced, along with the calculation times. It will also provide guidance in which parameters to prioritize when developing a new product and the available range of those parameters.

The thesis is proposed by and executed at Saab AB, in particular the *Business Area Surveillance* in Gothenburg. Saab's Surveillance area provides solutions for safety and security, surveillance and decision support, along with threat detection and protection. Saab's product portfolio contains airborne, ground-based and naval radars, as well as electronic warfare and combat systems. Figure 1.1 shows a ground-based radar from Saab. [1]



Figure 1.1: A ground-based radar from Saab AB. [2]

1.2 Purpose

The aim of the thesis work is to develop a method that evaluates concepts and new products with regard to structural analysis in an early stage of product development. The method should implement theories for high level optimization in combination with Design of Experiments (DOE) on an appropriate product.

1.3 Objective

The main goal of the project is to determine how the DOE method is most optimal applied in the early stages of product development with regard to structural analysis and optimization. The method will be applied on a large and complex product from Saab's product portfolio. It will be done in order to determine which parameters that have the largest influence on the product and how to interpret the results obtained from the

software. The project should elucidate and describe the different DOE methods which are available within HyperStudy [3] and how to apply them in order to obtain relevant results.

1.4 Limitations

There are a number of limitations throughout the project. They are listed below.

- The work is applied on a system level, i.e., changes regarding details of the design will not be made.
- The parameters that are varied in the DOE are different materials and geometry properties of the concepts.
- The different DOE methods are limited to those available in HyperStudy, in order to learn how to use the software for the optimization process.
- The other software that are used besides HyperStudy are MSC. Nastran [4], HyperMesh [5] and HyperView [6].
- The software versions that are used are limited to those available. HyperMesh, HyperView and HyperStudy are of version 2017.2 and MSC. Nastran is of version 2018.0.
- The method that is developed regards structural optimization and analysis and is not a general optimization method within all fields.

1.5 Expected outcomes

The project's expected outcomes are listed below.

- A method for parameter optimization in an early stage of concept generation.
- A description of the different available DOE methods.
- An evaluation of how different parameters effect the structural response of an authentic, complex system.

2 Theory

This chapter includes theory about the Finite Element Method and Structural Optimization used throughout the project. Different DOE methods and post-processing plots that are available in the software HyperStudy are explained, along with information about sandwich structure and how the beam bending was calculated analytically.

2.1 Finite Element Method

The Finite Element Method, abbreviated FEM, is a numerical method which solves general differential equations in an approximate manner. The equations are assumed to hold over a certain region which may be one, two or three dimensional. One characteristic feature of FEM is that the region is divided into smaller parts called Finite Elements, FE, which are geometrically simple subdomains or elements [7][8]. The unknown variables of the FE are approximated by a linear combination of algebraic polynomials and undetermined coefficients. This represents the values of unknown variables at the nodes of the element. The nodes are often located at the boundary of the elements and two neighbouring elements often share nodes. By satisfying the weak form of the governing equations over each element, algebraic equations among the undetermined coefficients are obtained. The algebraic equations from the elements are assembled using continuity and equilibrium considerations. In combination with the boundary and initial conditions, the algebraic equations can be solved for the unknowns [7][8]. FEM makes a problem with infinitely many degrees of freedom, DOF, to a problem with finite number of unknowns. The accuracy of the approximation increases with increasing amount of elements and consequently increasing number of nodes and unknowns.

2.2 Structural Optimization

Structural optimization measures which structure that fulfills boundary conditions and withstand loads the best. A structural optimization problem is formulated by choosing one (or more) objective function(s) that should be maximized or minimized. This can, for example, be to decrease weight or increase stiffness. The problem also contains constraints, which for example can be how much material that can be used or the maximal weight that the structure can have [9]. In a structural optimization problem, there are some functions and variables which are present. They are described below

- *Objective function (f)*, which is a function used to classify designs. The objective function f returns a number which indicated the goodness of the design, for every possible set of design variables \mathbf{x} .
- *Design variable (\mathbf{x})*, which is a function or vector that describes the design. The design variable \mathbf{x} can be changed during the optimization and may represent choice of material or geometry.
- *State variable (\mathbf{y})*, which is a function or vector that represents the response of a given structure, \mathbf{x} .

Structural optimization problem with one objective function can take the form [9]:

$$(\text{S0}) \begin{cases} \text{minimize } f(x,y) \text{ with respect to } x \text{ and } y \\ \text{Subject to } \begin{cases} \text{behavioral constraints on } y \\ \text{design constraints on } x \\ \text{equilibrium constraint.} \end{cases} \end{cases} \quad (2.1)$$

There is also a possibility that there are several objective functions, it is then called a multiple criteria optimization problem. Assume it has the same constraints as for (S0). The multiple criteria optimization can then be written as Equation 2.2, where the number of objective functions is i . Although, since not all objective functions, in general, are minimized towards the same goal, the multiple criteria optimization is not a standard optimization [9].

$$\text{Minimize } f_1(\mathbf{x},\mathbf{y}), f_2(\mathbf{x},\mathbf{y}), \dots, f_i(\mathbf{x},\mathbf{y}) \quad (2.2)$$

In (S0), three different types of constraints are included [9].

- *Behavioural constraints*, constraints on the state variable \mathbf{y} . The behavioural constraints are usually written as $g(y) \leq 0$ where g is a function that represents the outputs.

- *Design constraints*, involving the design variable \boldsymbol{x} .
- *Equilibrium constraint*, the equilibrium constraint for a discrete structural problem is presented in Equation 2.3 [9].

$$K(\boldsymbol{x})\boldsymbol{u} = \boldsymbol{F}(\boldsymbol{x}), \quad (2.3)$$

where $K(\boldsymbol{x})$ is the stiffness matrix, \boldsymbol{u} is the discretized vector of accuracy vector and $\boldsymbol{F}(\boldsymbol{x})$ is the force response. Both the stiffness matrix and the force vector are generally a function of the design [9].

2.3 Design of Experiments

Design of Experiments, DOE, is an efficient way of executing different experiments of concepts. Through DOE, it is possible to measure the impact of and correlation between different parameters [10]. There are several different methods of DOE that can be used in the design exploration tool HyperStudy [3] and which one to use is dependent of what parameters and properties the parameterized object has. Some of the different DOE methods that are available in the software HyperStudy are described below.

2.3.1 Full Factorial

The method Full Factorial changes one variable at a time and the remaining are kept constant. This method estimates the impact of a single factor when the other parameters are at selected and fixed conditions, meaning that it evaluates all possible combinations of the input variables [11]. For a case consisting of k parameters at L levels, i.e., how many values the parameter is evaluated in, the number of runs will be L^k . Consequently, this method takes effects and interactions into consideration and estimates the impact of a single factor which also makes it very time consuming [12].

2.3.2 Fractional Factorial

In the method Fractional Factorial, a chosen fraction of the combinations from the Full Factorial are evaluated. The result of this is the inability to completely resolve all of the main effects and interactions. It usually ends with higher order interactions which often are confounded with each other or two-factor interactions, meaning that one variable depends on another variable. Although, the Fractional Factorial is not as time consuming as the Full Factorial method, which is beneficial. It is often used when there is a need to screen many parameters quickly. The number of evaluations in the Fractional Factorial method is determined by l^{k-p} , where l is the number of levels of each parameter, k is the number of parameters and p is the fraction of the Full Factorial which is used [11].

How much the interactions are confounded is determined by the resolution of the method. In the software HyperStudy there are three different resolutions to choose between, they are called III, IV and V. In resolution III, the effects are estimated, but may be confounded with two-factor interactions. In resolution IV, the main effects are resolved unconfounded of two-factor interactions, but the two-factor interactions are confounded with respect to other two-factor interactions. Resolution V resolves the effects with respect to each other and the two-factor interactions are resolved with respect to each other [13]. When increasing the resolution, more evaluations are necessary so a decision about if the results can be confounded or not must be made.

2.3.3 Plackett-Burman

The Plackett-Burman method can be used to screen many factors quickly. The number of required evaluations for the Plackett-Burman method is a multiple of 4, e.g., 4, 8, 12, 16 and so on. This method is often compared to the Fractional Factorial since they both are used for the same purpose, which is to screen many factors quickly. The difference between the two methods is that the number of evaluations required for the Plackett-Burman method is a multiple of 4 while the number of evaluations for the Fractional Factorial is an exponential. This means that the Plackett-Burman method prevents the large gaps between the evaluations that the Fractional Factorial gives, due to being calculated as an exponential, when the number of evaluations increases [11]. Although, the Plackett-Burman will not resolve two-factor interactions so it is only used when the main effects are of interest [14].

2.3.4 Modified Extensible Lattice Sequence (MELS)

The Modified Extensible Lattice Sequence, MELS, is a lattice sequence and is designed to spread out points equally in a space by minimizing clumps and empty spaces. It can be applied either on an existing set of data points to provide equal coverage or by extending the lattice sequence. The amount of evaluations is determined by the user, but in order to get a fitting function of good quality, there is a minimum number of evaluations that should be done. In order to calculate the number of evaluations needed, Equation 2.4 is recommended. MELS is used for exploring the entire design space and creating fitting functions to the exact output responses [15].

$$Q(N) = 1.1 \cdot (N + 1) \frac{N + 2}{2}, \quad (2.4)$$

where Q is the number of evaluations and N is the number of variables used in the optimization.

2.3.5 Hammersley

Hammersley is a sampling method and it uses a quasi-random number generator to uniformly sample a unit hypercube, where the random numbers are based on Hammersley points. It uses fewer samples than random sampling when providing reliable estimations of output descriptive statistics. A k -dimensional hypercube with good, uniform properties is provided, which is an advantage over other available hypercube methods since it provides good uniform properties of each dimension individually. As in MELS, the number of evaluations is determined by the user. But in order to get a good quality fitting function, there are a minimum number of combinations that should be evaluated. When calculating the number of evaluations, Hammersley uses the same equation as MELS, that is Equation 2.4 [16].

2.4 Plots

In HyperStudy, there are several post-processing plots available to present different aspects of the result. Three different plots were used in this study and how they should be interpreted is described below. These plots were chosen because they contained necessary results for the DOE study or for the studied cases and outputs used throughout the project.

2.4.1 Evaluation plot

The Evaluation plot, see Figure 2.1, shows the values of an output or input variable for each evaluation. The number of evaluations is defined on the x -axis and the wanted input or output is defined on the y -axis. Consequently, the plot shows which evaluation that obtained which particular value. This is important to know if a certain output value is wanted. In the summary tab, each evaluation is listed with its obtained values. When the minimum or maximum is wanted, the Evaluation plot shows which evaluation that obtained the smallest or largest value. When the number of the evaluation is known, the settings of the parameters that resulted in the desired solution can be found in a tab called “summary” tab [17]. In Figure 2.1, it is visible that the 10th evaluation obtained the largest displacement.

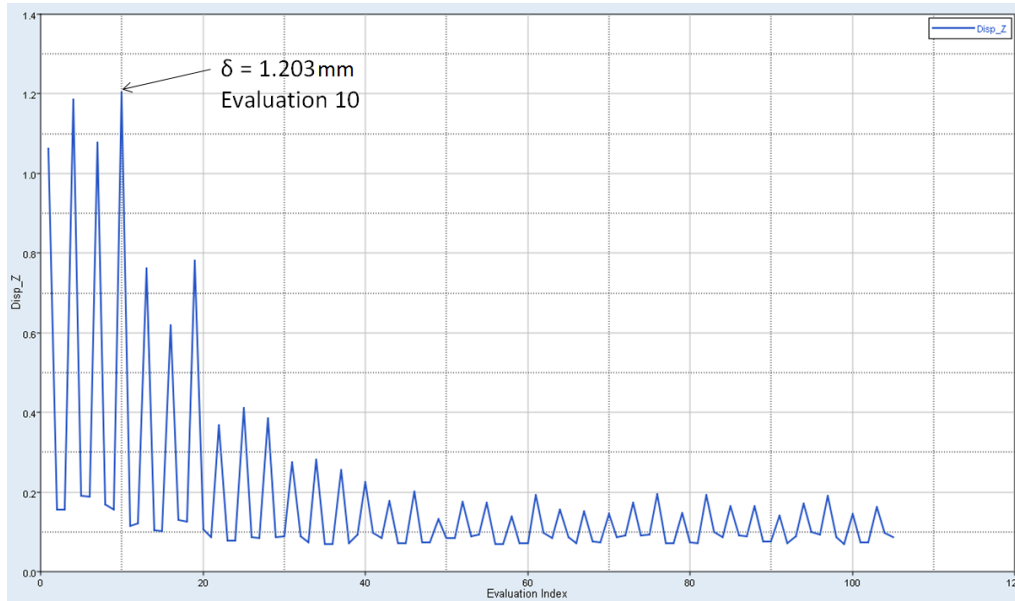


Figure 2.1: Evaluation plot, the vertical axis shows the displacement in mm and the horizontal shows all evaluations. The plot shows the displacement in z -direction and the arrow points at the evaluation that obtained the largest displacement. The value of the largest displacement is $\delta = 1.203$ mm.

2.4.2 Histogram plot

The Histogram plot is a form of distribution plot, as seen in Figure 2.2. It presents the frequency, as well as the total range of the output response values. Consequently, it shows the available range that the output variable can have, which is useful if the goal is to maximize or minimize an output value [18]. In Figure 2.2, the blue poles represent how many times a simulation resulted in a certain value. For instance, in Figure 2.2, the displacement in the z -direction often ended up in the solution 0.11 mm. The simulations obtained this value around 75 times according to the frequency scale, which is found to the left in the plot. The probability scale to the right visualizes how large the probability of a certain result is. As can be seen on the scale to the right in Figure 2.2, the probability is much larger for the result which is obtained more often than for a result which rarely is obtained. This plot shows the range of the output value through the largest and smallest values available for the output. In Figure 2.2, the range is 0.11 mm to 1.16 mm. The plot gathers equivalent results in the same poles, so all results in one pole might not be exactly the same. Although, the difference is not remarkable and does not affect the overall impression of the simulation. The red line illustrates the probability that the output is equal to a certain value and the green line shows the probability that the output is less than or equal to a particular value.

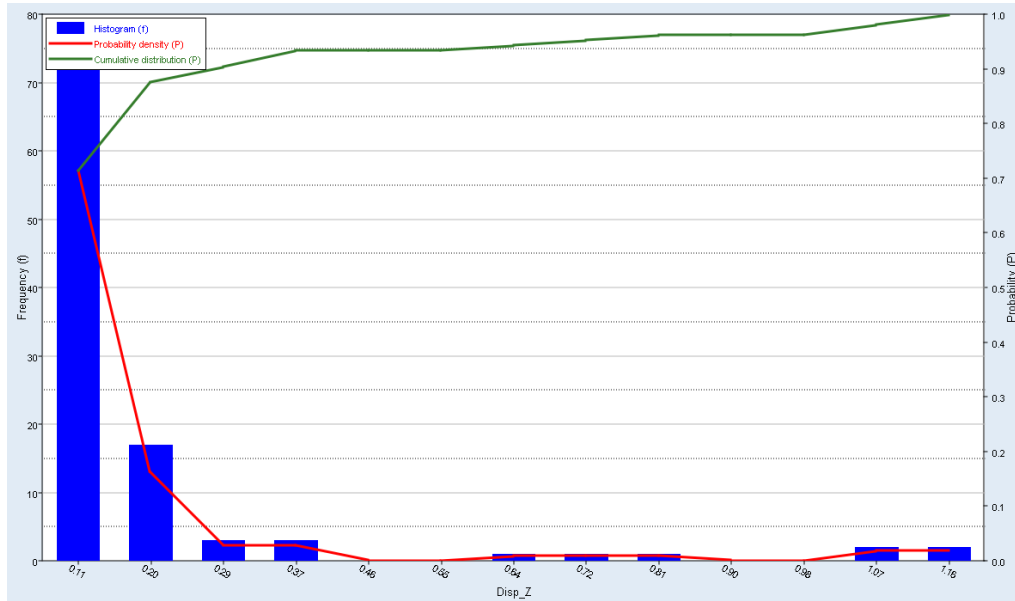


Figure 2.2: Histogram plot visualizes how often the simulations end up in with a certain solution when varying different parameters in the model. The horizontal axis shows the range of the output, the left vertical axis shows the frequency of the results and the right vertical axis shows the probability of the solution to obtain the result.

2.4.3 Pareto plot

The Pareto plot shows the effects that each variable has on the solution in hierarchical order, see Figure 2.3. This plot shows which variable that has a large impact on the solution and which ones that has minor or no impact. In Figure 2.3, the parameter “Case” has the largest effect and “Material_Sandwich” has the second largest. This provides a guideline when developing new concepts since it shows which parameters to focus on and which that can be neglected. The line that is included in the plot shows the cumulative effect of the variables. It is important since it displays how much the visible parameters affect the solution. If all variables are displayed, the cumulative line goes to 100%, but if the case has many variables then it might not be possible to show them all. The cumulative line is therefore useful because it is necessary to see if the shown parameters stands for a large part of the influencing parameters. Figure 2.3 shows that for the second most influential parameter “Material_Sandwich”, the value of the cumulative line is the two most influential parameters added together. For the third most influential parameter “Thickness_Height”, the three most influential parameters are added together and so on [19].

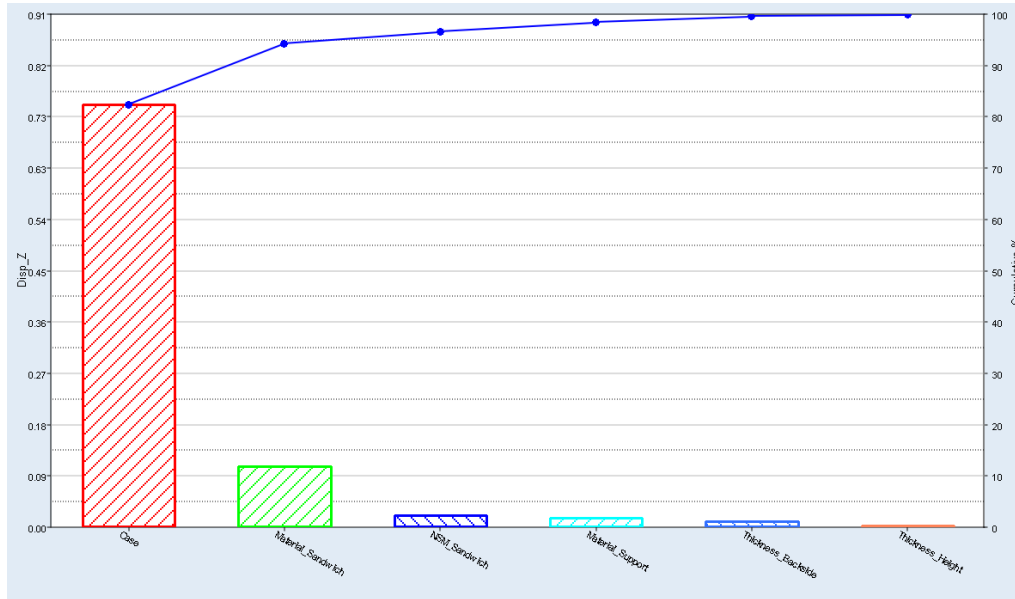


Figure 2.3: A Pareto plot visualizing which parameters that are influencing the magnitude of the displacement. The horizontal axis shows the different parameters which are displayed, the parameter with the largest influence is to the left. The vertical axis shows the value of the displacement in the z -direction in mm.

2.5 Sandwich structure

Here, the sandwich design consists of three layers, two skins on each side of a thick, low-density and low average strength material denoted the core. The normal stresses of the core will be small compared to those of the skins [20]. The purpose of a sandwich structure is to have a stiff and relatively light component [21]. A sandwich material can contribute to weight savings, having good fatigue properties, as well as good thermal and acoustical insulation. Although, if using a core with significantly low density, the stiffness and strength will be reduced and this increases the risk of complete failure of the sandwich structure [22]. Three different cases throughout the project consisted of sandwich structure in order to investigate how the different properties regarding composite elements can be parameterized. In Figure 2.4, a sandwich structure is presented.

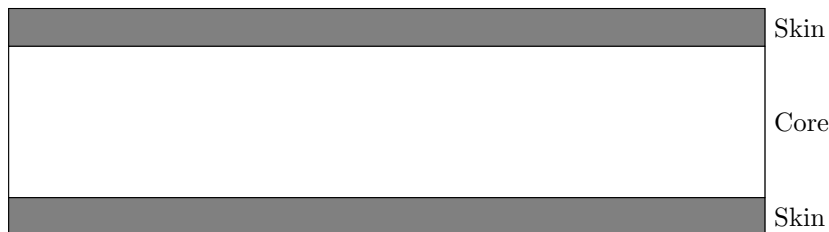


Figure 2.4: Sandwich structure

2.5.1 Core material

The benefits and properties of two different core materials used in the sandwich structures in this project are explained below.

Honeycomb

The honeycomb core consists of thin foils which are perpendicular to the skin [20]. Honeycomb can be produced in a variety of cell shapes, but the most common is the hexagonal shape [23]. One benefit that honeycomb has is that it has a high strength to weight ratio, as well as high compressive strength. It is also beneficial that the honeycomb can be made out of different materials, for example, composite, paper or aluminum [21]. The material properties used for the composite honeycomb (ECA-(i)) and aluminium honeycomb in the thesis are

given in Tables 2.1 and 2.2, respectively. For the composite honeycomb, E_x and E_y is the Young's modulus in the x and y material coordinate direction [24], respectively. G_{xy} is the in-plane shear modulus, G_{xz} and G_{yz} are the transverse shear modulus for the different directions, ν is the Poisson's ratio and ρ is the mass density. The difference in definition between the composite and aluminum honeycomb is that the aluminum honeycomb is isotropic and consequently, E is the Young's modulus and G is she shear modulus. The two materials are defined differently since they are defined using different material cards, MAT1 and MAT8 [24].

Table 2.1: The anisotropic material properties used in the composite honeycomb [25], defined as a MAT8 [24].

Honeycomb	
E_x	22 MPa
E_y	12 MPa
G_{xy}	0.54 MPa
G_{xz}	0.52 MPa
G_{yz}	0.28 MPa
ρ	29.0 kg/m ³
ν_{xy}	0.99 [-]

Table 2.2: The isotropic material properties used for aluminium honeycomb, defined as a MAT1 [24].

Aluminum honeycomb	
E	230 MPa
G	88.46 MPa
ν	0.3
ρ	100 kg/m ³

Rohacell

Rohacell is a material made out of foam and consists of a closed cell structure. This makes it possible to produce sandwich components in one single step [26]. Foam cores are often used in the marine industry due to that the cells are closed and that each cell is isolated from other cells [21]. The material properties used for Rohacell in this thesis are given in Table 2.3.

Table 2.3: The anisotropic material properties used in Rohacell [27], defined as a MAT8 [24].

Rohacell	
E_x	36 MPa
E_y	36 MPa
G_{xy}	13 MPa
G_{xz}	13 MPa
G_{yz}	13 MPa
ρ	32.0 kg/m ³
ν_{xy}	0.99 [-]

2.6 Bending

The displacements of plates and beams which are investigated in different cases throughout the project are calculated analytically. This is done in order to be able to compare and verify the results obtained by the simulations in the software. The chapters below describe how the different displacements are calculated.

2.6.1 Bending of a beam

The midpoint displacement of a simply supported beam with a perpendicular force applied across the middle is calculated through Equation 2.5. The moment of inertia for a rectangular cross section is used [28].

$$\delta = \frac{PL^3}{48EI}, \quad (2.5)$$

where P is the perpendicular force, L is the length of the beam, E is the Young's modulus of the material and I is the moment of inertia.

2.6.2 Bending of beam with Sandwich structure

When calculating bending of a sandwich structure, it can be analyzed as an I-beam where the core is the middle beam and the skins are the flanges. The core, i.e., middle beam, is assumed to have a very small thickness since the core does not contribute to the stiffness of the beam [23]. The moment of inertia for the different parts are calculated using Equation 2.6. The three different parts of the I-beam are analyzed as rectangles and added together using the parallel axis theorem, also known as Steiner's theorem.

$$I = \frac{bt^3}{12}, \quad (2.6)$$

where b is the width and t is the thickness of a rectangular cross section.

The effective thickness of the core is calculated using the Young's modulus for both the core and the skins, which can be seen in Equation 2.7 [23].

$$b_c = \frac{bE_{\text{core}}}{E_{\text{skin}}}, \quad (2.7)$$

where b is the width of the beam, E_{core} is the Young's modulus of the core material and E_{skin} is the Young's modulus of the skin material.

When calculating the midpoint displacement for a simply supported sandwich beam with a perpendicular force in the middle, the denominator is split into two parts. This can be seen in Equation 2.8. It is divided due to the different Young's moduli of the skin and the core materials.

$$\delta = \frac{FL^3}{48E_{\text{skin}}I_{\text{skin}} + 48E_{\text{core}}I_{\text{core}}}, \quad (2.8)$$

where F is the force, L is the length of the beam, E_{skin} and E_{core} are the Young's modulus of the material used in the skin and core, respectively. I_{skin} and I_{core} are the moment of inertia for the skin and the core, respectively [28].

3 Methodology

The software which were used are described, along with the process of the parameterization. The flow chart in Figure 3.1 shows the steps in the parameterization.

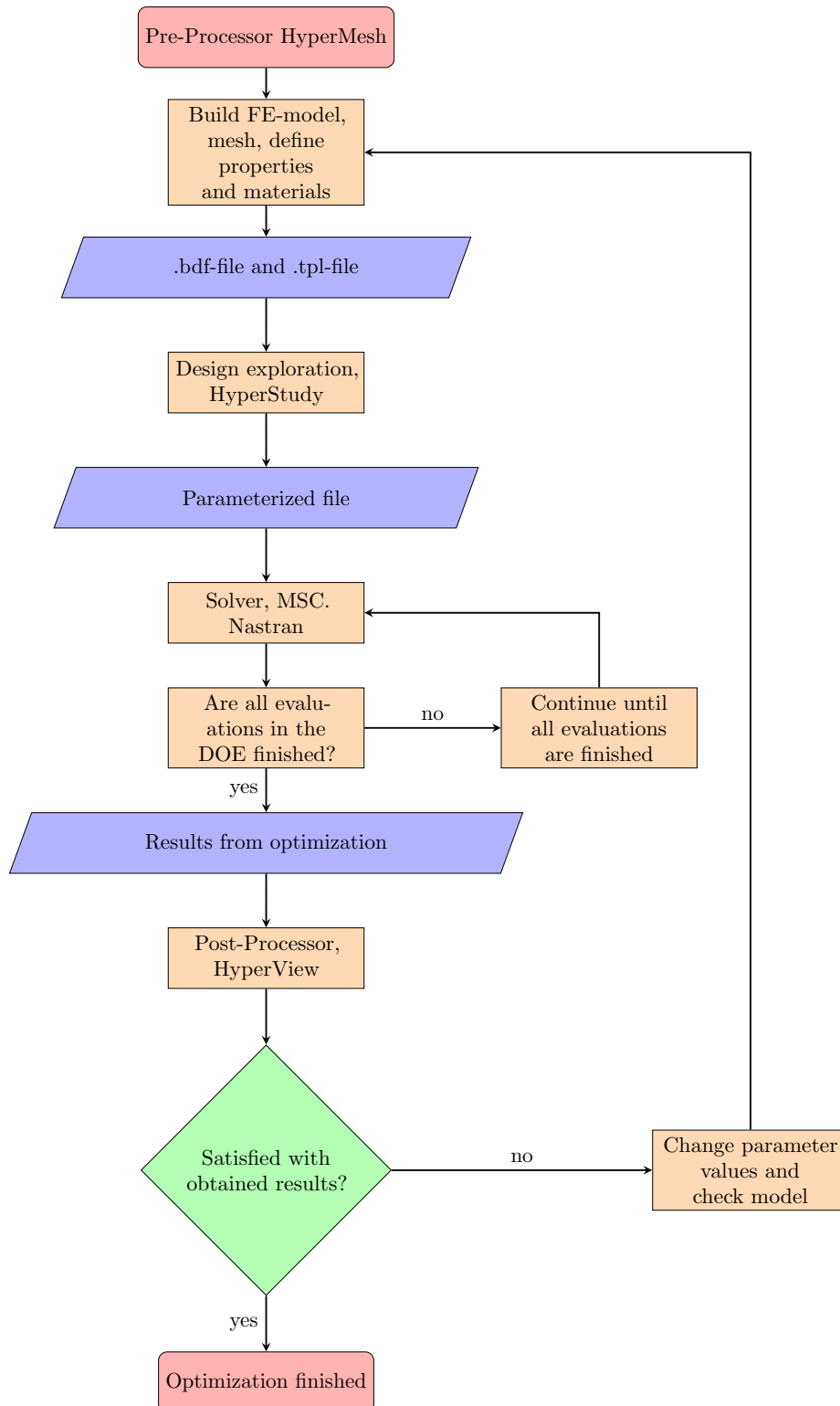


Figure 3.1: Flow chart of the process

3.1 Software

Different software were used during the project. A description of what they were used for and in what order they were used is described in the flowchart found in Figure 3.1. The three software HyperMesh [5], HyperView [6] and HyperStudy [3] are all part of the HyperWorks suite. The red boxes in Figure 3.1 represent the first and last steps of the process. The orange boxes represent the different steps, the purple boxes represent output and input between the different steps and the green box represents when the process demands that a decision is made. In Figure 3.1, the first purple box says .bdf-file and .tpl-file (template-file). This means that files consisting of this format were received as outputs from the step before and were used as inputs into the next step. The step that says “Are all evaluations in the DOE finished?” was not considered as a question since this step was done in the software and was not an conscious choice in the process.

3.1.1 HyperMesh

The software HyperMesh is a multi-disciplinary finite element pre-processor [5]. It was used for preparation of the FE-model by building the models and meshing them, i.e., dividing the geometry into smaller elements. It was also used for defining load cases and specific details, such as material properties and thicknesses of different components [29]. From HyperMesh, files which were accessed and parameterized in HyperStudy were obtained. The used version of HyperMesh was 2017.2.

3.1.2 MSC. Nastran

MSC. Nastran, called Nastran, is a multidisciplinary structural analysis tool and it was used for static analysis [4]. It was used as the solver in this project. Nastran version 2018.0 was used.

3.1.3 HyperView

HyperView is a post-processing and visualization environment [6]. It visualizes data interactively as well as captures and standardizes the post-processing activities. It was used in order to check the results obtained from HyperStudy. The used version of HyperView was 2017.2.

3.1.4 HyperStudy

HyperStudy is a design exploration tool for engineers and designers that automatically creates design variants, manages evaluations and collects data [3]. It is useful for exploring, understanding and improving designs by the use of different optimization methods. It also has beneficial post-processing tools in order to ease the understanding and interpretation of the results [3]. Different optimization methods are available within the software and they provide information about which parameters that have the largest influence on the new concept. The used version of HyperStudy was 2017.2.

3.2 Parameterization

The parameterization was executed in the software HyperStudy by editing an imported .tpl-file. The .tpl-file and .bdf-file that were needed were obtained from HyperStudy, as can be seen in the flowchart in Figure 3.1. The .tpl-file contained all information about the parameters that was needed in order to execute the parameterization and simulation. The different steps that were included from the parameterization setup to the evaluation of the DOE can be seen in Figure 3.2.

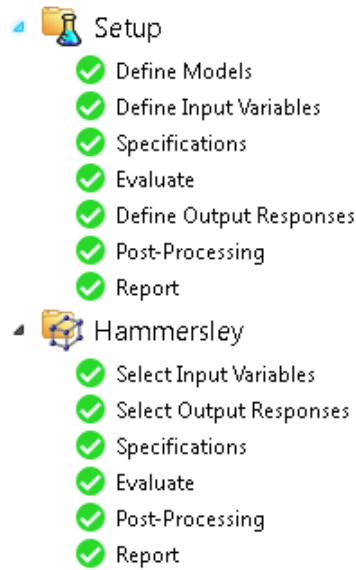


Figure 3.2: The different steps of a setup and a Hammersley DOE in HyperStudy

In the step Define Models, shown in Figure 3.3, the files which were used in the parameterization were specified together with which solver that was used when executing the simulations. The .tpl-file that was to be parameterized was defined under “Resource” and the input file, which is a .bdf-file that contained all components and properties that the model included, was defined in “Solver input file”. The editing and parameterizing were done in the .tpl-file using the HyperStudy Editor. It opened the stated file and consequently the parts which were to be parameterized were included in the file. When the parts were found, the entire space which regarded a particular value was marked and thereafter, a parameter was created. The format used throughout the project was that each property had eight spaces and consequently, all eight spaces were marked. As mentioned above, the template file was based on the .bdf-file obtained from HyperMesh and it contained the entire model, including the bulk file (.blk-file), demanded output, boundary conditions and load cases.

+ Add Model		- Remove Model		Model Resources					
	Active	Label	Varname	Model Type	Resource	Solver input file	Solver execution script	Solver...uments	Comment
1	<input checked="" type="checkbox"/>	Model 1	m_1	{ } Parameterized File	D:/.../HyperStudy/Rigidf...	Rigidforce.bdf	Nastran (nastran)	{file}	...

Figure 3.3: Figure shows how the resource, solver input file and solver execution script were defined in the “Define Models” step. The Resource tab includes the .tpl-file with complete file path, the Solver input file contains the .bdf-file and which solver to use was defined under Solver execution script.

When creating a real parameter, three values needed to be defined. They were

- Lower bound
- Nominal value
- Upper bound

The lower bound defined the lower limit while the upper bound defined the upper limit of the variable range. The nominal value is the value which is default if the variable was deactivated and it was also used as the initial value in an optimization. This value was chosen freely and it was not required to be the average of the upper and lower bound, nevertheless it often was. Although, the nominal value is required to be within the range of the upper and lower bounds [30]. When the parameterized variable was a string, the input was a list with the names of the files that were to be included in the parameterization and optimization. See Figure 3.4 for parameterization with real values and Figure 3.5 for parameterization with strings. The chosen format defined how many decimals the lower and upper bound consisted of. This can be observed in Figure 3.4 where the format is 8.3, meaning that it allowed three decimals, which both bounds contained. There were also two

different choices called “Set percent” and “Set value” and they were used when a nominal value was defined and then the upper and lower bounds could be put to $\pm 20\%$ or ± 20 of the nominal value. In Figure 3.5, the format was 5s, meaning that a string was parameterized. In the “List” that can be seen in Figure 3.5, the name of all strings that the parameterization varied between are mentioned.

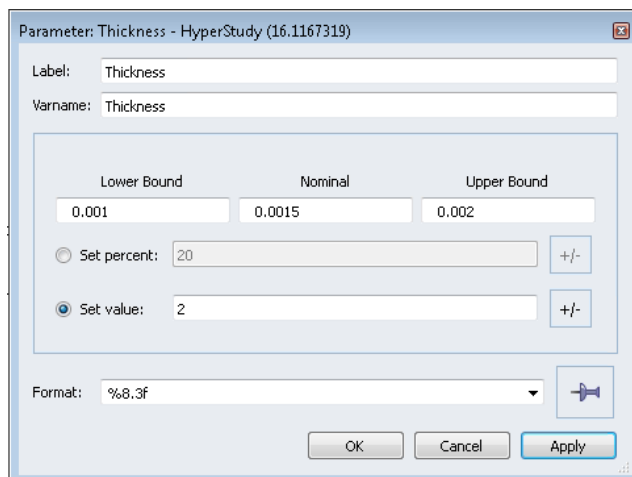


Figure 3.4: Defining a real parameter with Lower Bound, Nominal and Upper Bound values.

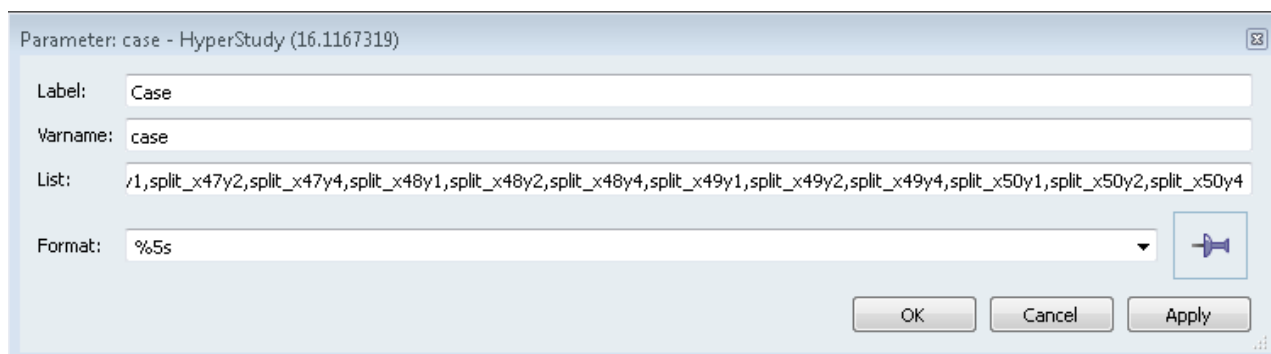


Figure 3.5: A string is parameterized. The name of the .blk-files that are parameterized are listed in the “List” box.

When the parameterization was complete, the “Solver input file” was needed to be defined. In this project, that meant the .bdf-file obtained from HyperMesh which contained the model. Nastran was defined as the Solver execution script and then the variables were imported. In the step called “Define Input Variables”, seen in Figures 3.6 and 3.7, it was possible to choose which of the defined parameters that were to be active in the simulations. In Figure 3.6 only the variable “Case” is active. Figure 3.7 shows the different data types that the variables could have. It visualizes that the parameter could be changed between Real, Integer and String. If the value contains decimals, the data type is put to real and the mode is continuous. If the variable only contains discrete values, the data type can be put to either real or integer, but the mode is required to be put to discrete. If the variable is a string, the data type should be string and the mode is categorical.

The step where the input variables were defined is equivalent to defining the design variable. In the step, the different variables regarding change of material, geometry and thicknesses etc. were defined. They were varied in the different cases in order to observe which combination of design variables that gave the desired output.

	Active	Label	Varname	Model Parameter	Model Type	Data Type	Mode	Values	Distribution Role
1	<input checked="" type="checkbox"/>	Case	m_1_case	m_1.case	{ } Parameterized File	String	Categorical	whole,spli...	Design
2	<input type="checkbox"/>	Thickness	m_1_Thickness	m_1.Thickness	{ } Parameterized File	Real	Continuous	N/A	Design

Figure 3.6: Define Input Variables, this case contains one string and one real parameter, but only the parameter called “Case” is active.

	Active	Label	Varname	Model Parameter	Model Type	Data Type	Mode	Values	Distribution Role
1	<input checked="" type="checkbox"/>	Case	m_1_Case	m_1.Case	{ } Parameterized File	String	Categorical	G8_z0y0,G...	Design
2	<input checked="" type="checkbox"/>	Thickness_Back...	m_1_Thickness...	m_1.Thickness...	{ } Parameterized File	Real	Continuous	N/A	Design
3	<input checked="" type="checkbox"/>	Thickness_Height	m_1_Thickness...	m_1.Thickness...	{ } Parameterized File	Real	Continuous	N/A	Design
4	<input checked="" type="checkbox"/>	NSM_Sandwich	m_1_NSM_San...	m_1.NSM_Sand...	{ } Parameterized File	String	Categorical	2.042-7, 2...	Design
5	<input checked="" type="checkbox"/>	Material_Sandw...	m_1_Material_S...	m_1.Material_Sa...	{ } Parameterized File	Real	Discrete	2, 9, 10	Design
6	<input checked="" type="checkbox"/>	Material_Support	m_1_Material_S...	m_1.Material_Su...	{ } Parameterized File	Real	Discrete	12, 13	Design

Figure 3.7: Define Input Variables, this case contains two string, two real and two discrete parameters.

When the “Define Input Variables” step was complete, one of the three different methods available in the “Specifications” step needed to be chosen. The available methods were

- Nominal run
- System bounds check
- Sweep

The nominal run only evaluated the variables at their nominal values. The system bounds check evaluated the system at the nominal values, and thereafter at the lower and upper values. Sweep evaluated the system by sweeping from the lower to upper values. In the step Evaluate, the method that was specified in the Specifications step was evaluated.

In the step “Define Output Responses”, the desired output was specified. There were two different ways of specifying the output. It was either done manually, or by dragging the .op2-file obtained in the evaluations step into the “Define Output Responses” window. When creating the output responses by dragging the file, the result files from the first run were used. All solutions ended up in a folder called “Approaches” and were thereafter sorted in different folders dependent of what type of simulation that had been run. The simulations from the setup file ended up in folders called “nom.#” and the folder from the DOE simulations obtained the name “doe.#”. The #-symbol mentions the number of the evaluation of the simulation or DOE that was done. In these folders, there are sub-folders called “run.#”, where # is the number of the evaluation. As mentioned before, the result files which were located in the folder “run_0001” were used when creating output responses. In the post-processing step, the results obtained from the output responses were analyzed using different plots that were used in the thesis. The plots are described in section 2.4.

The output response step was equivalent to the step defining the output response function in the structural optimization, see section 2.2. It was now defined which output that was desired with regard to the design variables which were defined in the input step. Consequently, the DOE method used this information to calculate which parameters that had the largest influence on the output and which parameters that could be neglected due to having minor influence on the output.

After the setup-step was finished, a DOE simulation could be specified. It was done by adding an “Approach” and thereafter it was possible to choose between DOE, Fit, Optimization or Stochastic simulation, see Figure 3.8. Since this thesis regarded the method DOE, it is the only approach which was investigated further. When creating a DOE simulation, the defined Input Variables and Output Responses from the setup step were also defined in the DOE. It was possible to add more output responses to the DOE if desired. After all output responses were defined, a DOE method must be chosen. The different methods available in HyperStudy can be seen Figure 3.9 and the choice regarding which method to use was dependent of which parameters that were defined. The different methods which were relevant for the cases in this thesis are defined in section 2.3.

Consequently, the DOE study had the same evaluation and post-processing as the Setup did, e.g., Evaluation, Distribution and Pareto plots.

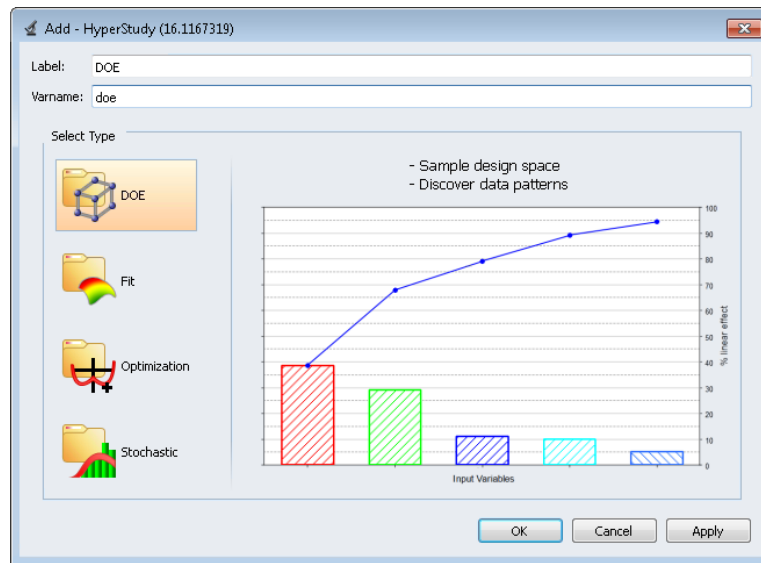


Figure 3.8: Choose between different approaches.

	Mode	Label	Varname	Details
1	<input checked="" type="radio"/>	Modified Extensible Lattice Sequence	Mels	
2	<input type="radio"/>	D - Optimal	DOpt	
3	<input type="radio"/>	Fractional Factorial	FracFact	
4	<input type="radio"/>	Full Factorial	FullFact	
5	<input type="radio"/>	Plackett Burman	PlackBurm	
6	<input type="radio"/>	Taguchi	Taguchi	Requires at least (3) variables.
7	<input type="radio"/>	Central Composite	Ccd	Discrete and Categorical vari...
8	<input type="radio"/>	Box Behnken	Box	Discrete variables must have...
9	<input type="radio"/>	Latin HyperCube	LatinHyperCube	
10	<input type="radio"/>	Hammersley	Hammersley	
11	<input type="radio"/>	User Defined	User	
12	<input type="radio"/>	Run Matrix	RunMatrix	
13	<input type="radio"/>	None	None	

[Show less ...](#)

Figure 3.9: The different DOE methods to choose between in HyperStudy.

4 Results - Sample cases

The project began by executing three simple model cases and the methodology and results from the different cases are described below. The first case consisted of a three point bending with a plate, i.e., it had a perpendicular line force across the middle of the plate. In the second case, the plate consisted of a sandwich structure with a perpendicular line force across the middle of the plate. The third case consisted of a plate with sandwich structure where the core was divided into smaller panels (see Figure 4.23) and a perpendicular force was applied along the middle of the plate. The project started out with simple cases in order to learn how to create and mesh models, as well as apply DOE using structural optimization. The cases were also parameterized in HyperStudy and the results were analyzed. The parameterization started with changing values within variables and later changing the geometry and mesh of the model.

4.1 Plate

The first case consisted of a simply supported plate with the dimensions 10 m x 1 m x t , where t is the thickness of the plate.

4.1.1 Methodology

The first case consisted of a single plate; it was created in order to learn to use the software that was used along the project. In the software HyperMesh, the plate was modelled and thereafter meshed using shell elements, see Figure 4.1. Consequently, the model was exported and opened in HyperStudy. The model consisted of two different analyses, one linear static and one natural frequency analysis. The model was simply supported and in the case with a linear static analysis, a perpendicular line force of 90 N was applied. The boundary conditions were not constrained regarding rotation around the y -axis, which is degree of freedom 5 and abbreviated DOF 5. Only one side was constrained in DOF 1, i.e., translation in x -direction, in order for the plate to be able to flex.

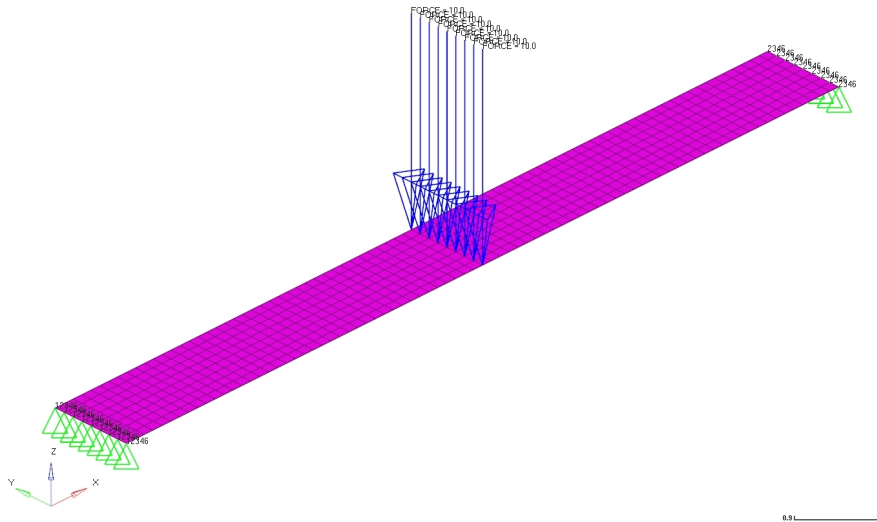


Figure 4.1: Plate with applied force and constraints

The main objective functions for the two cases were to minimize midpoint displacement and to maximize natural frequency for the linear static and natural frequency case, respectively. The mass was also demanded as output for the two cases. The design variables, i.e., parameters, were the thickness and the material of the plate. The thickness varied between 1 mm and 2 mm and the material changed between steel and aluminum. The simulations were run in Nastran through HyperStudy and the cases were analyzed using different DOE methods in order to learn how the different methods work.

Since the model was made out of shell elements, the specified values and parameterization were done according to the definition of PSHELL elements. The element's definition, according to Nastran, can be seen in Figure 4.2.

Figure 4.3 shows how the parameterization was done in the .tpl-file through HyperStudy. All three material properties, MID1, MID2 and MID3 were parameterized in order to get the membrane, bending and transverse shear of the shell elements. Figure 4.4 shows how the parameterization was displayed when the parameterized file was opened as a text-file (.txt-file) in a text editor outside HyperStudy.

PSHELL **Shell Element Property**

Defines the membrane, bending, transverse shear, and coupling properties of thin shell elements.

Format:

1	2	3	4	5	6	7	8	9	10
PSHELL	PID	MID1	T	MID2	12I/T**3	MID3	TS/T	NSM	
	Z1	Z2	MID4						

Figure 4.2: Definition of the PSHELL property in MSC. Nastran. [24]

```

$$$$-----$$$$
$$$$ Property Definition for Surface and Volume Elements -----$$$$
$$$$-----$$$$
$$$$
$$$$ PSHELL Data
$$$$
$HMNAME PROP .....1"Shell_thick" 4
$HWCOLOR PROP .....1.....6
PSHELL .....1.....0.015.....1.....1.....

```

Figure 4.3: The parameterization in HyperStudy. The values marked in blue were parameterized. According to the definition in Figure 4.2, thickness = T and the material ID = MID1, MID2 and MID3 were parameterized.

```

$
$$$$-----$$$$
$$$$ Property Definition for Surface and Volume Elements -----$$$$
$$$$-----$$$$
$$$$ PSHELL Data
$$$$
$HMNAME PROP .....1"shell_thick" 4
$HWCOLOR PROP .....1.....6
PSHELL .....1{templ_ex_on}{mat, %81}{templ_ex_off}{templ_ex_on}{thickness, %8.3f}{templ_ex_off}{templ_ex_on}{mat, %81}{templ_ex_off} .....{templ_ex_on}{mat, %81}{templ_ex_off}
$$$$ HYPERMESH TAGS
$$$$-----$$$$
$$$$ BEGIN TAGS
$$$$ END TAGS
$$$$
$$$$ MAT1 Data
$$$$
$HMNAME MAT .....1"Steel" "MAT1"
$HWCOLOR MAT .....1.....5
MAT1 .....1 21E+10 .....0.37 8000.0
$$$$
$HMNAME MAT .....2"Aluminium" "MAT1"
$HWCOLOR MAT .....2.....6
MAT1 .....2 69E+9 .....0.334 2712.0

```

Figure 4.4: The parameterization of the first case. When opening the .tpl-file in a text editor, the parameterization is shown.

4.1.2 Linear static simulation

According to the DOE, the smallest midpoint displacement was obtained when the thickness of the plate was $t = 0.002$ m and the material was steel. The simulations showed that the value of the displacement for this case was $\delta = 0.0134$ m. In order to verify that the simulations were set up properly, the displacement was calculated by hand using the bending equation. Equation 4.1 was used together with the Young's modulus for steel, which is 210 GPa, and a plate thickness of 2 mm. A rectangular cross section was used when calculating the moment of inertia. The midpoint displacement for the simply supported plate with a perpendicular line force of 90 N applied along the middle of the plate is seen in Equation 4.1.

$$\delta = \frac{PL^3}{48EI} = 0.0134\text{m} \tag{4.1}$$

As can be seen, the displacement obtained from the simulations was equal to the result which was obtained analytically. This proved that the results obtained from the simulations for this case can be trusted. The displacement of the plate can be seen in Figure 4.5.

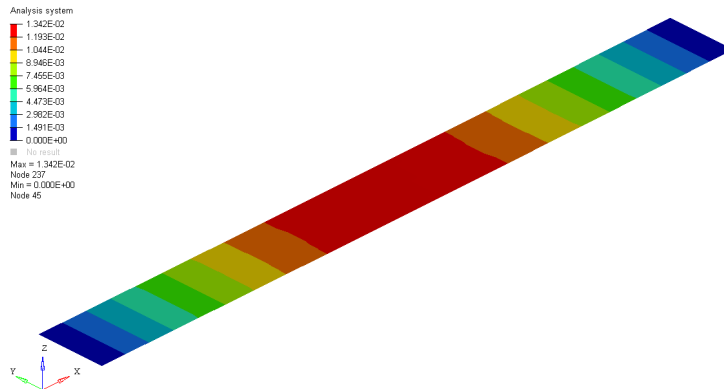


Figure 4.5: The displacement of the plate. The scale ranges from the blue = 0 to the red = $1.342 \cdot 10^{-2}$ mm.

The results from the parameterization was obtained from the Hammersley method which was evaluated 20 times. Figure 4.6 shows the Evaluation plots for the two parameters. It can be seen that the smallest midpoint displacement, which was the main objective function, was obtained for evaluation 20 and the smallest mass was obtained for evaluation 1, i.e., the outputs demand two different designs to be fulfilled.

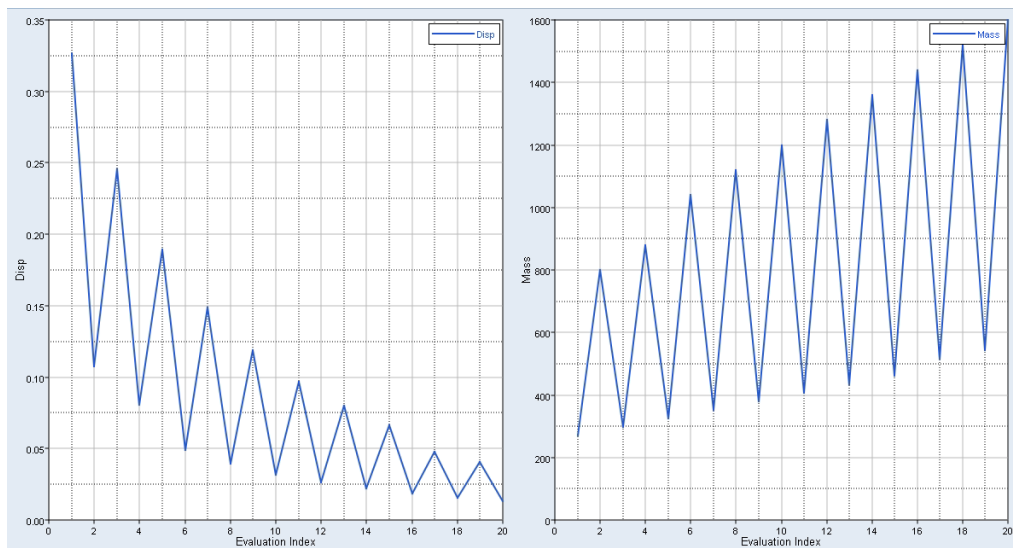


Figure 4.6: Evaluation plot. The left plot shows midpoint displacement and the right plot shows mass.

The Histogram plot shown in Figure 4.7 shows how the results regarding displacement and mass were distributed. The range of the different parameters can be seen on the respective x -axis. The smallest possible displacement was 0.03 m and the largest was 0.31 m according to the plot. The Pareto plot in Figure 4.8 shows which parameters that influenced the solution the most. For the displacement, the thickness of the plate influenced more than the material and vice versa for the mass.

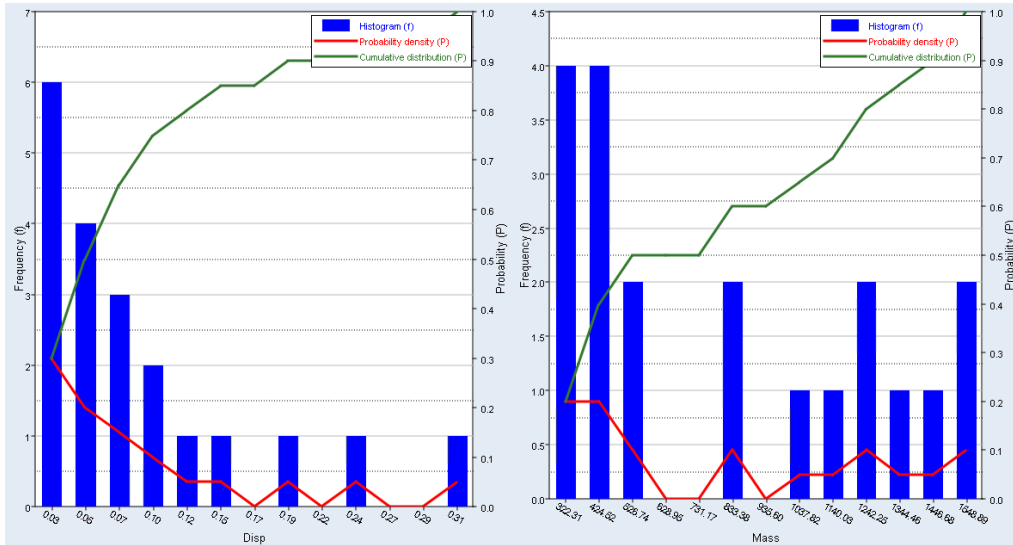


Figure 4.7: Histogram plot. The left plot shows the displacement and the right shows the mass.

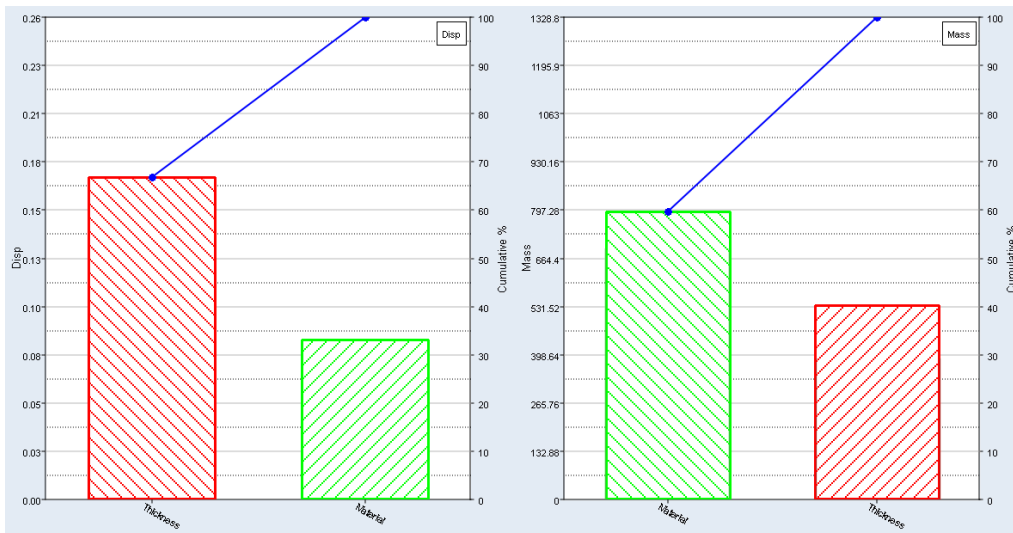


Figure 4.8: Pareto plot shows the parameters' influence on the solution. The plot to the left displays displacement and the plot to the right displays the mass.

4.1.3 Natural Frequency simulation

The Evaluation plot, Figure 4.9, shows the results regarding midpoint displacement and natural frequency in the first mode for the 20 different evaluations executed in the Hammersley DOE. It is possible to decipher that evaluation 7 obtained both the smallest midpoint displacement and the largest natural frequencies. The main objective function regarded to maximize the natural frequency and here, both outputs can be fulfilled at the same time since the same case gave the smallest displacement and the largest natural frequency. The Histogram plot in Figure 4.10 shows which result of the midpoint displacement and natural frequency that occurred most frequently and which range the results had. The plot shows that the smallest and largest obtained natural frequency was 3.16 Hz and 5.90 Hz, respectively. This information is beneficial to have when developing a product towards a specific natural frequency or midpoint displacement. It informs about how many evaluations, and therefore combination of parameters, that obtained the particular frequency or if it is outside of the obtained range. The Pareto plot in Figure 4.11 shows that the material had a larger influence than the plate thickness regarding displacement. The plate thickness influenced the solution to around 95% regarding the eigenfrequencies.

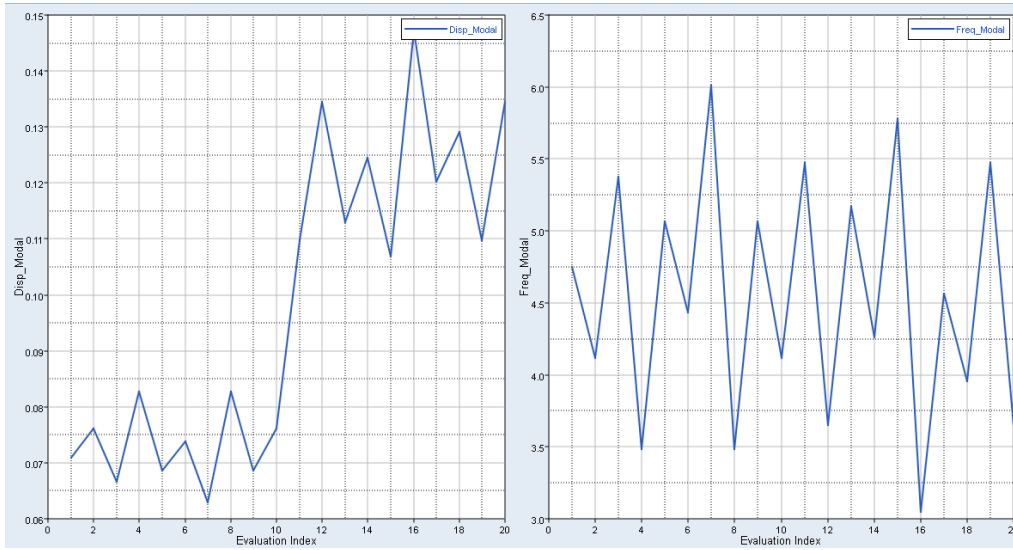


Figure 4.9: Evaluation plot displaying midpoint displacement to the left and natural frequencies to the right.

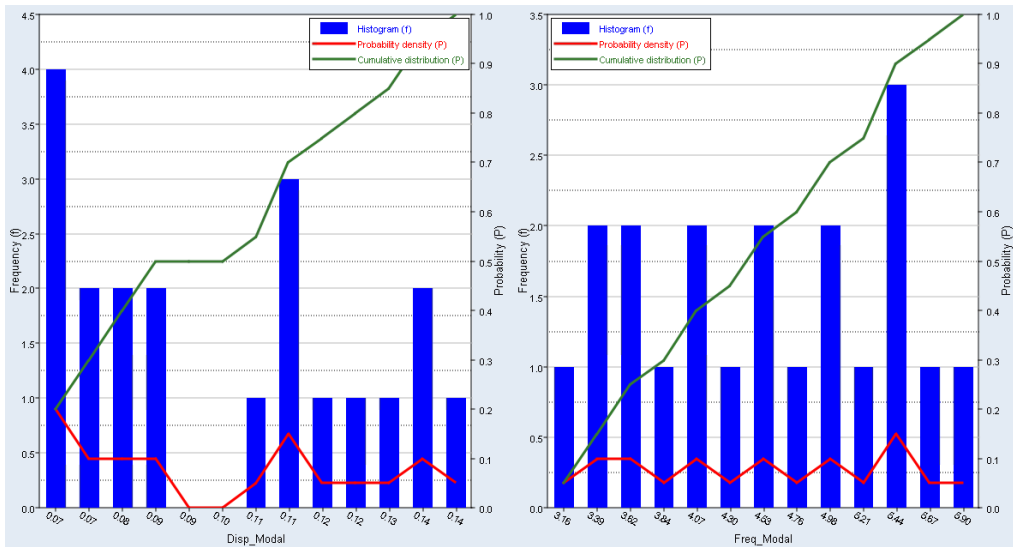


Figure 4.10: Histogram plot midpoint displaying displacement to the left and natural frequencies to the right.

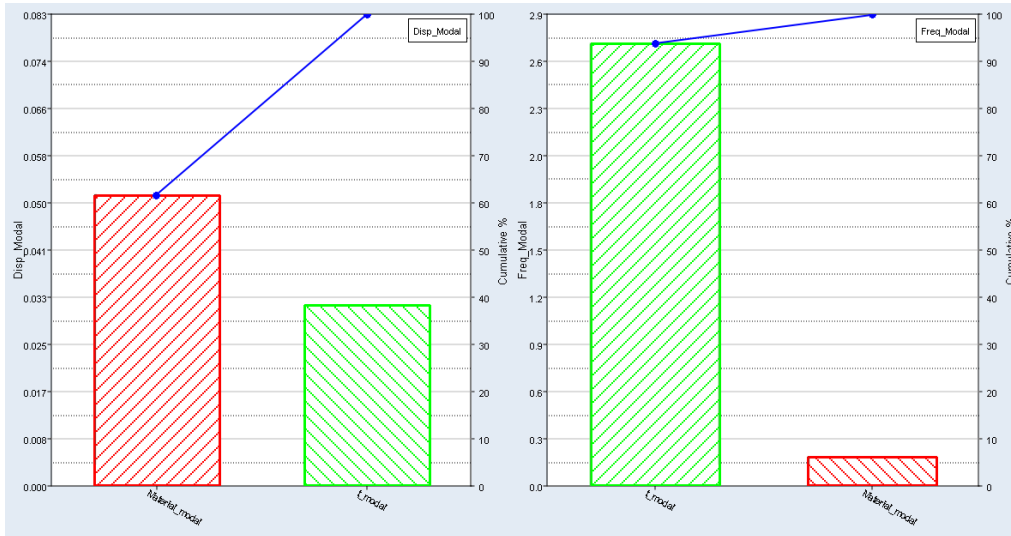


Figure 4.11: Pareto plot shows how much the parameters influence the solution.

4.2 Sandwich Structure

In the second case, a simply supported plate consisting of a sandwich structure was analyzed. It had the dimensions 10 m x 1 m x t , where t initially contains two skin thicknesses of 1 mm each and a core thickness of 32.5 mm.

4.2.1 Methodology

The second case can be seen in Figure 4.12 together with the constraints and loads. It was modelled and meshed using composite elements, called PCOMP [24], in HyperMesh. The definition and how the properties were defined in a PCOMP element can be seen in Figure 4.13. Two different models were created, one linear static case and one natural frequency case. Only the linear static case had the applied force of 10 N across the middle of the plate.

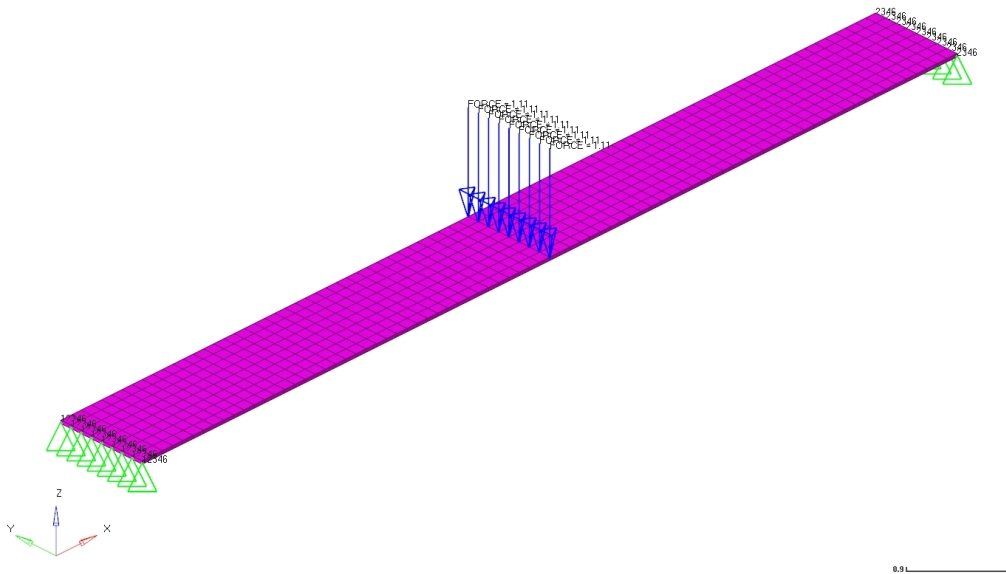


Figure 4.12: Sandwich plate with perpendicular force and constraints.

PCOMP Layered Composite Element Property

Defines the properties of an n-ply composite material laminate.

Format:

1	2	3	4	5	6	7	8	9	10
PCOMP	PID	Z0	NSM	SB	FT	TREF	GE	LAM	
	MID1	T1	THETA1	SOUT1	MID2	T2	THETA2	SOUT2	
	MID3	T3	THETA3	SOUT3	-etc.-				

Figure 4.13: Definition of the PCOMP property in Nastran. [24]

The main objective functions for the two cases linear static and natural frequency were to minimize midpoint displacement and maximize natural frequency, respectively. The mass was also obtained for the two cases, although only to observe how it varies between the cases. The cases consisted of two design variables, the thickness of the skins and the material of the core. The thickness of the skins was parameterized with values between 1 mm and 2 mm and the parameters were linked together in order for the skins to always have the same thickness, even when varying. The core material was parameterized and changed between Honeycomb and Rohacell. The thickness of the core was fixed and set to 32.5 mm and the material of the skins was set to an aramid fiber laminate. Figures 4.14 and 4.15 show the parameterization, where Figure 4.14 shows the parameterization in HyperStudy and Figure 4.15 shows how it is displayed in the .tpl-file when opening it in a text editor. Different DOE methods were evaluated in order to see how the methods work and which parameters that influence the output.

```

$$$$-----$
$$$ Property Definition for Surface and Volume Elements -----$
$$$-----$
$HMNAME PROP ..... 1"PComp" 4
$HWCOLOR PROP ..... 1 ..... 6
PCOMP ..... 1 ..... 0.0 ..... 0.0
..... 3 ..... 0.001 ..... 0.0 ..... YES ..... 4 ..... 0.0325 ..... 0.0 ..... YES
..... 3 ..... 0.001 ..... 0.0 ..... YES

```

Figure 4.14: The parameterization in the HyperStudy editor.

```

$
$$$
$$$-----$
$$$ Property Definition for Surface and Volume Elements -----$
$$$-----$
$HMNAME PROP ..... 1"PComp" 4
$HWCOLOR PROP ..... 1 ..... 6
PCOMP ..... 1 ..... 0.0 ..... 0.0 ..... YES{templex_on}{Mat_Core, %8i}{templex_off} 0.0325 ..... 0.0 ..... YES
..... 3{templex_on}{t_skin, %8.4f}{templex_off} ..... 0.0 ..... YES
..... 3{templex_on}{t_skin, %8.4f}{templex_off} ..... 0.0 ..... YES

```

Figure 4.15: The parameterization when opening the .tpl-file in a text editor.

4.2.2 Linear static simulation

The midpoint displacement for the sandwich structure with a perpendicular line force of 10 N was calculated analytically by using Equation 4.2 and the result was the same regardless of which core material that was used.

$$\delta = \frac{FL^3}{48E_{skin}I_{skin} + 48E_{core}I_{core}} = 0.0186m \quad (4.2)$$

In the simulations, the obtained midpoint displacements varied with core material. The lack of influence from the core material in the analytical solution might be due to that the skin and core materials had very different Young's moduli, see Table 4.1. Even if Rohacell had a larger Young's modulus than Honeycomb, the difference

was negligible in comparison to the difference between the Young's modulus of the skin and the core materials.

Table 4.1: Young's modulus of the skin and core materials.

Material	Young's modulus [MPa]
Skin	20000
Composite Honeycomb	22
Rohacell	36

The Evaluation plot, Figure 4.16, shows the midpoint displacement and mass for the 20 different evaluations using the DOE method Hammersley. In the plot showing the objective function midpoint displacement, there is a clear reduction in displacement after the 10th evaluation. It can be explained by that HyperStudy changed the core material in the sandwich from Honeycomb to Rohacell at this evaluation. In Figure 4.16, it can also be seen that the mass was larger in every other simulation. It can be explained by that the value for the thickness changes between a smaller and a larger value. The Histogram plot, as well as the Evaluation plot, show that the evaluations only obtain two different values regarding the mass, see Figure 4.17, which is reasonable since it oscillates between two values. The oscillation can be explained by using the Pareto plot, Figure 4.18, which shows that the design variable thickness almost exclusively influences the mass.

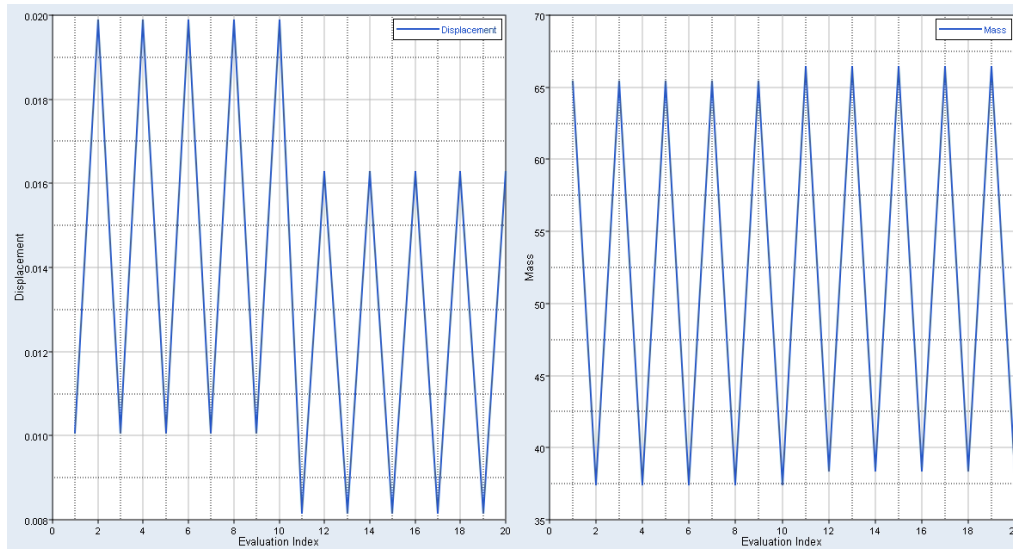


Figure 4.16: Evaluation plot. The midpoint displacement is plotted to the left and the mass to the right.

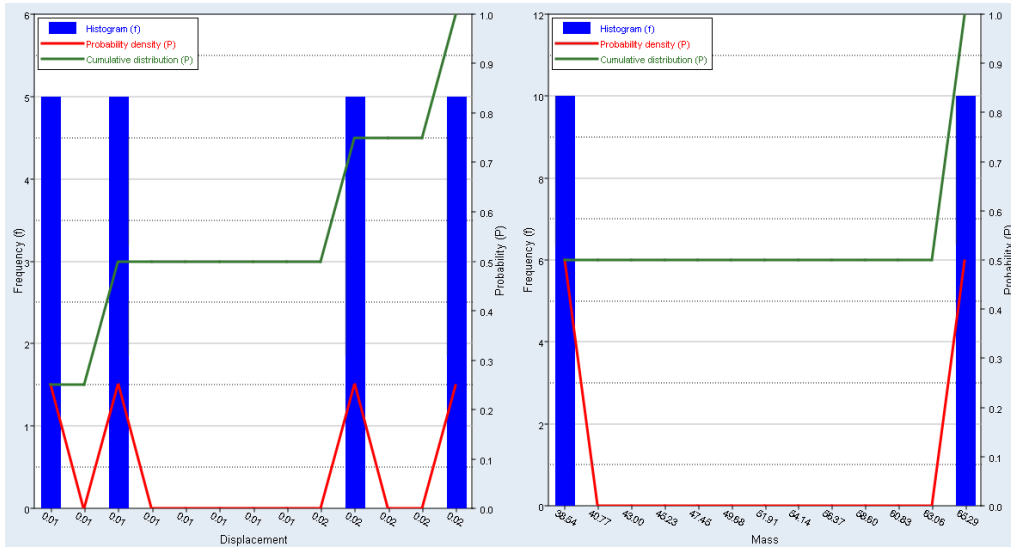


Figure 4.17: Histogram plot. The left plot visualizes the midpoint displacement and the right shows the mass. The displacement obtained four different values in the simulations and the mass obtained two.

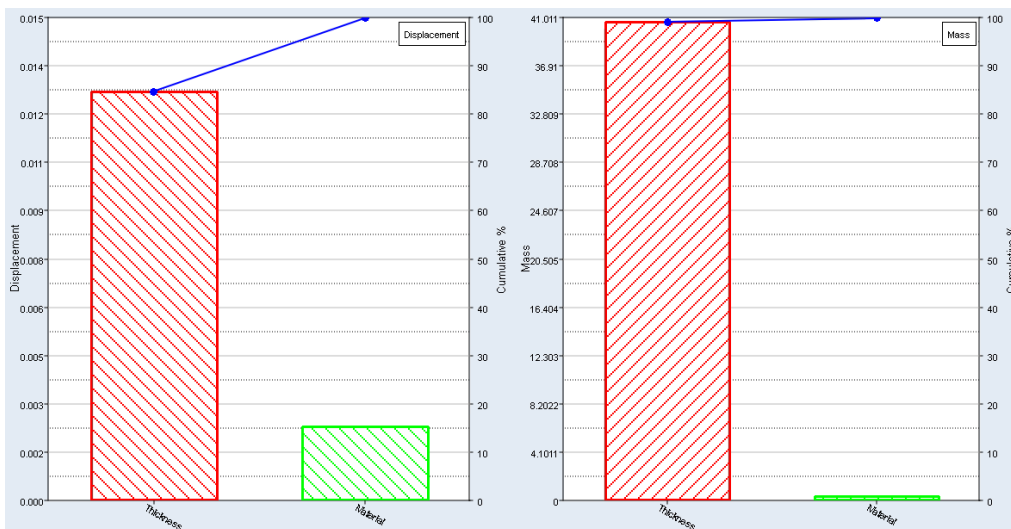


Figure 4.18: Pareto plot. The left plot shows the parameters' influence on the midpoint displacement and the right plot shows the parameters influence on the mass. The thickness had a larger influence than the material had for both cases.

4.2.3 Natural Frequency simulation

In the Evaluation plot, Figure 4.19, it is visible that the natural frequency for the first mode oscillates between values, while the midpoint displacement is reduced for each new case. In the Histogram plot, Figure 4.20, it can be seen that the natural frequencies only result in a couple of different values while the displacement has many different solutions. This can be analyzed together with the Pareto plot, Figure 4.21, which shows that the natural frequency almost exclusively is influenced by the material of the core and the midpoint displacement is almost exclusively influenced by the thickness of the skins.

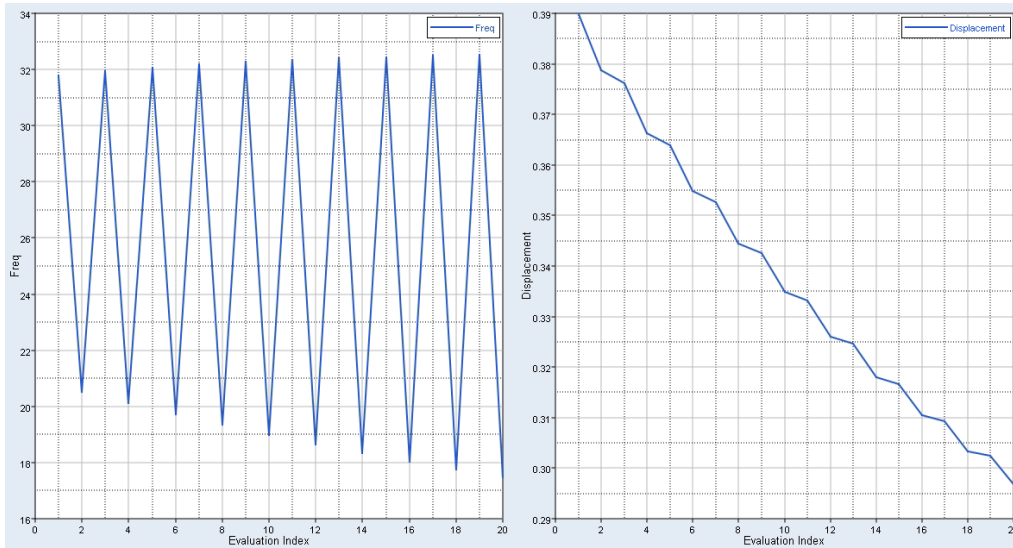


Figure 4.19: Evaluation plot. The left plot displays the natural frequencies and the right displays the midpoint displacement.

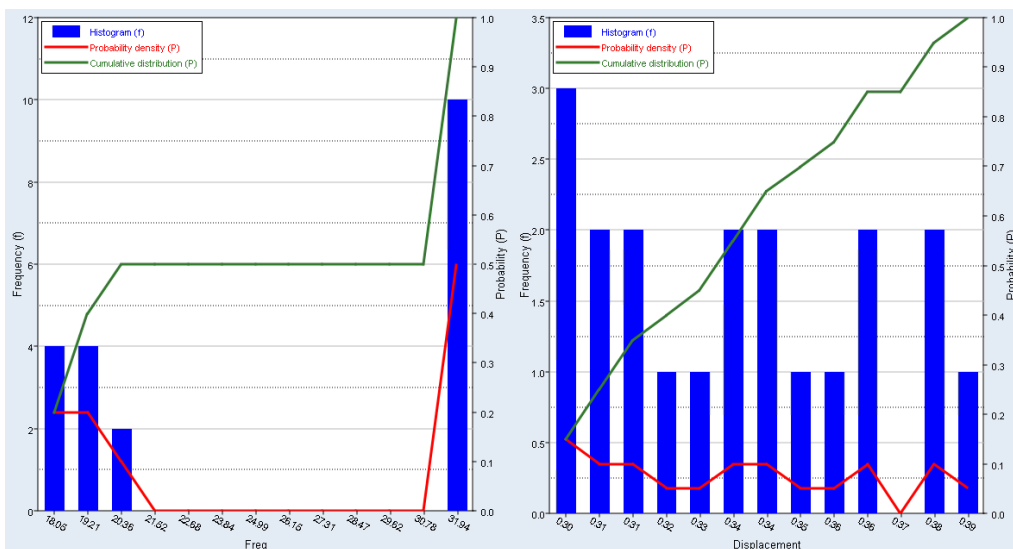


Figure 4.20: Histogram plot. The left displays the natural frequencies and the right displays the midpoint displacement.

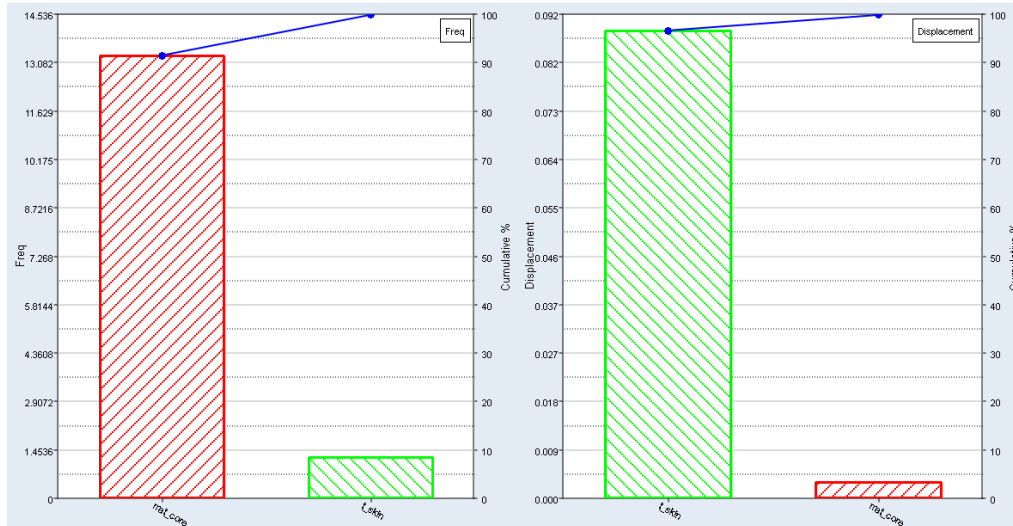


Figure 4.21: Pareto plot. The left plot displays which parameters that influenced the natural frequencies and the right displays which parameters that influenced the midpoint displacement. The design variable `mat_core` regards the core material and `t_skin` regards the thickness of the skins.

4.3 Divided sandwich structure

This case consists of a plate with sandwich structure where the skins are modelled with shell elements and the core with solid elements. This was necessary in order to be able to split the core into smaller parts, called panels. The analyzed plate had dimensions 10 m x 1 m x t , where t initially contains two skin thicknesses of 1 mm each and a core thickness of 32.5 mm.

4.3.1 Methodology

The model consisted of a sandwich structure which was made out of shell and solid elements. The goal with the case was to see how the midpoint displacement, which also was the main objective function, was affected if the core was split into smaller parts, called panels. The mesh was made fine because when splitting the core into panels, elements were deleted in order to be certain that there was a gap between the panels. If the elements were smaller, it minimized the gaps between the panels and also made the position of the gaps more accurate. Since only the core was to be split and the skins were to remain in one piece, composite elements could not be used since they were modelled as one component. Consequently, the skins were made out of shell elements and the core with solid elements, see Figure 4.22. Due to that the core was modelled with solid elements, the core material had to be defined using the material card MAT9. The values regarding the honeycomb were calculated using an excel document used at Saab and the used values can be seen in Table 4.2 and the used density was $\rho = 1400 \text{ kg/m}^2$. The split core can be seen in Figure 4.23 and the entire model can be seen in Figure 4.24. In the linear static analysis, the model had a perpendicular line force of 10 N applied in a rigid that is attached to nodes across the middle of the plate. The constraints were the same as in the previous cases, DOF 5 was not constrained on either side and only one side was constrained in DOF 1.

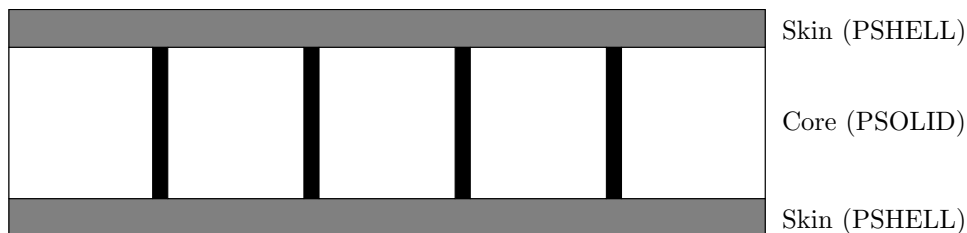


Figure 4.22: Sandwich structure with a split core

Table 4.2: The MAT9 card for Honeycomb used in the core [24]. The matrix is symmetrical.

G_{11}	G_{12}	G_{13}	G_{14}	G_{15}	G_{16}
50 MPa	50 MPa	35 MPa	0	0	0
	G_{22}	G_{23}	G_{24}	G_{25}	G_{26}
	50 MPa	35 MPa	0	0	0
		G_{33}	G_{34}	G_{35}	G_{36}
		400 MPa	0	0	0
			G_{44}	G_{45}	G_{46}
			0.6 MPa	0	0
				G_{55}	G_{56}
				20 MPa	0
					G_{66}
					30 MPa

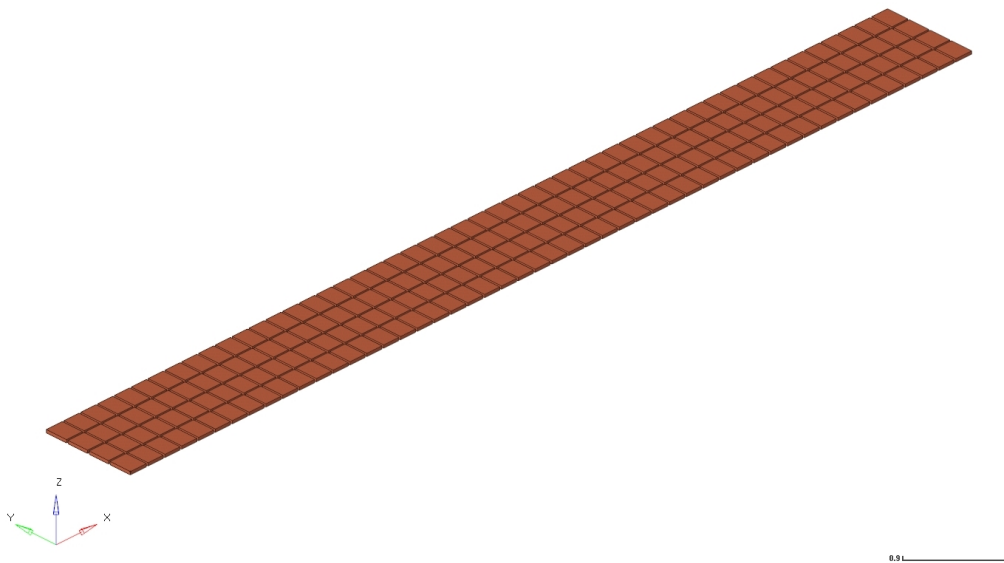


Figure 4.23: The core divided into panels. Figure shows the case in which the core is split into 50 parts in the x -direction and 4 parts in the y -direction.

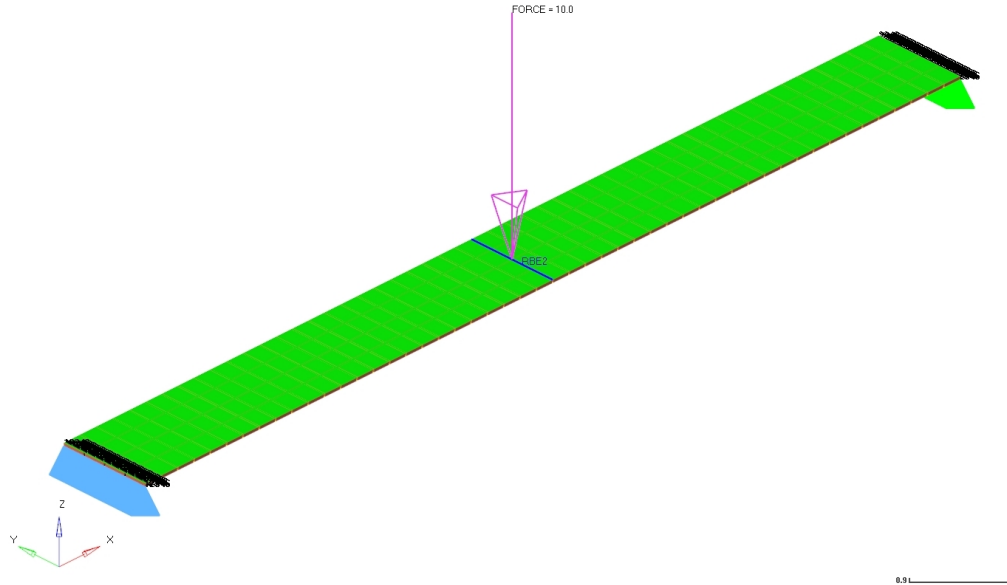


Figure 4.24: The entire model with skins, core, force and constraints. The skins were one pieces while the core was split in parts.

When the model had been created and meshed, the different cases in which the core was split into a different amount of panels were created. The core was split into a maximum of 50 parts in the x -direction of the core, so the x -direction ranged between 1 and 50 panels. The y -direction was split into 2 and 4 parts, so the number of parts ranged between 1, 2 and 4 parts in the y -direction. This resulted in 150 different cases, ranging from one whole plate to a core consisting of 50x4 panels. The applied force was put in a rigid that was connected to the middle nodes in the upper skin. This was done in order for the node number, in which the force was applied, to remain constant for all cases. This was necessary for the parameterization since it resulted in that all cases could use the same .bdf-file and only the .blk-file needed to be parameterized. The parameters regarding the thicknesses of the skins were attached to each other and parameterized between 1 mm and 2 mm. The geometry and mesh for the different cases were, thus, put into .blk-files, which were parameterized as strings in HyperStudy. The parameterization was executed by entering the names of all the .blk-files which were to be run. The execution of this can be seen in Figures 4.25, 4.26 and 4.27.

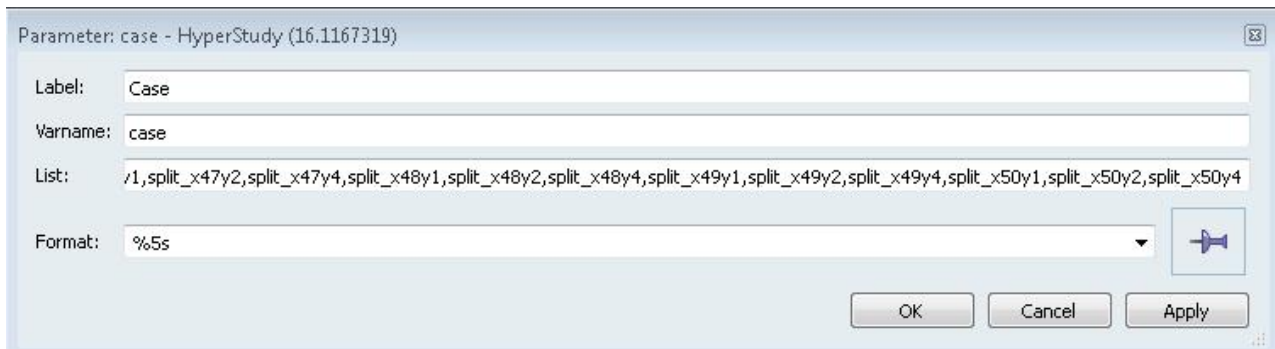


Figure 4.25: The name of the .blk-files which were to be run in the parameter. The used format means that the parameter is a string.

```

$$-----$
$$              Bulk Data Cards              $
$$-----$
INCLUDE 'd:\hej\Case 3\Hyperstudy\{templax_on}\case, %5s\{templax_off}.blk'

```

Figure 4.26: The parameterized .tpl-file, the name of the file is the parameter.

```

$$$$-----$$$$
$$$  Property Definition for Surface and Volume Elements  $$$
$$$$-----$$$$
$$$
$$$  PSHELL Data
$$$
$HMNAME PROP ..... 1 "Skin_upper" 4
$HWCOLOR PROP ..... 1 ..... 7
PSHELL ..... 1 ..... 1 ..... 0.001 ..... 1 ..... 1
$
$HMNAME PROP ..... 3 "Skin_lower" 4
$HWCOLOR PROP ..... 3 ..... 17
PSHELL ..... 3 ..... 1 ..... 0.001 ..... 1 ..... 1
$$$
$$$  PSOLID Data
$$$
$HMNAME PROP ..... 5 "Core" 5
$HWCOLOR PROP ..... 5 ..... 32
PSOLID ..... 5 ..... 4

```

Figure 4.27: Parameterization of the upper and lower skins.

4.3.2 Linear static analysis

The main objective function demanded from the simulation was to minimize the magnitude of the midpoint displacement in the x -direction. The other demanded outputs were effective von Mises stresses and strains as well as maximum shear in the core and skins. The results were checked in HyperView and were thereafter categorized in MATLAB through separating the different cases by how many times the y -axis is split. Thereafter, the results were normalized by the value obtained for the case with the whole core in order to be able to see the relative change in the results. There was a large change between the normalized results regarding the stresses and strains in both parts of the plate. The cases with equal amount of panels in the x -direction had larger stresses than the cases with an unequal amount of panels. This could be due to that the panels were split in the middle for the equal cases, which also is where the force was applied. The normalized displacements in x -direction was always larger than 1, which was reasonable since this means that the displacement becomes larger when the core is split into smaller panels.

The parameters were evaluated using the DOE method Hammersley and the number of evaluations were 327 according to the formula used to calculate this, see section 2.3.5 and Equation 2.4. The main objective function during this case was to minimize the magnitude of displacement, so these results are shown in Figures 4.28, 4.29 and 4.30. The Evaluation plot shows that the midpoint displacement oscillated between two values during the evaluations. This can also be seen in the Histogram plot, Figure 4.29, which only contain two poles, i.e., two different solutions, of around 160 evaluations each. In the Pareto plot in Figure 4.30, it can be seen that for the magnitude of the midpoint displacement, the parameter regarding thickness of the skins had a larger influence than the parameter regarding how many panels that the core was divided into. According to the normalized results, the magnitude of displacement increased with the number of panels. The plot regarding how the normalized magnitude of displacement changes when the number of panels increased can be seen in Figure 4.31. The x -axis in the plot represents how many times the core is split on the length, i.e., x -axis. The y -axis represents the change in percent compared to a whole core, i.e., the midpoint displacement obtained for the split cases were divided by the displacement obtained for the whole core. The three different lines represent how many panels the core has in the y -direction, the blue line has one, the red has two and the pink has four panels in height.

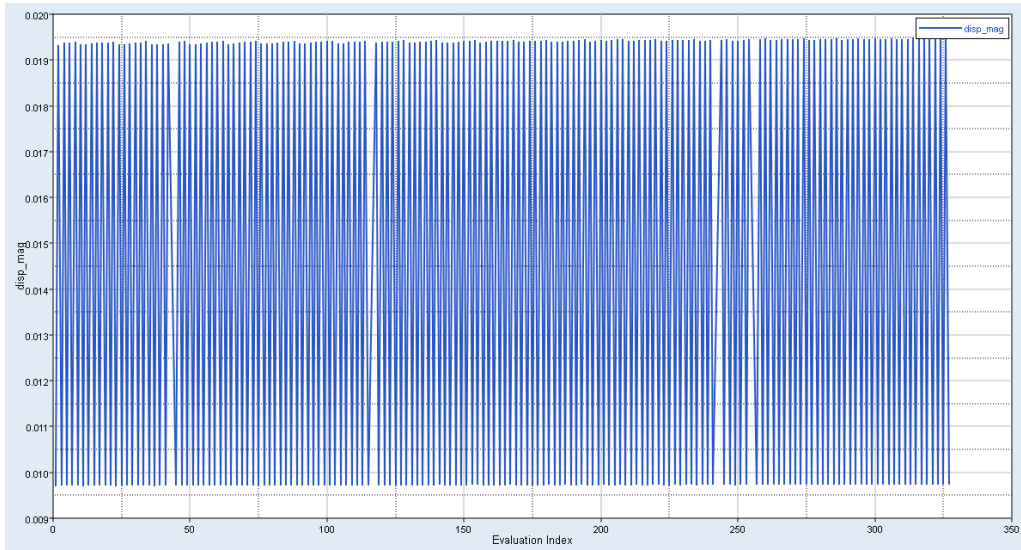


Figure 4.28: Evaluation plot for magnitude of midpoint displacement.

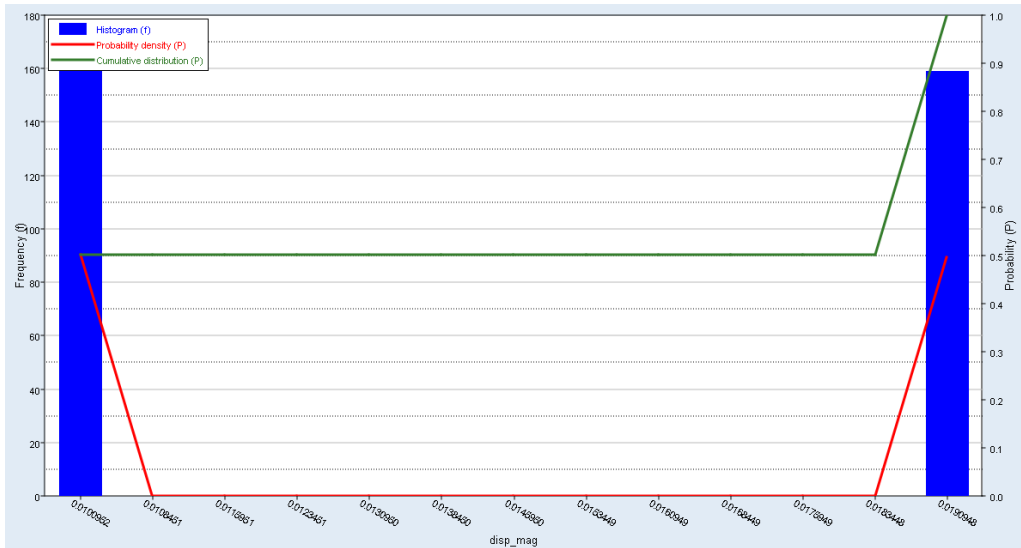


Figure 4.29: Histogram plot for magnitude of midpoint displacement.

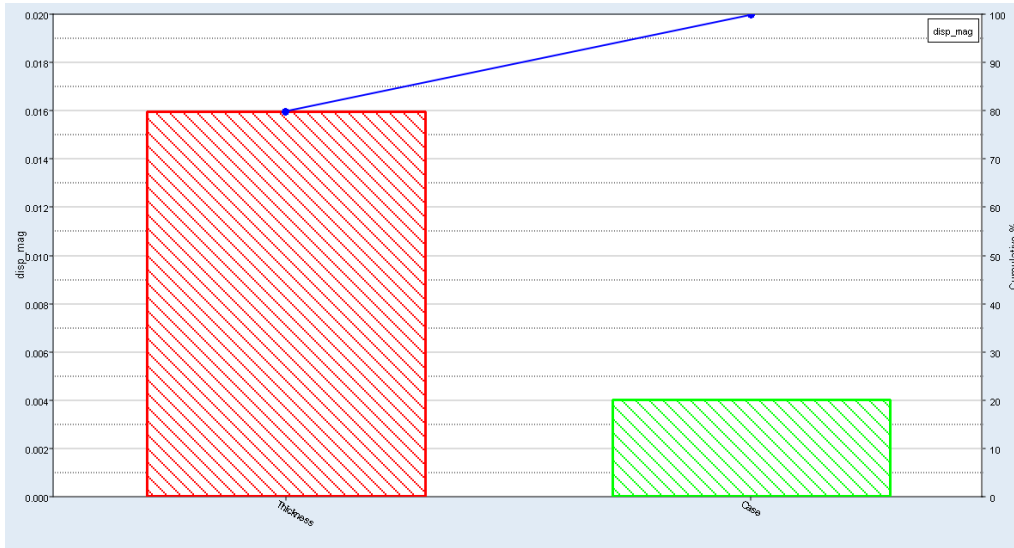


Figure 4.30: Pareto plot for magnitude of midpoint displacement.

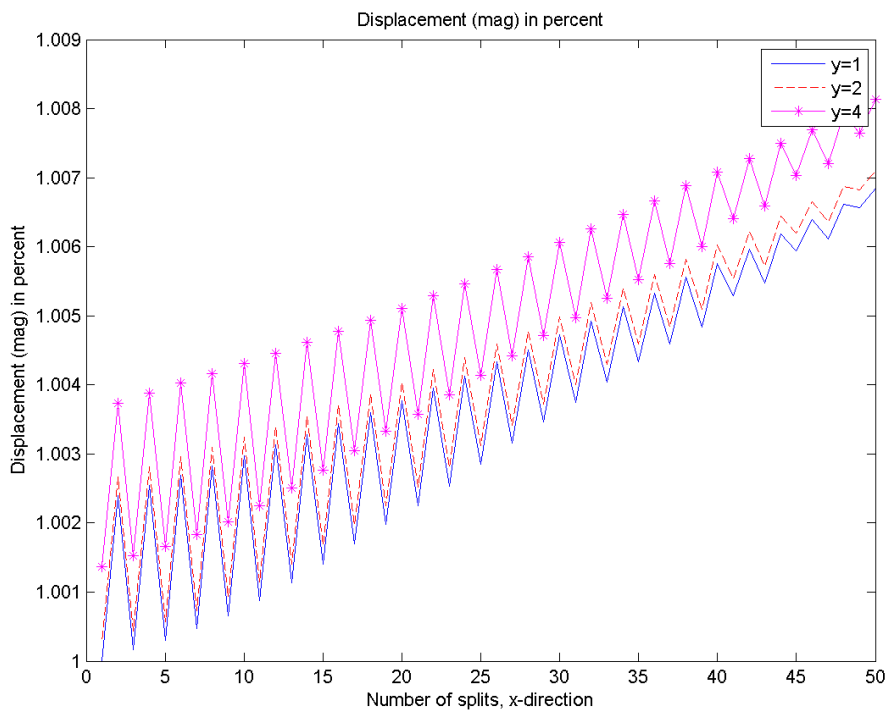


Figure 4.31: The percentage change of the magnitude of midpoint displacement.

5 Results - Authentic case

The authentic, advanced case regarded an antenna from Saab's product portfolio. It was analyzed and parameterized in order to explain how the method can be applied on an authentic, complex product. The case began with that an existing model was studied and thereafter a new simplified version of the model was created, in which the number of existing components was reduced. The simplified model was thereafter compared to the original model, in order to verify that the behavior of the simplified model resembled the behavior of the original. Thereafter, another model was created, analyzed and parameterized, and it consisted of an antenna which was twice as high as the antenna that the simplified model consisted of. The antenna was changed in order to evaluate a concept which still was in the concept evaluation phase.

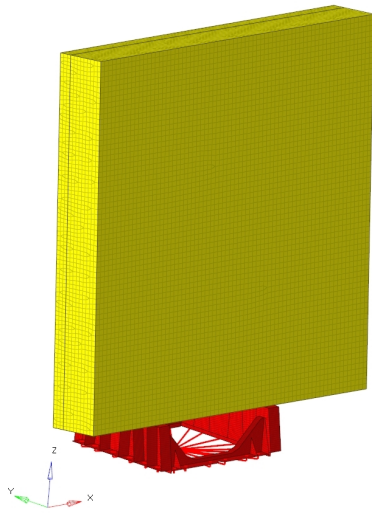
5.1 Methodology

The different steps described in this chapter are:

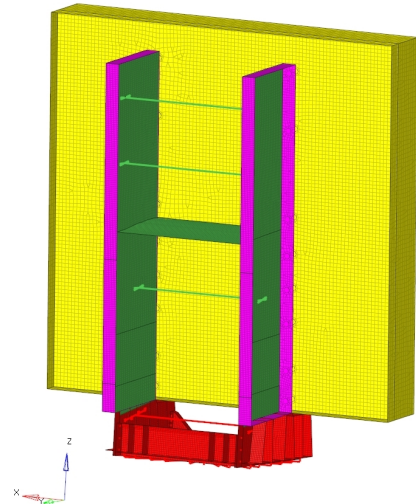
- Build FE-model - both G4 and G8 structures
This section describes how the two different FE-models were built with the ability to parameterize them later on in mind.
- Parameterize
The parameterization that was executed is described in this section, along with the values of the different parameters and why they are varied.
- Linear static analysis
An acceleration was applied in the x -, y - and z -direction, respectively. The results regarding the objective function to minimize the maximum displacement in the x -direction are presented.
- Natural frequency analysis
An analysis regarding the natural frequencies was made. The results regarding the objective function to maximize the first natural frequency are presented.

5.1.1 Build FE-model

The model was based on an original antenna from Saab's product portfolio, but it was simplified. The new, simplified model was created using shell and composite elements. The model was simplified through replacing the antenna elements, called multi packs, with an equally distributed nonstructural mass, i.e., mass that does not contribute to the stiffness, across the sandwich plate. It was added due to that the authentic model can contain a different amount of multi packs, cables and other equipment mounted on the back of the antenna. Consequently, the weight of the antenna was affected. The antenna of the simplified model, shown in Figures 5.1, had measurements 2 m x 2 m and is called G4. The yellow parts in Figure 5.1 are called antenna, the green and pink parts are called the back structure and the red part is called bottom. The bottom is the part which makes it possible to mount the radar on a, for example, a vehicle or a boat. The antenna and back structure were tilted 5° around the x -axis, see Figures 5.2a and 5.2b. The original case consisted of different types of plates between the back structure and they were all replaced with beams. The original model also contained a plate between the support structure and consequently, a plate was added to the simplified model.

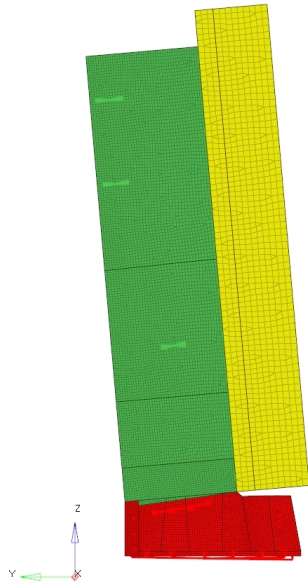


(a) Antenna G4 from the front.

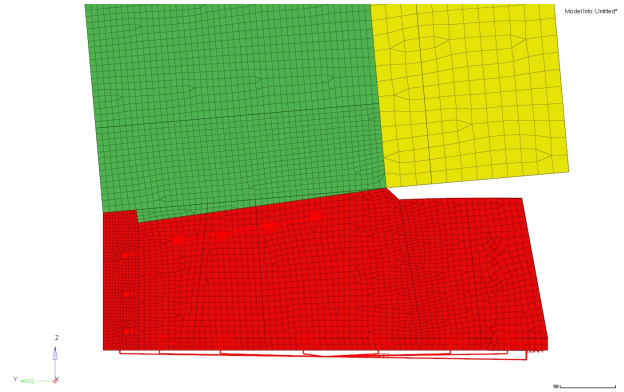


(b) Antenna G4 from the back.

Figure 5.1: Simplified G4 model. The yellow parts are the antenna, the green and pink parts are the back structure and the red part is the bottom.



(a) The antenna and back structure were tilted 5° backwards around the x -axis.



(b) The antenna and back structure were tilted 5° . Figure displays how the transition from the tilted part to the bottom is modelled.

Figure 5.2: The antenna and back structure were tilted 5°

The natural frequencies obtained from the original and simplified cases were compared by dividing the results from the simplified model by the results from the original model for each mode. This was done in order to get a relative difference regarding how much the natural frequencies change when the model was simplified. The change in percentage between the natural frequencies of the two models can be seen in Table 5.1. The mode shapes were checked in order to be certain that the behaviour of the models resembled each other, even though one model was simplified. The modal shapes for the first three modes of the simplified model can be seen in Figures 5.3, 5.4 and 5.5. In the first mode, Figure 5.3, the back support twists around the z -axis. Consequently, the antenna moves as well, although the main movement comes from the back supports. The second mode, Figure 5.4 rotates back and forth around the x -axis. The third mode, Figure 5.5, is also a rotation around the

z -axis, although in this case, the main movement comes from the antenna.

Table 5.1: Percentage change of natural frequencies between the original and simplified model.

Mode	Percentage change [%]
Mode 1	-10.63
Mode 2	-0.90
Mode 3	-5.15

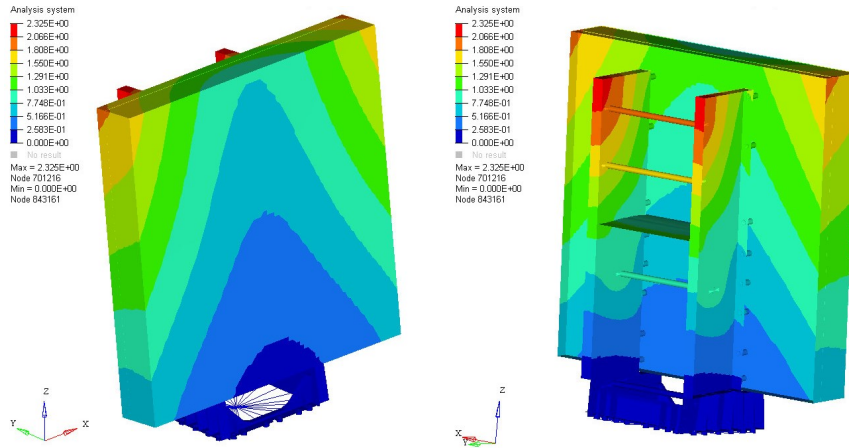


Figure 5.3: The first mode shape of the simplified model. The scale regards normalized displacement and ranges from the blue = 0 to red = 2.325.

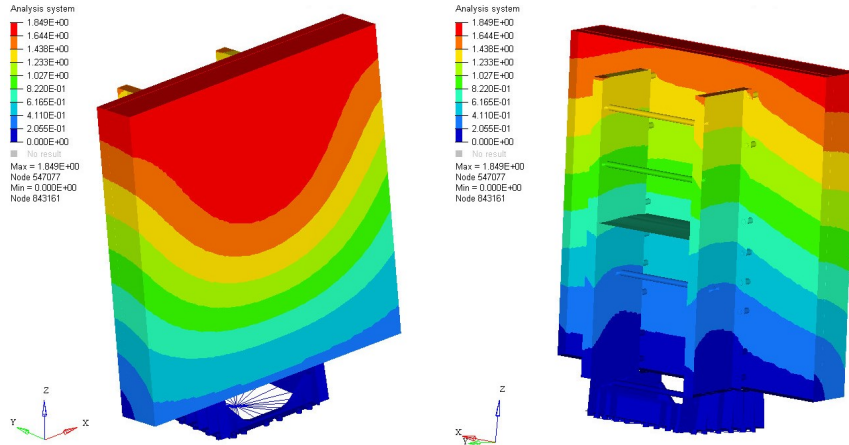


Figure 5.4: The second mode shape of the simplified model. The scale regards normalized displacement magnitude and ranges from the blue = 0 to the red = 1.849.

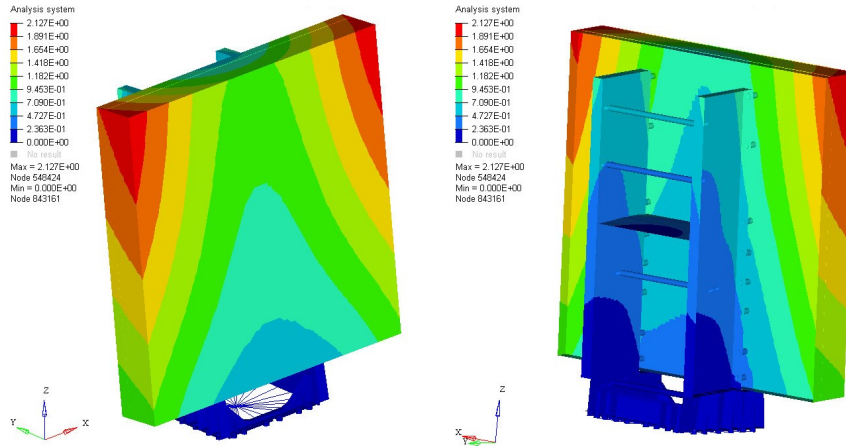
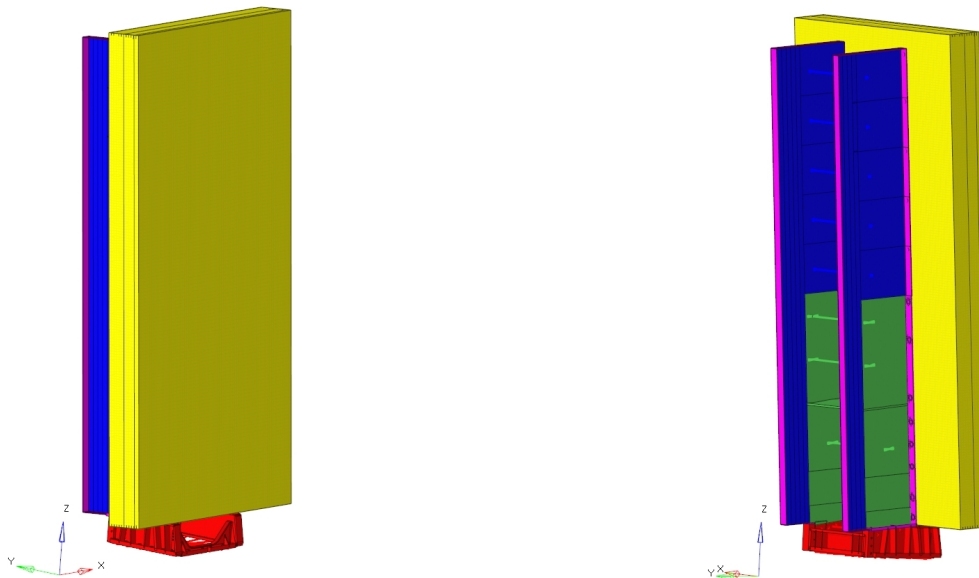


Figure 5.5: The third mode shape of the simplified model. The scale regards normalized displacement magnitude and ranges from the blue = 0 to red = 2.127.

After the simplified and original model were compared to each other and the results were assumed to be acceptable, the simplified model was used to build a new model called G8, see Figures in 5.6. The antenna on the new model was made twice as high as the antenna from the simplified case, i.e., the height measured to 4 m instead of 2 m. The width of the antenna remained constant with 2 m. The new model was analyzed and parameterized with regard to how much the original back structure had to extend in order to have acceptable results from a structural analysis point of view. Consequently, the main objective function in the analysis was to minimize the maximum displacement. In Figure 5.6, the original back structure is green and the extended back structure is blue. The height and width were modelled as different parts, called panels, so it would be possible to vary the heights and widths of the back structure during the optimization.



(a) The G8 model from the front. The parts are the same as in the G4 antenna.

(b) The back structure divided into different parts in the G8. The green part in the back structure is from the G4 case and the blue parts are the height and width plates which were parameterized.

Figure 5.6: G8 model from the front and back.

5.1.2 Parameterization

For the parameterization, the back structure was divided into eleven different cases. The first one consisted of the back structure from the simplified G4 case, i.e., only the green parts in Figure 5.6. The remaining cases consisted of five cases where the height varied and five cases where the width varied. When changing the back structure, it was only extended in one direction at a time. Thus, when the height varied, the width was constant with the smallest width possible, i.e., as wide as the back structure was in the simplified G4 case. When the width varied, the height was constant and at its maximum. All parameters and their values can be seen in Table 5.2 and the parameters regarding the width and height of the back structure were divided into two different parts. This was done in order to ease the understanding of which cases that varied in height and which that varied in width. Although, they were all included in the same design variable in the DOE and it was called “Case”. When the parameters were imported into HyperStudy, it calculated that 105 evaluations were needed to be executed by using Equation 2.4. That HyperStudy calculated that 105 evaluations were needed means that 105 different cases were created since consequently, each evaluation was a new case. The other parameters that were parameterized can be seen in the list below. Their different values which were used in the simulations can be seen in Table 5.2, along with the type of the parameter, i.e., if the parameter was a real or a discrete value or a string.

- Nonstructural mass

The parameter nonstructural mass changed between three different discrete values which represent the mass of the multi packs, cables and other equipment which, in reality, were mounted on the antenna. By adding nonstructural mass, the model could be simplified while still taking the weight of the different equipment into consideration. The nonstructural mass that was added can be seen in Table 5.2 and it was also shown how the different values affected the mass of the sandwich plate. The sandwich plate is pointed at in Figure 5.8. As mentioned before, the nonstructural mass was a parameter due to that the antenna could, in reality, contain different amount of multi packs, cables and other equipment. Since these were removed in the simplified model, they were replaced with an equally distributed mass across the sandwich plate instead. Although, the mass did not contribute to any stiffness, but it showed how the antenna behaved at different weights.

- Core material in sandwich plate

The core material used in the sandwich plate varied between three different materials. They were aluminum honeycomb, composite honeycomb and Rohacell. The material properties for these materials can be found in section 2.5.1. The core material was chosen as a parameter since it was still uncertain which core material that was the most beneficial to use for this case. The method then showed which material that contributed to the best solution with regard to the objective function.

- Material of back structure

The material of the back structure, i.e., the blue and pink parts in Figure 5.6, were parameterized. The material varied between steel and aluminium, see Table 5.2, since these were the two most relevant materials. The material of the back structure was a parameter in order to see how much the material of the back structure affects objective functions, i.e., to minimize the maximum displacement and to maximize the first natural frequency of the antenna.

- Thickness BackWidth

Thickness BackWidth can be seen in Figure 5.10a. The thickness of the shell elements were varied in order to see how much the support structure could reduce the maximum displacement, which was the objective function for the linear static analysis.

- Thickness BackHeight

Thickness BackHeight can be seen in Figure 5.10b. The thickness of the elements were varied along the back structure. It was investigated to see how the thickness of the back structure affected the maximum displacement of the antenna, which was one of the main objective functions.

Table 5.2: The parameters which were parameterized in the G8 model.

Parameter	Values	Type of parameter
Nonstructural mass (represents the mass of the multi packs, cables and other equipment which are mounted on the antenna)	204.2 kg/m ² = 1800 kg (weight of sandwich plate) 224.2 kg/m ² = 1975 kg (weight of sandwich plate) 254.2 kg/m ² = 2213 kg (weight of sandwich plate)	String - Categorical
Core Material in sandwich plate	Aluminium honeycomb, Composite honeycomb and Rohacell	Real - Discrete
Material of back structure	Steel and Aluminium	Real - Discrete
Thickness BackWidth	5-10 mm, with 7.5 mm as nominal value	Real - Continuous
Thickness BackHeight	5-10 mm, with 7.5 mm as nominal value	Real - Continuous
Support structure height	z0y0 : Height = 1850 mm, Width = 475 mm z1y0 : Height = 2250 mm, Width = 475 mm z2y0 : Height = 2650 mm, Width = 475 mm z3y0 : Height = 3050 mm, Width = 475 mm z4y0 : Height = 3450 mm, Width = 475 mm z5y0 : Height = 3850 mm, Width = 475 mm	String - Categorical
Support structure width	z5y1 : Height = 3850 mm, Width = 520 mm z5y2 : Height = 3850 mm, Width = 565 mm z5y3 : Height = 3850 mm, Width = 610 mm z5y4 : Height = 3850 mm, Width = 655 mm z5y5 : Height = 3850 mm, Width = 700 mm	String - Categorical

In Figure 5.7a the different panels are shown, along with the width of the back structure. The blue areas were new for this case and the gray was the original back structure of the antenna, i.e., the back structure from the simplified G4 model. So the blue panels were added one by one and the gray part remained constant. In Figure 5.7b, the different widths used in the parameterization can be seen. As in the height case, the blue panels were the ones which were added on one by one and the gray was constant. The bottom structure, seen in red, did not change between the different cases. Figure 5.8 shows that the yellow part is the sandwich material which had a varying, equally distributed nonstructural mass and core material.

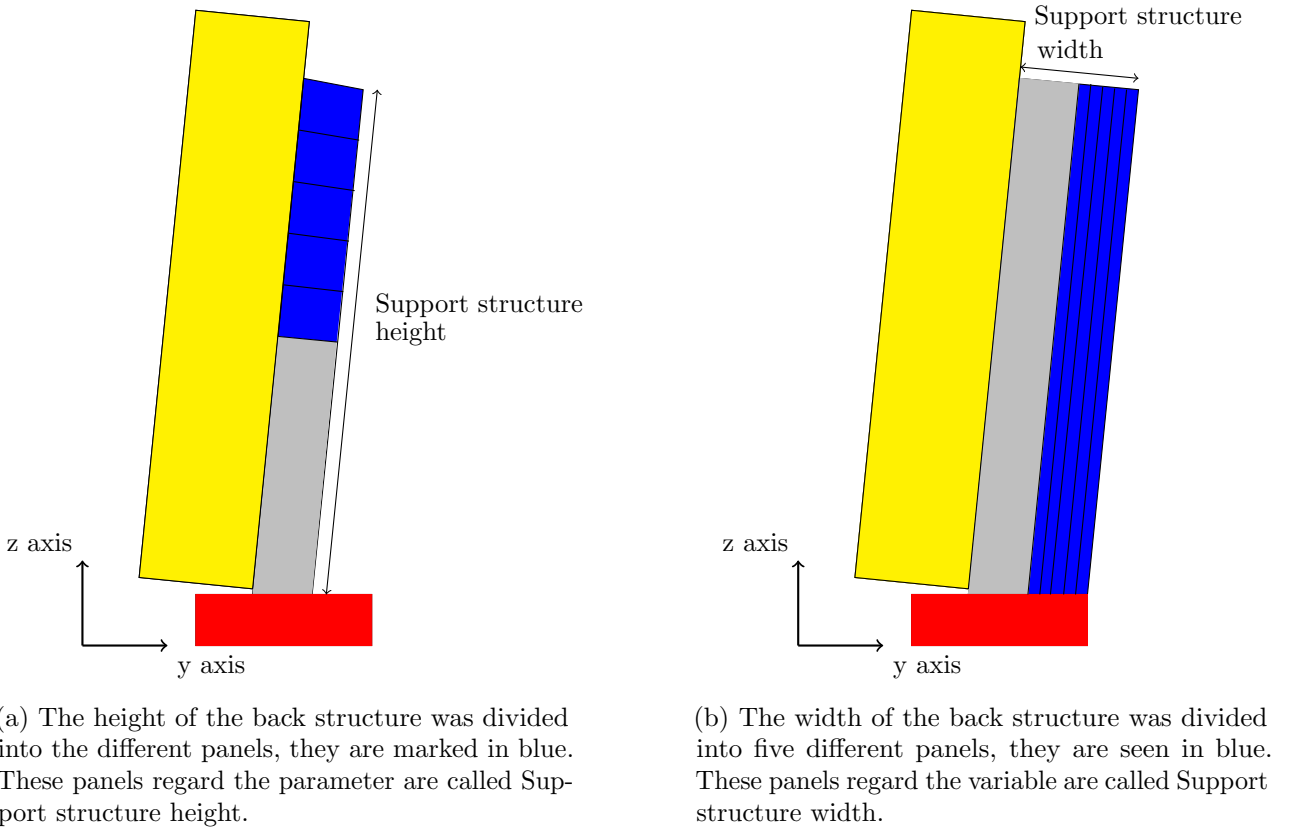


Figure 5.7: The parameters regarding the back structure. The blue panels were the support structure height and support structure width parameters. The red box was the bottom structure and the gray parts are constant for the two different cases.

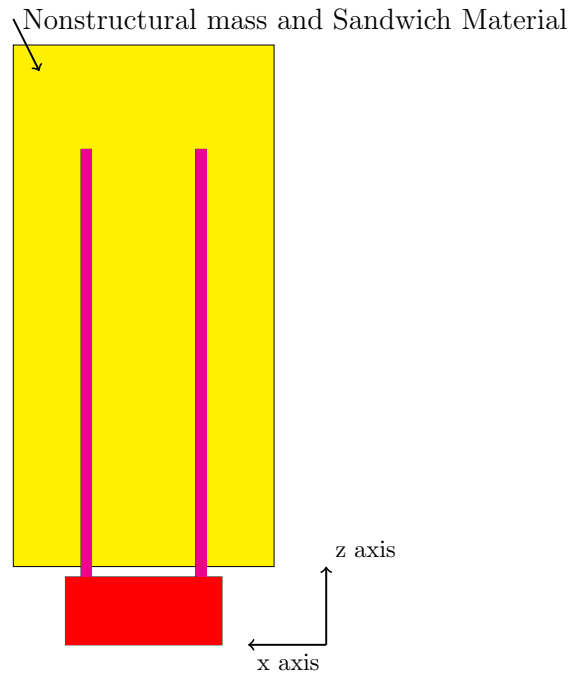


Figure 5.8: Back of the antenna. The yellow part represents the sandwich plate which is where the equally distributed nonstructural mass was applied and where the core material was changed. The red part was the bottom structure which did not change from the simple case.

The parameters called BackHeight and BackWidth are explained in Figures 5.9, 5.10a, 5.10b and 5.11. The blue part is the entire back structure and the pink parts are the supports which surround the back support.

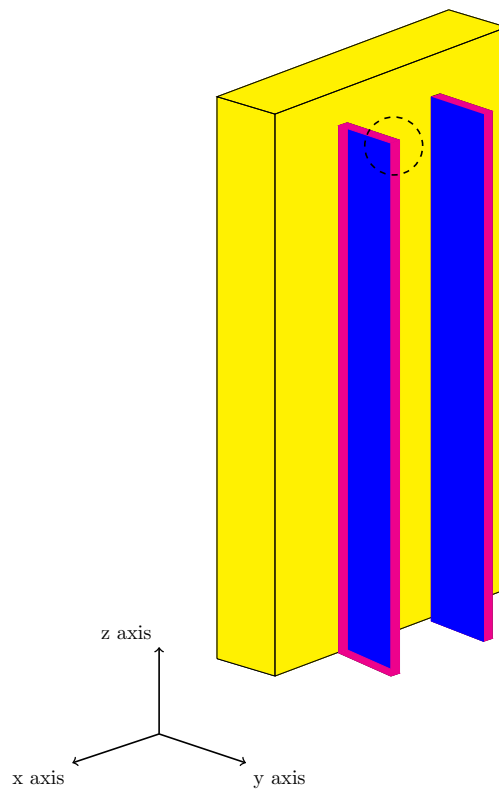
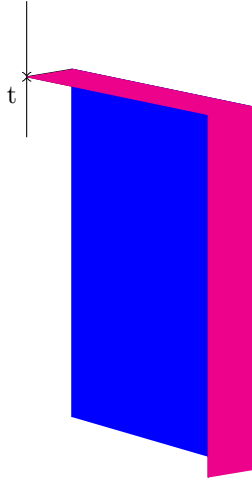
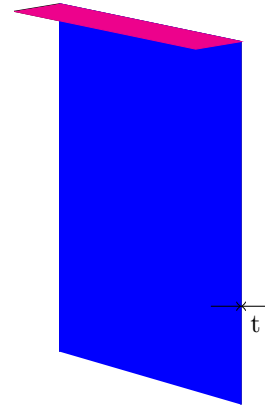


Figure 5.9: G8 model. The black circle shows where Figures 5.10a and 5.10b are zoomed.



(a) Zoomed view from Figure 5.9, the variable Thickness BackWidth is marked with a t .



(b) Zoomed view from Figure 5.9, the variable Thickness BackHeight is marked with a t . The Support Structure in front of the plate was removed in order for the BackHeight plate to be visible.

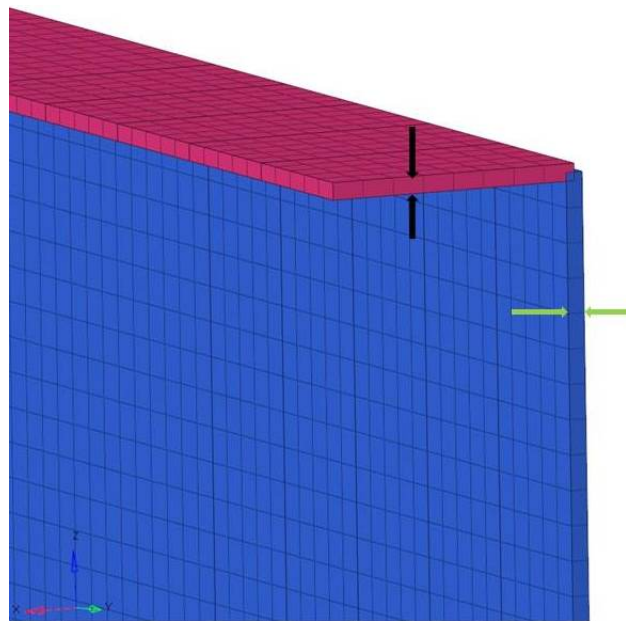


Figure 5.11: The marked area in Figure 5.9 was zoomed in the HyperMesh model for visualization. The Support Structure in the front was removed in order to see the parameter Thickness BackHeight. Thickness BackHeight is marked with green arrows and Thickness BackWidth is marked with black arrows.

5.2 Linear static analysis

The DOE used for this case was the Hammersley and it was, as mentioned before, evaluated 105 times. The number of evaluations was calculated by HyperStudy using Equation 2.4. The load case for the linear static analysis consisted of an acceleration of 9820 mm/s^2 , applied in x -, y - and z -direction, respectively. The main objective function was to minimize the maximum displacement for all three cases of acceleration. Other outputs that were demanded from the simulations were:

- Axial force in screws that attach the antenna to the back structure.

- Shear stress in screws, calculated as $\sqrt{Shear1^2 + Shear2^2}$ due to that, in HyperStudy, the shear stresses were defined as components in the screws local coordinate system. In order to get the resulting shear stress, they were calculated using the mentioned formula. The screws attach the antenna to the back structure.
- Composite Stress 2D, von Mises in plies 1,2 and 3 individually. Plies are referring to the different layers of the sandwich, so in this case the composite contains three plies, two skins and one core.
- Stress 2D, von Mises (in components z_1 and z_2 , which have different directions in the coordinate system.)

The main objective function regarding this case was to minimize the maximum displacement and here, the displacement in the x -direction was chosen. Thus, the Evaluation, Histogram and Pareto plot all show the results for displacement in x -direction. The Evaluation plot, Figure 5.12, shows that the smallest displacement was obtained in evaluation 15 and it had the value $\delta = 3.625$ mm. The parameter values which were used for evaluation 15 and thereby obtained the smallest displacement can be seen in Table 5.3. The Histogram plot, Figure 5.13, shows that the output values obtained different results in the range 3.90 mm to 10.52 mm. The Pareto plot, Figure 5.14, shows that the parameter called “Case” was the parameter that had the largest influence on the maximum displacement in the x -direction. The second and third most influential parameters were the core material of the sandwich and nonstructural mass, respectively. In Appendix A.1, the Evaluation, Histogram and Pareto plots for all the other demanded outputs can be found.

Table 5.3: The design variables and the used values for evaluation 15, which obtained the smallest displacement.

Parameter	Values
Nonstructural mass	204.2 kg/m ²
Core material in sandwich plate	Aluminum honeycomb
Material of back structure	Steel
Thickness BackWidth	5.60 mm
Thickness BackHeight	9.69 mm
Case	z1y0 - one height panel and original width.

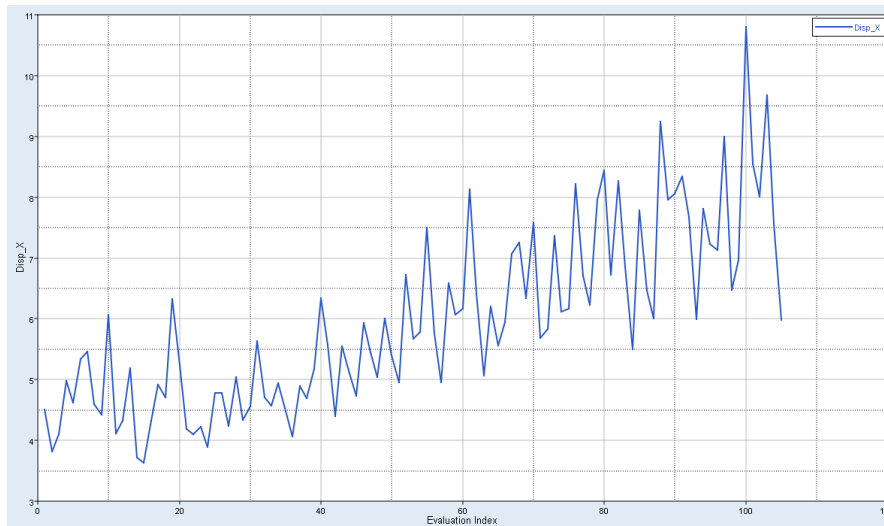


Figure 5.12: Evaluation plot presenting maximum displacement in the x -direction. Figure shows that the maximum displacement in x -direction is smallest at evaluation 15.

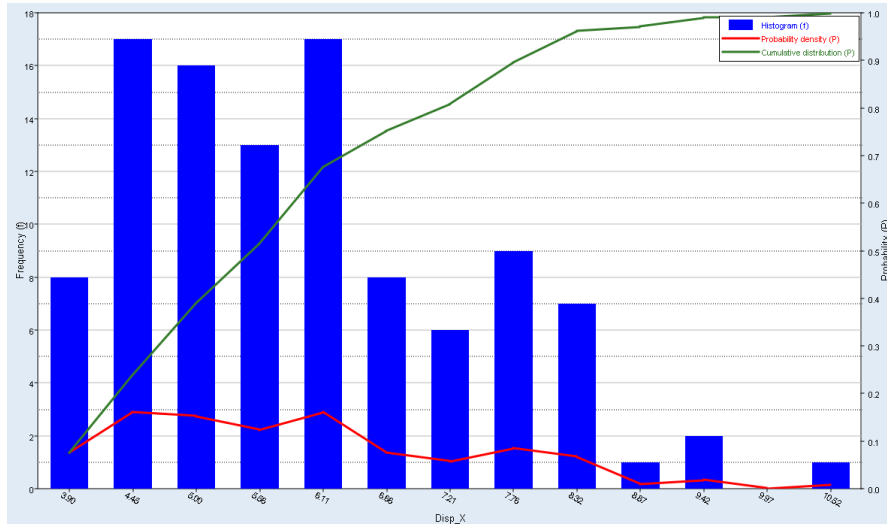


Figure 5.13: Histogram plot presenting maximum displacement in x -direction. Figure shows that the range that the maximum displacement has is between 3.90 mm and 10.52 mm. Most simulations end up with a maximum displacement between 4.45 mm and 6.11 mm, with a majority at 6.11 mm.

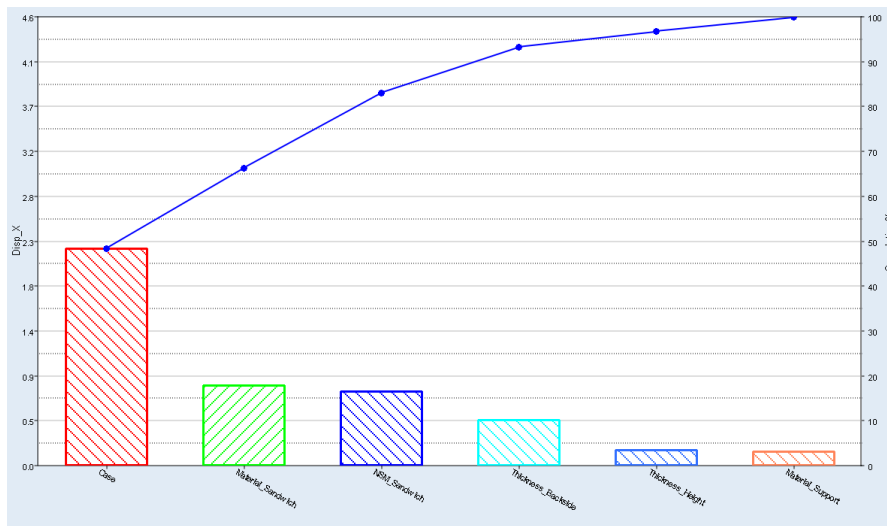


Figure 5.14: Pareto plot displays which parameter that influences the solution regarding the maximum displacement in x -direction the most. In this case, it is clear that the parameter “Case” influences the most with around 48%. Consequently, the sandwich material and nonstructural mass affect second and third most with 18% and 16%, respectively.

The main objective function, i.e., to minimize the maximum displacement in the x -direction, that was obtained from the 15th simulation was visualised in HyperView and the result can be seen in Figure 5.15. The case shown in the figure had an applied acceleration of 9820 mm/s² in the x -direction and it visualized the maximum displacement in x . The displacement is scaled with a factor of 200 in Figure 5.16 in order to clearly visualize the deformation.

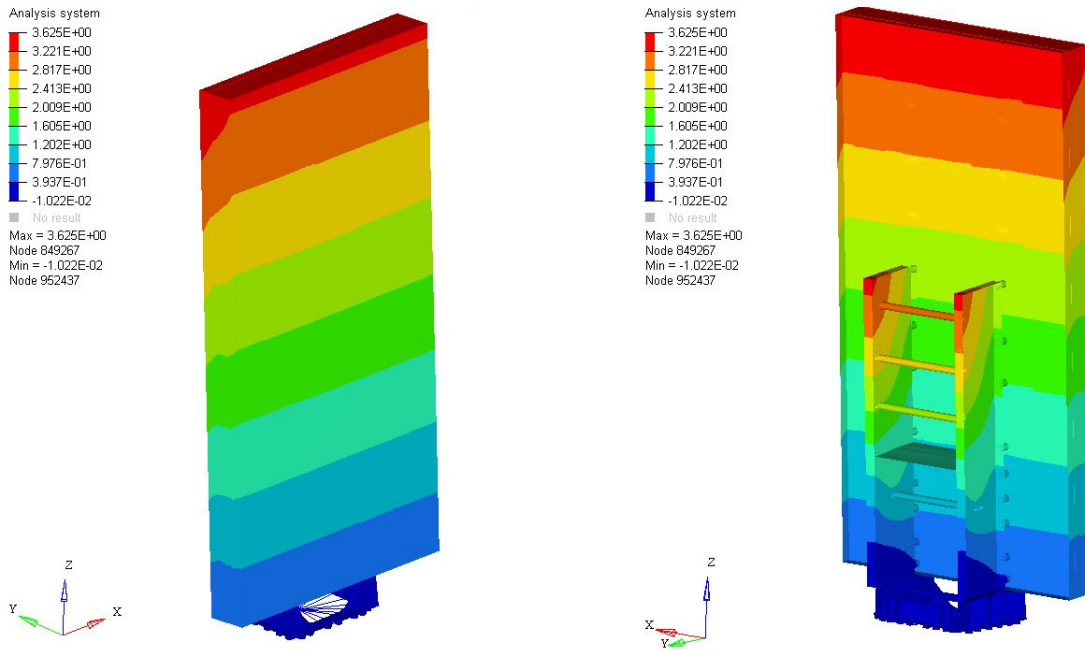


Figure 5.15: Displacement in x -direction. The scale ranges from blue = -0.0122 mm to red = 3.625 mm.

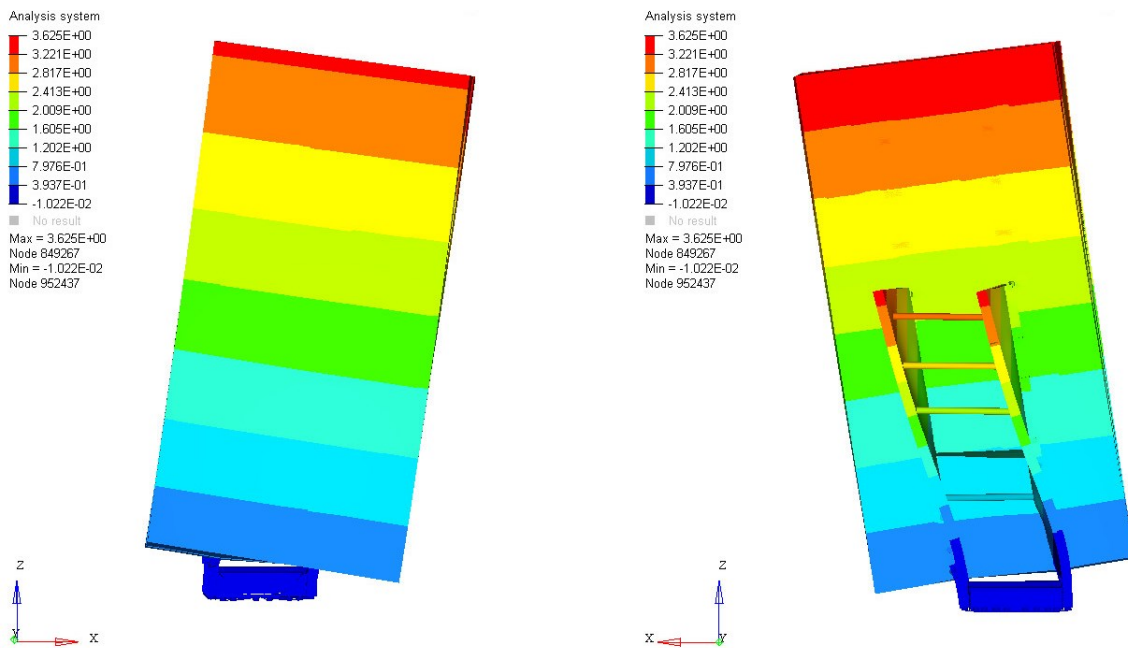


Figure 5.16: The displacement in x -direction is scaled with a scale factor of 200 for visualization. The scale ranges from blue = -0.0122 mm to red = 3.625 mm.

5.3 Natural Frequency analysis

A natural frequency analysis was done in order to find the first five symmetrical natural frequencies of the model. The simulation was executed by using Hammersley DOE consisting of 105 evaluations. The main objective function was to maximize the first natural frequency with symmetrical mode. Thus, the Evaluation, Histogram and Pareto plot all show the results for the natural frequency of the first mode. The Evaluation plot, Figure 5.17 shows that the largest first natural frequency was obtained from evaluation 36 with 9.34

Hz. Although, the results obtained from both evaluation 36 and 35, which were the evaluations with the two largest first natural frequencies, have unsymmetrical modes for the first and second frequencies. Due to the objective function being to find the first natural frequencies with the largest symmetrical modes, the results from the case with the third largest natural frequencies were analyzed instead. Although, the five first modes for evaluation 35 and 36 are shown in Appendix A.2. The third largest natural frequency was obtained in the 56th evaluation and had a first natural frequency of 8.94 Hz. The Histogram plot, Figure 5.18 shows that the output values obtain different results in the range from 1.78 Hz to 9.03 Hz. The Pareto plot, Figure 5.19, shows that the parameter called “Case” was the parameter that had the largest influence on the objective function, i.e., the first natural frequency in the first mode. The parameters that affect the solution second and third most were the core materials in the sandwich and nonstructural mass, respectively.

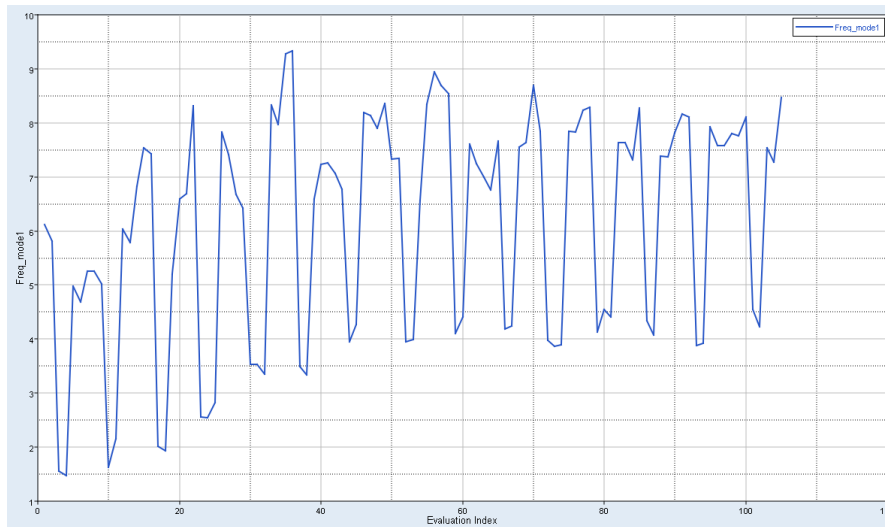


Figure 5.17: Evaluation plot presenting the natural frequencies for the first mode. It shows that the three largest frequencies were obtained from evaluation 36, 35 and 56.

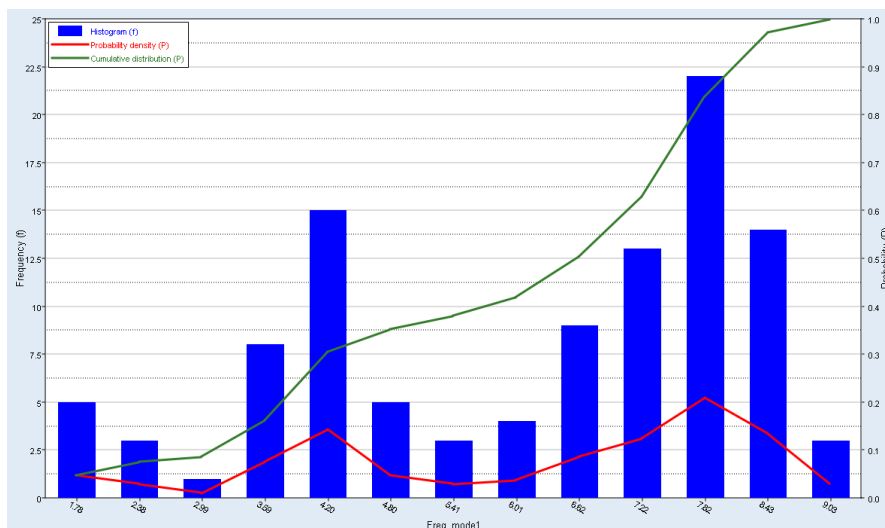


Figure 5.18: Histogram plot presenting the natural frequencies in the first mode. It shows that the range of the frequencies in the first mode was between 1.78 Hz and 9.03 Hz. Most simulations end up at a frequency between 7.22 Hz and 8.43 Hz, with a majority at 7.82 Hz.

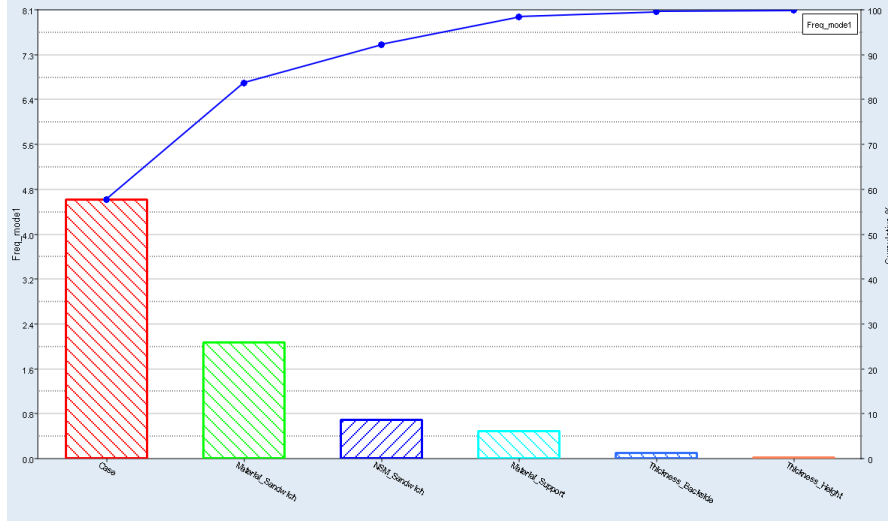


Figure 5.19: Pareto plot displaying which parameter that influences the solution regarding the natural frequencies at the first mode the most. In this case, it is clear that the parameter “Case” influences the most with around 58%. Consequently, the sandwich material and nonstructural mass affects second and third most with 26% and 8%, respectively.

The values of the design variables used during the simulation that obtained the largest first frequency, which was the 56th evaluation, can be seen in Table 5.4. The five first modes for the first frequency simulation can be seen in Figures 5.20, 5.21, 5.22, 5.23 and 5.24. When comparing the three first modal shapes in the G4 case, Figures 5.3, 5.4 and 5.5 to the three first modes for the G8 case, Figures 5.20, 5.21 and 5.22, they were similar. The conclusion from this was that the model behaved similarly for both the G4 and G8 cases, even though the antenna on the G8 was extended to be twice as high. The three first modes were, like the G4 case, a rotation around the z -axis, a rotation around the x -axis and a rotation around the z -axis, respectively. In the fourth mode, Figure 5.23, the back structure moves back and forth along the x -axis and for the fifth mode, the antenna flexes back and forth in the y -direction. The mode shapes were normalized by mass normalization in Nastran in order for the eigenvector to result in a unit value of generalized mass, i.e., the modal mass is 1.

Table 5.4: The parameters and the obtained values at the 56th simulation.

Parameter	Values
Nonstructural mass	204.2 kg/m ²
Core material in sandwich plate	Aluminium honeycomb
Material of back structure	Steel
Thickness BackWidth	5.547 mm
Thickness BackHeight	8.457 mm
Case	z5y0 - Five height panels and original width.

Table 5.5: The five first natural frequencies obtained from the 56th simulation.

Mode	Frequency [Hz]
1	8.949
2	9.315
3	14.07
4	20.78
5	22.79

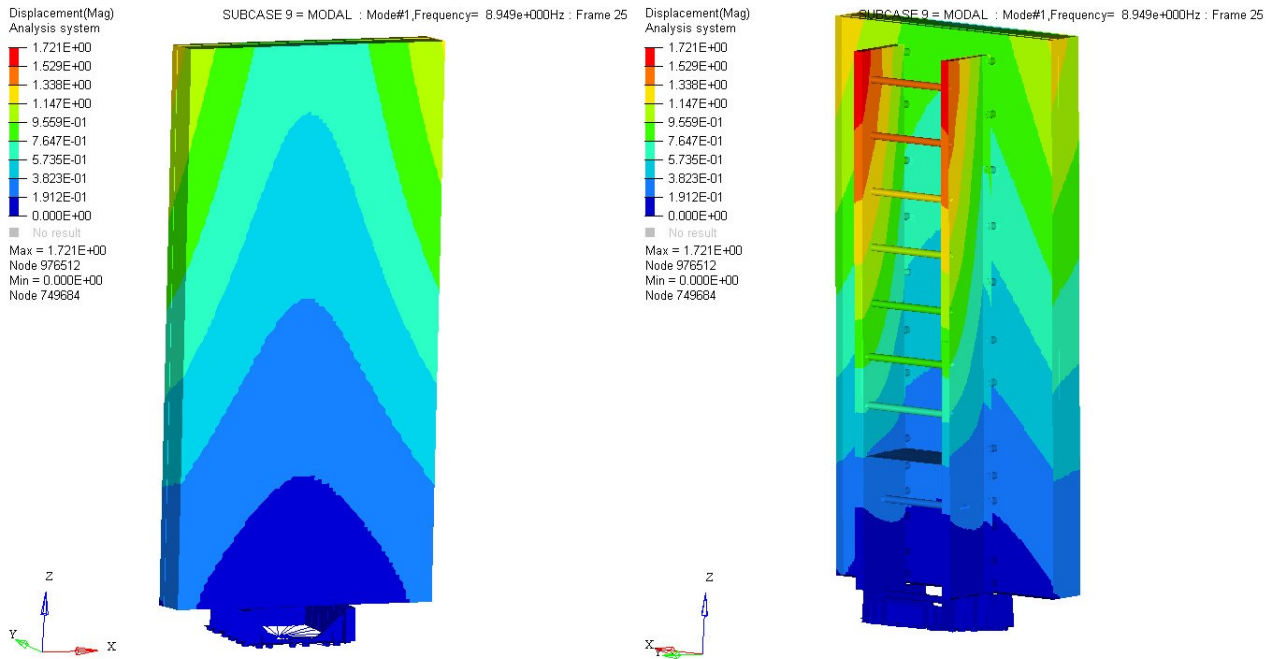


Figure 5.20: Mode 1, with frequency = 8.949 Hz. The scale ranges from blue = 0 to red = 1.721.

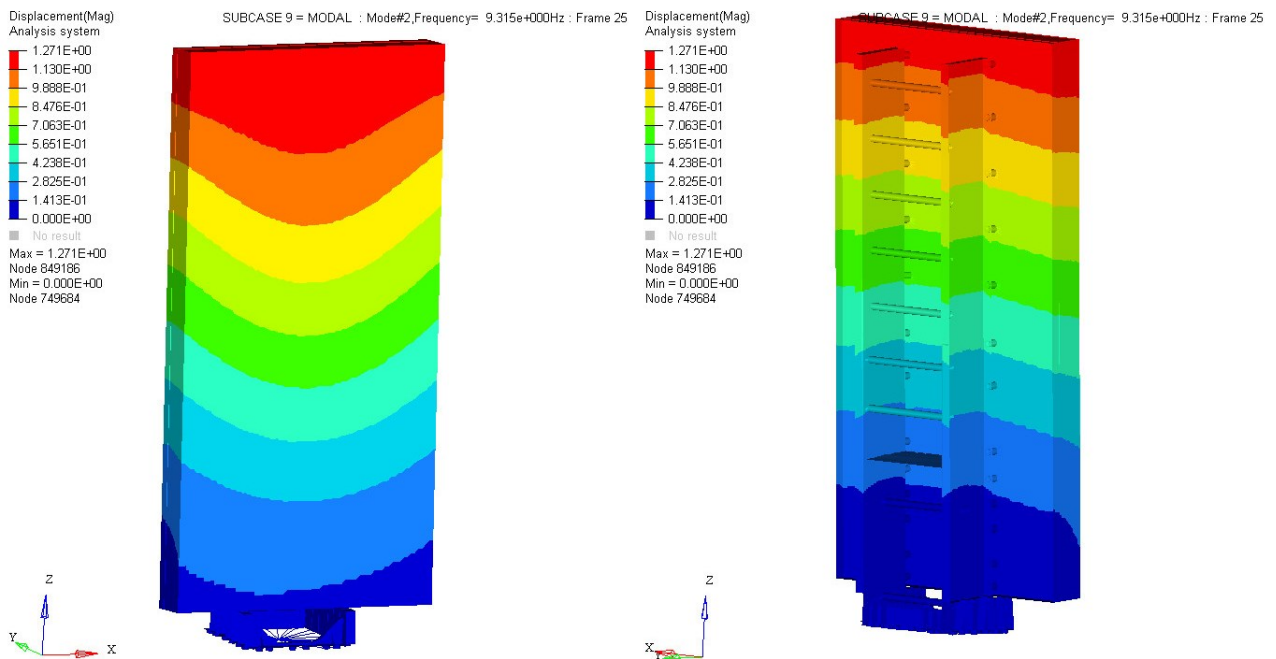


Figure 5.21: Mode 2, with frequency = 9.315 Hz. The scale ranges from blue = 0 to red = 1.271.

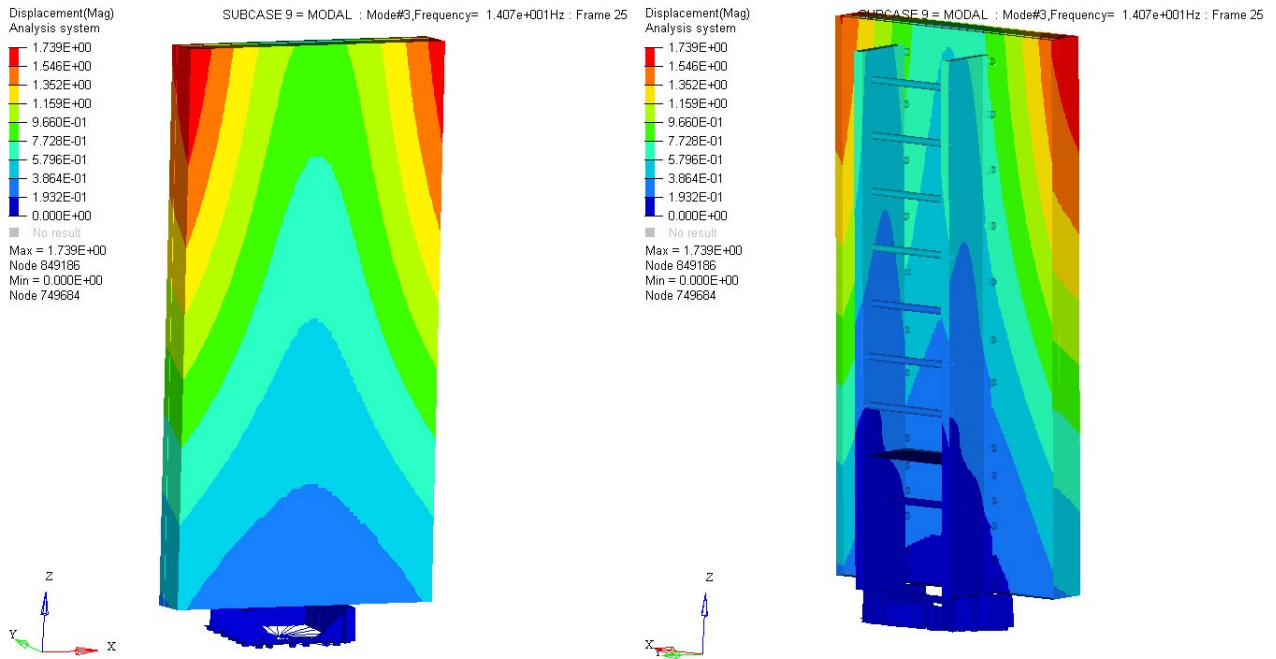


Figure 5.22: Mode 3, with frequency = 14.07 Hz. The scale ranges from blue = 0 to red = 1.739.

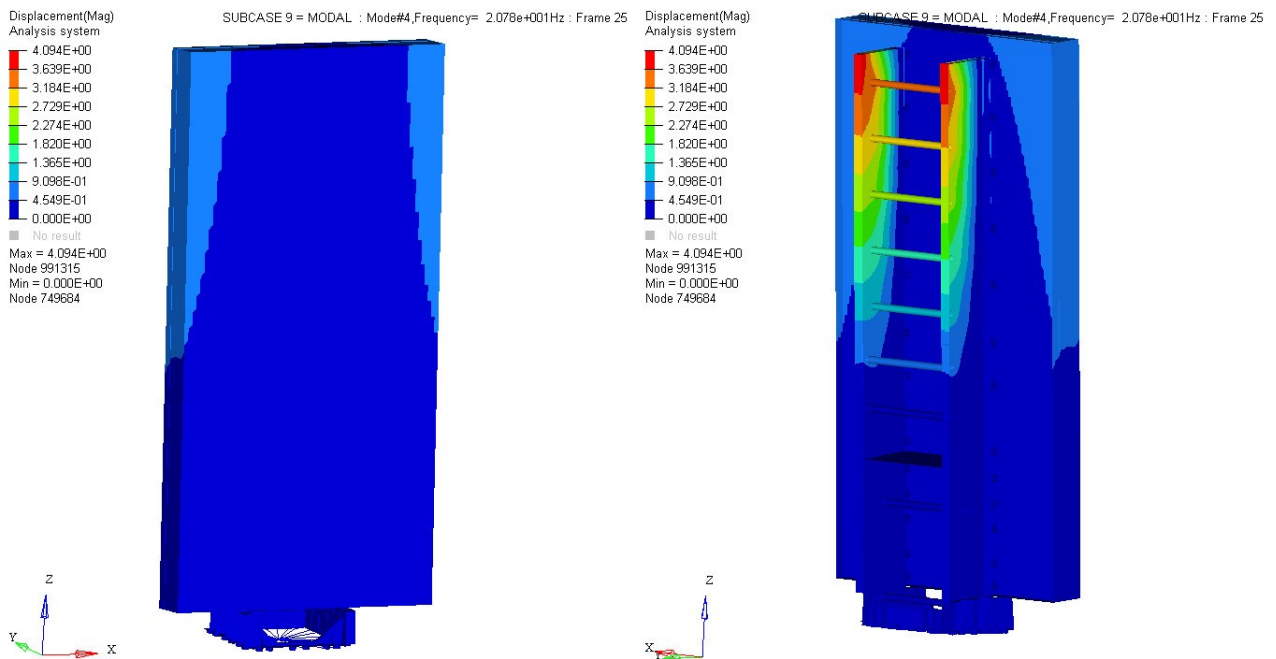


Figure 5.23: Mode 4, with frequency = 20.78 Hz. The scale ranges from blue = 0 to red = 4.094.

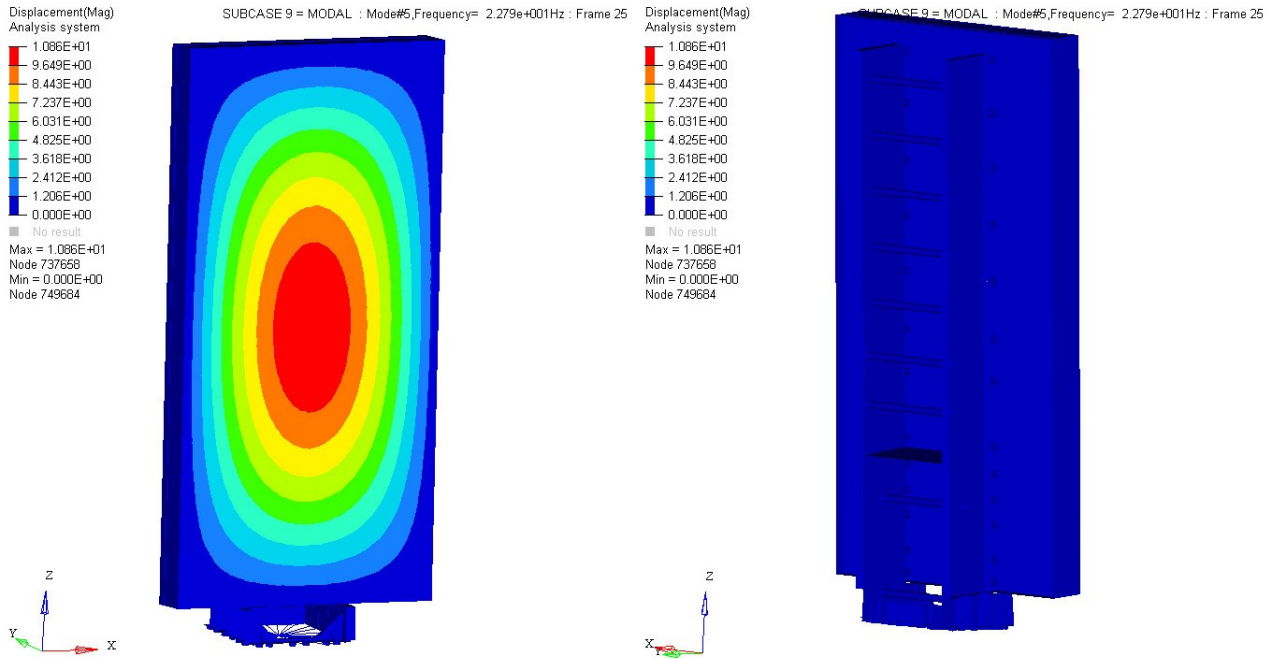


Figure 5.24: Mode 5, with frequency = 22.79 Hz. The scale ranges from blue = 0 to red = 10.86.

6 Discussion and Future Work

The discussion is divided into two different parts, one is about the developed method and one is about the G8-model that is built. The future work for each part is listed below the discussion.

6.1 Method

The purpose of the thesis was to determine a method that evaluates concepts and new products with regard to structural analysis and DOE. The work began with three sample cases in order to become familiar with the software that was used throughout the project. In the two first sample cases, different DOE methods were used in order to understand how they work. When doing more research, the method Hammersley seemed to suit the problems within this thesis and therefore, it was used as the DOE-method in the sample cases, as well as in the authentic, advanced case. The reason why only the Hammersley method was used was in order to eliminate error sources that might come with changing the method since they have different ways of changing and varying the parameters. If the model contains fewer design variables, the full factorial method could be used to estimate the impact of a single factor. Perhaps a DOE method like Hammersley, MELS or Plackett-Burman could be used in order to see which parameters that influence the solution the most. Thereafter, a full factorial could be evaluated with the two or three parameters with the largest influence in order to estimate the impact of each single factor and all possible combinations. Hammersley was used due to its sampling is more uniform than other hypercube methods and thereby get a better spread of the evaluation points. If more time would have been available, evaluations using MELS would have been made since it also is designed to spread out points equally in space. It would have been interesting to see if the results would have been different with a different DOE method. In summary, from the research done in this thesis, the MELS and Hammersley methods seem to have quite a similar course of action when choosing which points to evaluate in order to make them as uniform and equally spread out as possible.

In the third sample case, a string parameter was introduced for the first time. It was done in order to learn how to use strings in a parameter. For the third case, the geometry and mesh for each case were extracted and placed in another file, called .blk-file. Thereafter, it was included into the .bdf-file instead of being a part of the .bdf-file. The name of the file was thereafter made into a parameter, so the case could change the geometry and mesh between the different cases. One observation that was done when executing the parameterization was that each parameter only could contain one variable. So if, for example, the geometry is to change in more than one way, only smaller parts of the .blk-file should be parameterized. When changing the .blk-file in the advanced case, this was thought of too late. The file could have been varied in both the height and width at the same time, so the solution would show how the different heights and widths of the back structure affect the solution, respectively. But since the entire .blk-file with the mesh and geometry of the whole model was parameterized, it could not be done for this case.

For the analysis of the results obtained from the third case, the maximum value of the stresses and strains were demanded. Although, when analyzing the values and normalizing them, it was seen that some of the values regarding stresses and strains seemed unreasonable. This can be due to that a singularity point or an unphysical value was found when evaluating the maximal stress and strain. These results which were found might have been present in the elements directly where the force was applied. It is therefore important to look at the solution before extracting results and being certain about which results that are desired and which elements that are of interest.

One bug that occurred later in the thesis work was that HyperStudy was unable to read the result file with type .f06 in the advanced case. This affected the demanded output due to that HyperStudy could not extract the mass or natural frequencies and therefore, they could not be defined as an objective function for this case. Although, it was possible to open the files manually in HyperStudy and the .f06-file is then displayed in text. Thereafter, when the desired variables were found, the names of the variables were marked and chosen as a keyword. The values were thereafter marked and chosen as value. HyperStudy then extracted the results which were placed on that exact location manually from the result file. This method is not optimal, although it worked and the frequencies were obtained. One additional remark in HyperStudy regarding the Evaluation plot, found in section 2.4.1, which affected the post-processing was that it was not able press or select a point in the

plot and obtain information. If, for example, the minimum displacement is to be found, it would be beneficial to be able to press the point which has the smallest displacement in the plot and then obtain information about which evaluation it is and perhaps the values of the objective functions. Currently, the x -axis has to be studied in order to approximately see which parameter that obtained that value and thereafter search for it in a table. If the number of evaluations increase, it will be harder to tell approximately which evaluation that obtained a certain value. Although, this is not a major fault and all obtained results are available in a table in another tab in HyperStudy.

When executing structural optimization and DOE throughout the thesis work, the software HyperStudy has shown many of the features it possesses. It is a very versatile tool and is very useful when solving structural optimization problems. It eased the analysis and understanding of the obtained results due to post-processing tools that were available within HyperStudy, since they were easy to understand. The developed method will be able to save a lot of time in the concept generation phase, as well as showing what to focus on when developing new products. The method can evaluate numerous different concepts, the largest amount of concepts evaluated during one simulation in this thesis were 105, and thereafter inform about which parameters that were worth investigating further and which that can be neglected. It is also possible to have several different objective functions at one time, although this is often not used since the results usually do not correlate. If one objective function is to decrease mass and the other is to increase stiffness, they will most certainly not obtain the same solution. Although, it can be used as a check point in order to see how the change in variables affect the solution.

Future work regarding the method is mentioned below.

- Investigate other DOE methods more carefully to understand when the different methods are beneficial to use.
- Only parameterize the particular values or parts that are to vary. If changing one part of the mesh as a parameter, only parameterize that part of the .blk-file in order to be able to parameterize different parts of the file at the same time.
- The demanded output should be studied further in order to make sure that the requested output is a realistic result.
- Investigate the opportunity to make geometry changes in HyperStudy instead of creating all different concepts by hand.
- Investigate the other types of approaches which are available in HyperStudy, that is Fit, Optimization and Stochastic.

6.2 Model

Firstly, the core materials used in the simulations regarding the advanced case were Rohacell and two kinds of honeycomb, composite and aluminum. The composite honeycomb and Rohacell were defined as MAT8 in the simulations, but the aluminum honeycomb was defined as MAT1. It was defined this way due to how it was defined in the original model. Since the original and the simplified model were to be compared, the materials had to be equivalent. Although, since it is a honeycomb material, the material properties in the different directions vary. Therefore, the aluminum honeycomb has not given authentic results if they were to be compared to how it would behave in reality. Although, since the same information is given for the different cases, there should not be a difference in results between the models. Although, this probably has an impact on which parameters that contributed to achieving the smallest displacement and largest frequency, since the aluminium honeycomb was defined to be stiffer than it is in reality. Consequently, it also seems much stiffer than the composite honeycomb and Rohacell. Thus, it might be recommended to use aluminum honeycomb by the software, although this result is not trustworthy since it is not realistic and is not defined as the other materials.

Secondly, when continuing to develop the G8-case, a new model must be created. The model which was created in this thesis is very simplified and in order to get realistic results, some things should be improved. The nonstructural mass that was applied on the sandwich plate should be replaced with the multi packs, cables and

other equipment in order to see how they affect the stiffness and displacement of the antenna. Also, a back cover of the antenna is not included in the simplified model. The entire model is also modelled with only shell and composite elements with added thicknesses and perhaps solid elements might be needed in some places in the model. One additional remark is that the back structures should be investigated further. Currently, the entire back structure has the same thickness. However, perhaps the thicknesses can vary for the different heights and widths in the structure. Even the elements surrounding the back structure vary with the same thickness. Perhaps these parts can be divided and that different parts can obtain different thicknesses. By varying these parameters as well, the structure can be optimized further than when all elements have the same thickness.

Lastly, the parameters used in for the G8 model should be overlooked. The variation in height and width should be parameterized differently. Consequently, the entire .blk-file should not be parameterized, only the parts which regard a specific parameter. In that case, the influence of both the height and width of the back structure can be analyzed at the same time. Perhaps other parameters are interesting to examine, like for instance different materials in the back support along the height or different thicknesses of the parameter called BackHeight in the model. Also, as mentioned before, the material definitions should be investigated further.

Future work regarding the G8 model is mentioned below.

- Edit the material card regarding the aluminum honeycomb.
- Change thickness along the height in the support structure.
- Check the parameters used in the G8-model so they are relevant and add parameters which are missing.

7 Concluding remarks

The obtained results shows that by using structural optimization and DOE, the purpose of the project, which was to determine a method that evaluates concepts with regard to structural analysis and DOE, has been fulfilled. The method has been developed and tested through three different sample cases and thereafter applied on an authentic product from Saab's product portfolio. The method informs about which parameters that have the largest influence on the product behaviour in terms of displacement and eigenfrequencies, along with which combination of parameters that fulfill the objective function and how to interpret the results obtained from the DOE.

The developed method is very versatile when it comes to structural optimization. The design variables can be real or discrete values, or even strings which makes it possible to parameterize everything from a thickness in an element to complete geometries and meshes. Everything that is included in the .tpl-file is possible to parameterize, since it is the file that the parameterization is executed in. Therefore, by using this method, many parameters can be screened at the same time and the results will show which design variables to focus and which that can be neglected when developing and evaluating new concepts.

References

- [1] Saab AB. *About Us: Business Areas*. URL: <https://Saabgroup.com/about-company/organization/business-areas/> (visited on 04/29/2019).
- [2] Saab AB. URL: <https://Saab.com/land/istar/multi-role-surveillance-system/giraffe-4a/> (visited on 04/29/2019).
- [3] Altair Engineering, Inc. *Altair HyperStudy Overview*. 2019. URL: <https://altairhyperworks.com/product/hyperstudy> (visited on 02/01/2019).
- [4] MSC. *MSC Nastran*. URL: <http://www.mscsoftware.com/product/msc-nastran> (visited on 02/01/2019).
- [5] Altair Engineering, Inc. *Altair HyperMesh Overview*. 2019. URL: <https://altairhyperworks.com/product/HyperMesh> (visited on 02/01/2019).
- [6] Altair Engineering, Inc. *Altair HyperView Overview*. 2019. URL: <https://altairhyperworks.com/product/hyperview> (visited on 02/01/2019).
- [7] N. Ottosen and H. Petersson. *Introduction to the Finite Element Method*. Pearson Prentice Hall, 1992, pp. 1–6.
- [8] S. Rai, D. Ramana, and A. Manglik. *Dynamics of Earth’s Fluid System*. A.A. Balkema Publishers, 2002, p. 204. URL: <https://books.google.se/books?id=05EI8d1RwNkC&lpg=PA199&ots=XNZt6Gvm3m&dq=finite%5C%20element%5C%20method&lr&hl=sv&pg=PA204#v=onepage&q=finite%5C%20element%5C%20method&f=false> (visited on 05/20/2019).
- [9] P. W. Christensen and A. Klarbring. *An Introduction to Structural Optimization*. Springer Science + Business Media, 2009, pp. 1–7.
- [10] N. Jonnerby. “Weight Optimization of Radar Shelter using Design of Experiment”. 2018.
- [11] G. Box, J. Hunter, and W. Hunter. *Statistics for Experimenters: Design, Innovation, and Discovery*. Vol. 2. Hoboken, New Jersey: John Wiley & Sons, Inc., 2005.
- [12] Altair Engineering, Inc. *Full Factorial*. 2019. URL: https://www.sharcnet.ca/Software/Hyperworks/help/hst/hst.htm?fractional_factorial.htm (visited on 03/08/2019).
- [13] Altair Engineering, Inc. *Fractional Factorial*. 2019. URL: https://www.sharcnet.ca/Software/Hyperworks/help/hst/hst.htm?fractional_factorial.htm (visited on 03/08/2019).
- [14] NIST/SEMATECH. *5.3.3.5. Plackett-Burman designs*. URL: <https://www.itl.nist.gov/div898/handbook/pri/section3/pri335.htm> (visited on 01/31/2019).
- [15] Altair Engineering, Inc. *Modified Extensible Lattice Sequence (MELS)*. HyperWorks Help. 2019.
- [16] Altair Engineering, Inc. *Hammersley Sampling*. 2009. URL: https://www.sharcnet.ca/Software/Hyperworks/help/hst/hst.htm?hammersley_sampling.htm (visited on 05/06/2019).
- [17] Altair Engineering, Inc. *Evaluate*. HyperWorks Help. 2019.
- [18] Altair Engineering, Inc. *Distribution*. HyperWorks Help. 2019.
- [19] Altair Engineering, Inc. *Post-Processing for DOEs*. URL: https://www.sharcnet.ca/Software/Hyperworks/help/hst/hst.htm?fractional_factorial.htm (visited on 03/25/2019).
- [20] F. J. Plantema. *Sandwich Construction*. New York: John Wiley & Sons, Inc., 1966.
- [21] Caterham Group. *Sandwich Structures*. July 3, 2016. URL: <https://altairenligheten.com/in-depth/sandwich-structures/> (visited on 02/28/2019).
- [22] O. E. et al. *Marine Applications of Advanced Composite Materials. Fracture modes, damage tolerance and failure mitigation in marine composites*. Cambridge: Woodhead Publishing, 2015, pp. 79–102.
- [23] D. Zenkert. *An Introduction To Sandwich Construction*. Stockholm: Royal Institute of Technology, 2005.
- [24] MSC Software Corporation. *Quick Reference Guide*. 2017, pp. 2180–2185.
- [25] EURO-COMPOSITES. *Mechanical Properties of ECK Honeycomb*. 2010. URL: <https://www.euro-composites.com/en/portfolio/mechanical-engineering/> (visited on 02/13/2019).
- [26] Evonik. *Product Information. Rohacell*. URL: <https://www.rohacell.com/product/rohacell/en/> (visited on 02/21/2019).
- [27] Evonik. *ROHACELL HF*. 2019. URL: <https://www.rohacell.com/product/peek-industrial/downloads/rohacell%5C%20hf%5C%20product%5C%20information.pdf> (visited on 02/08/2019).
- [28] D. Roylance. *Beam Displacements*. Tech. rep. Cambridge, MA 02139: Department of Materials Science and Engineering, Massachusetts Institute of Technology, Nov. 2000, pp. 1–3. URL: <http://web.mit.edu/course/3/3.11/www/modules/bdisp.pdf> (visited on 05/20/2019).
- [29] *HyperMesh Introduction*. 2011, pp. 1–5.

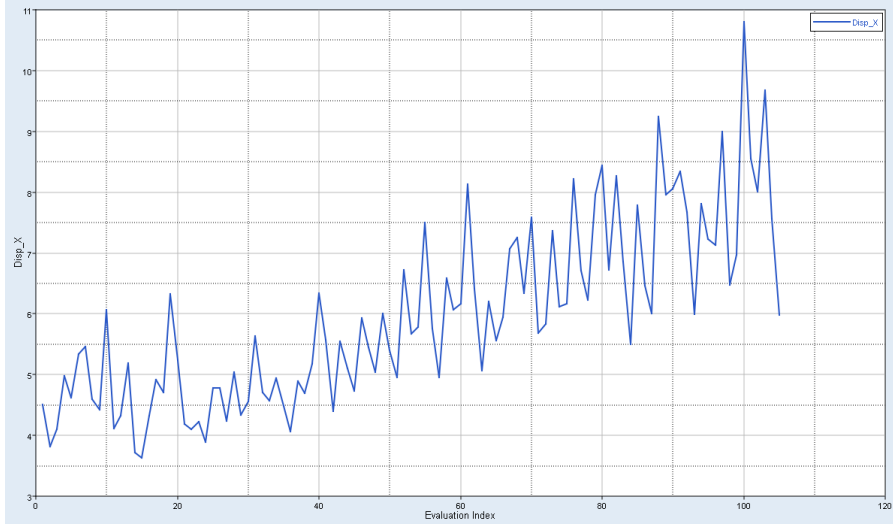
- [30] Altair Engineering, Inc. URL: https://www.sharcnet.ca/Software/Hyperworks/help/hst/hst.htm?hyperstudy_input_data.htm (visited on 05/13/2019).
- [31] NIST/SEMATECH. *5.3.3.4. Fractional factorial designs*. URL: <https://www.itl.nist.gov/div898/handbook/pri/section3/pri334.htm> (visited on 01/31/2019).

Appendices

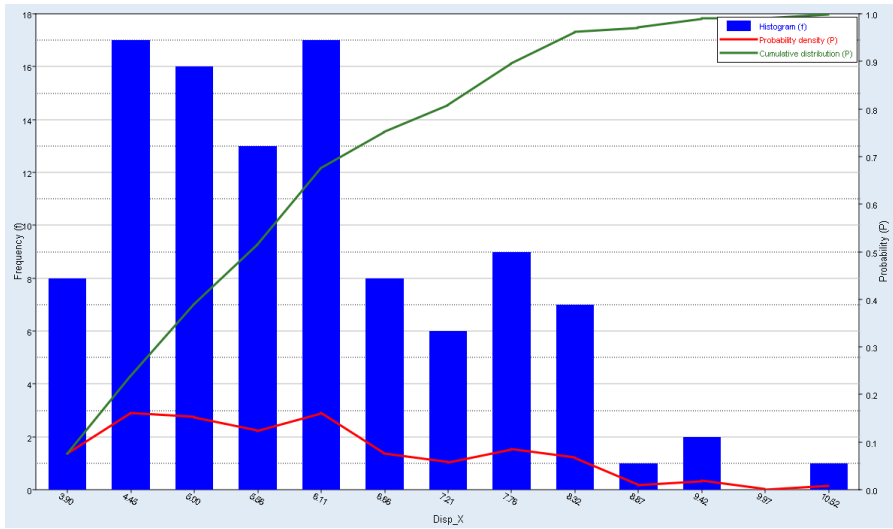
A G8 model

All obtained results from the objective functions defined in the linear static and natural frequency case can be seen below. The results for one objective function is shown at a time.

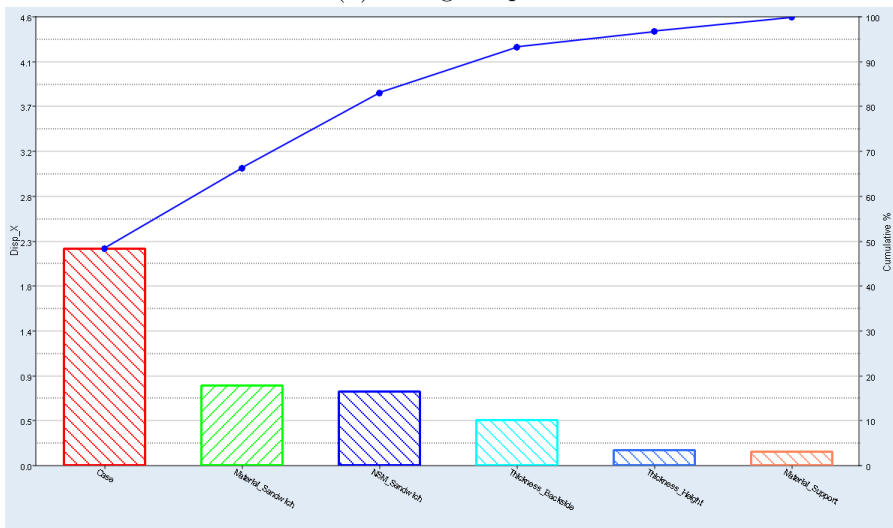
A.1 Linear static analysis



(a) Evaluation plot.

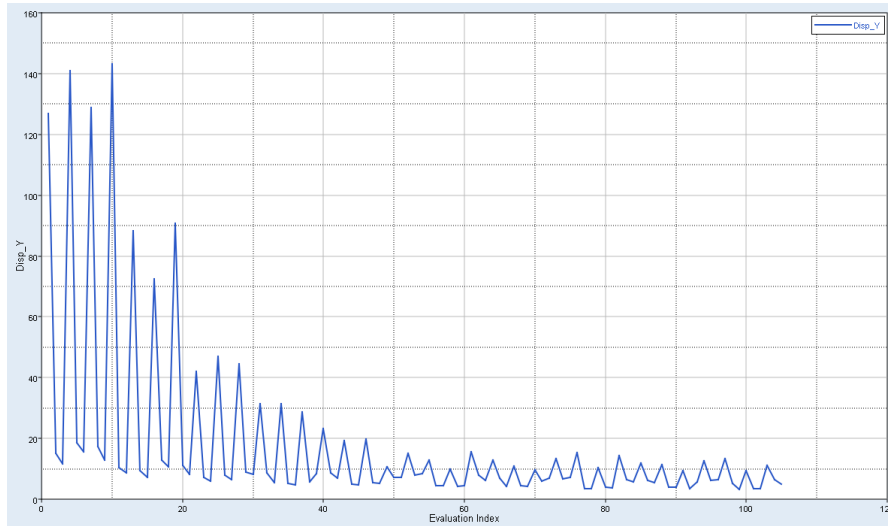


(b) Histogram plot.

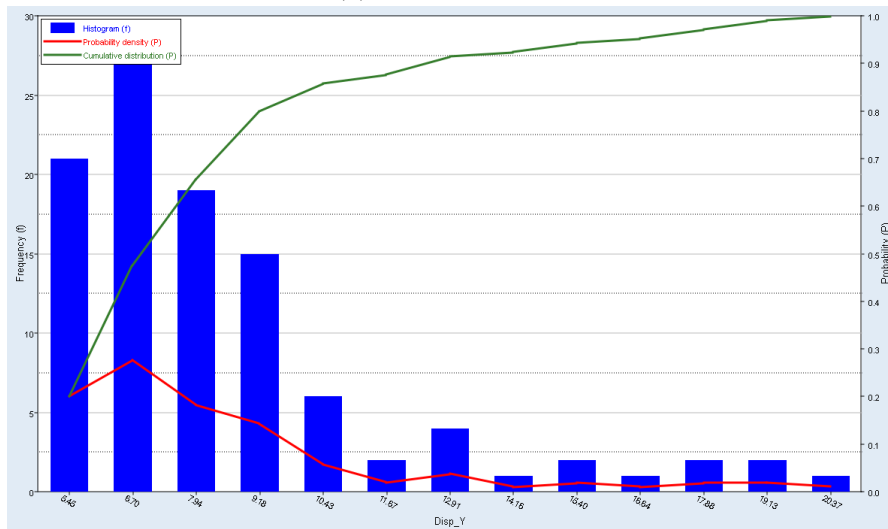


(c) Pareto plot.

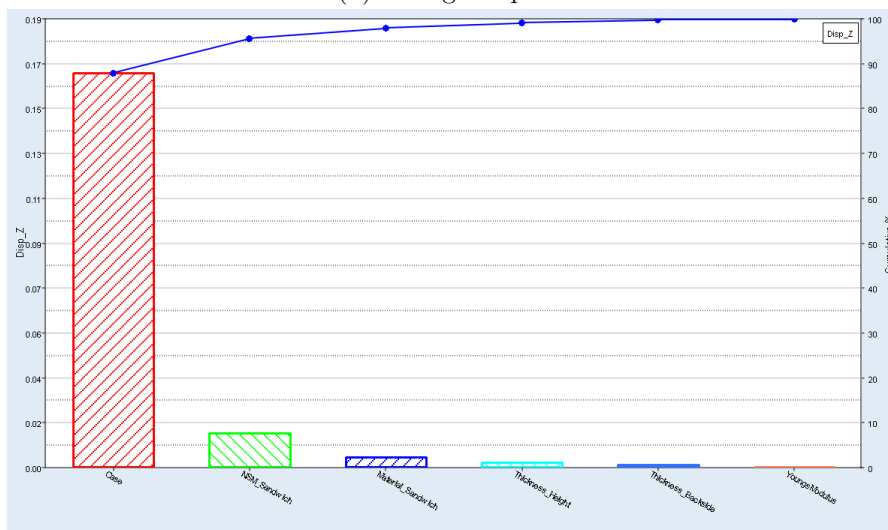
Figure A.1: The plots regarding displacement in x for the linear static case.



(a) Evaluation plot.

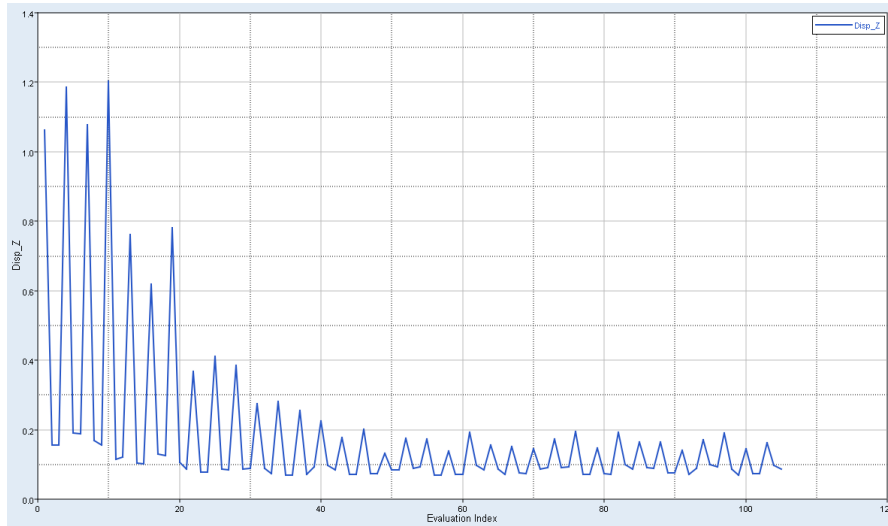


(b) Histogram plot.

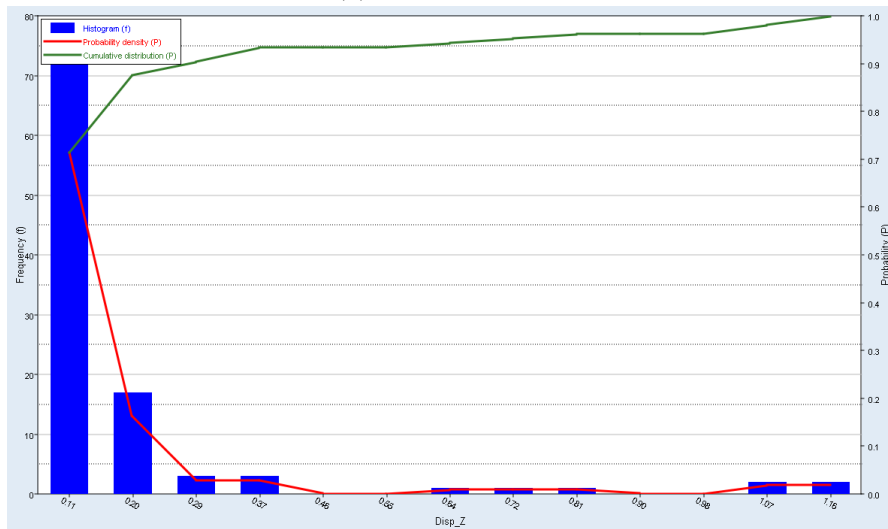


(c) Pareto plot.

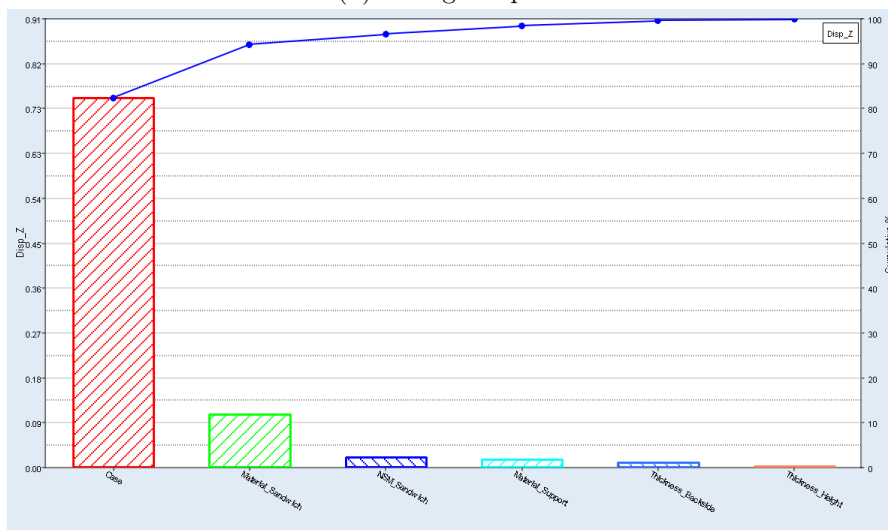
Figure A.2: The plots regarding displacement in y for the linear static case.



(a) Evaluation plot.

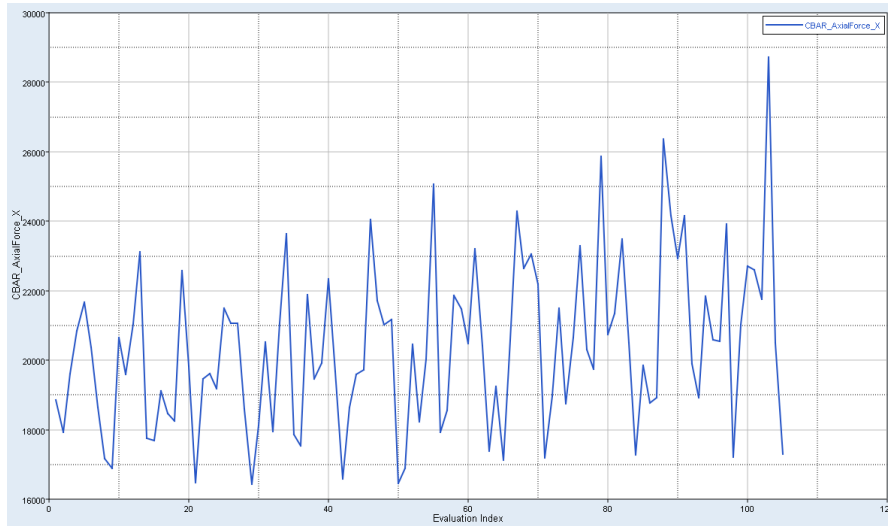


(b) Histogram plot.

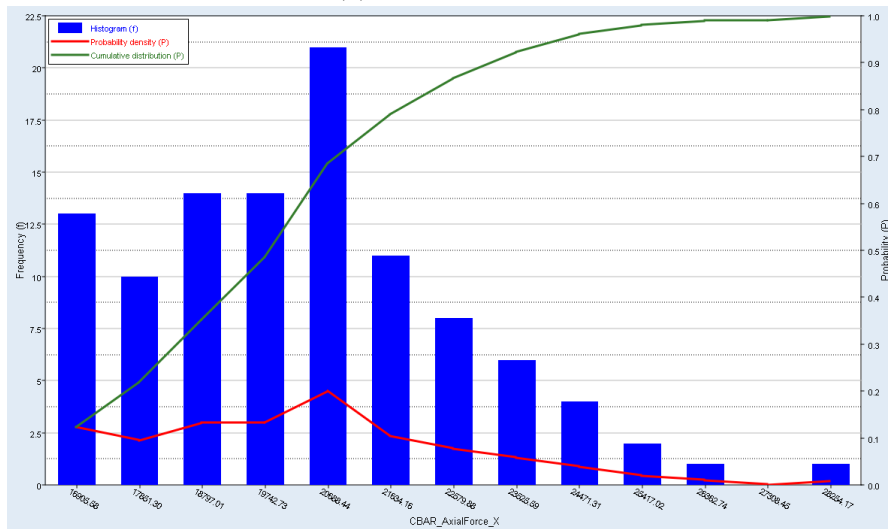


(c) Pareto plot.

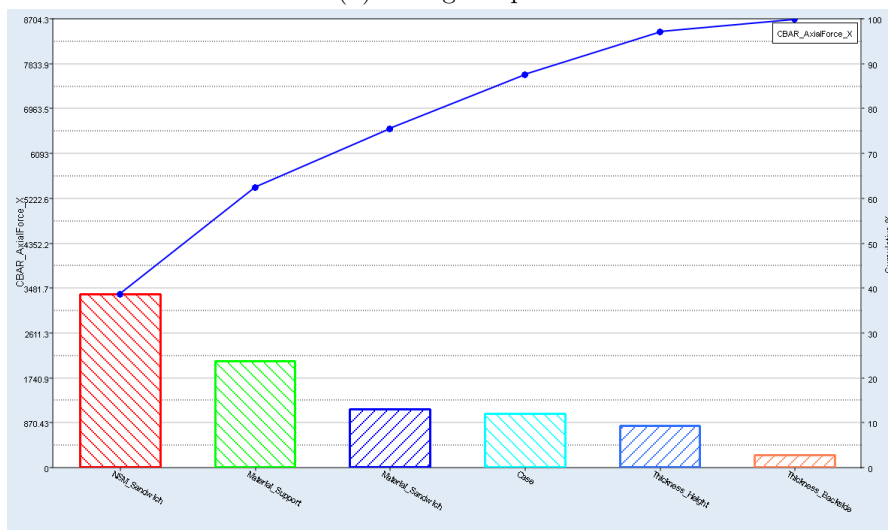
Figure A.3: The plots regarding displacement in z for the linear static case.



(a) Evaluation plot.

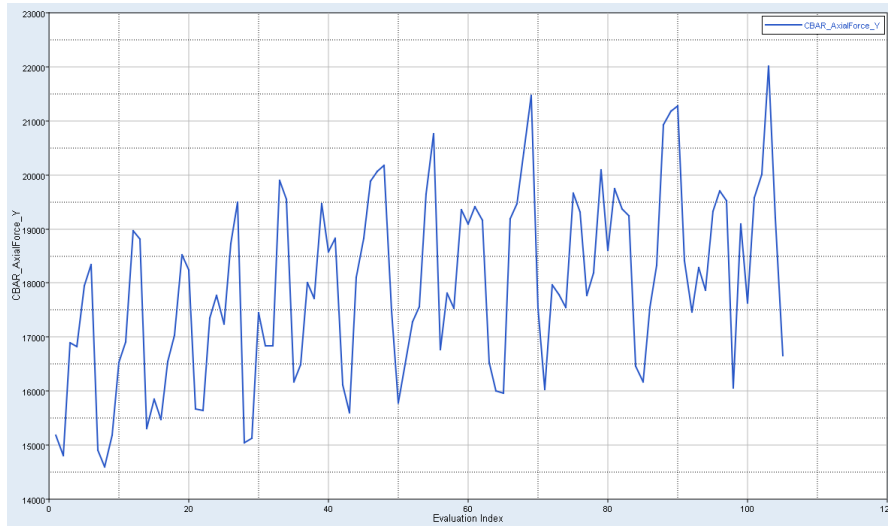


(b) Histogram plot.



(c) Pareto plot.

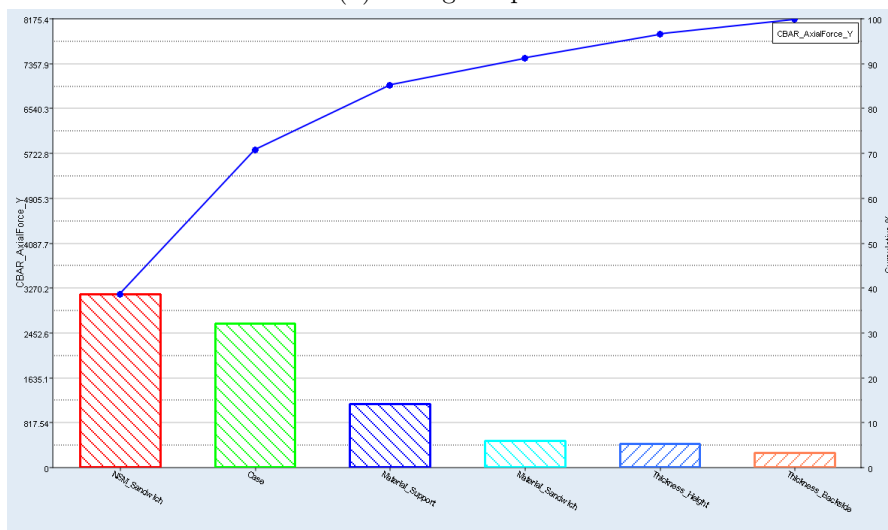
Figure A.4: The plots regarding axial forces in screws in the x -direction for the linear static case.



(a) Evaluation plot.

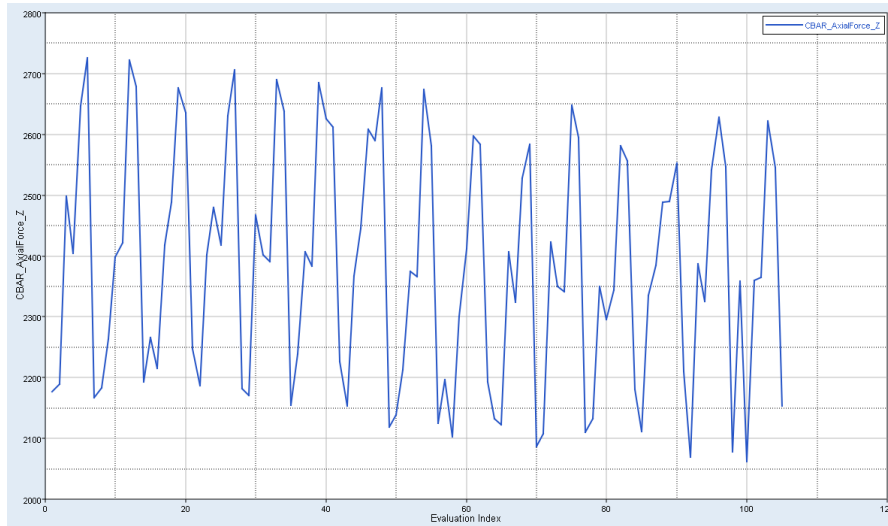


(b) Histogram plot.

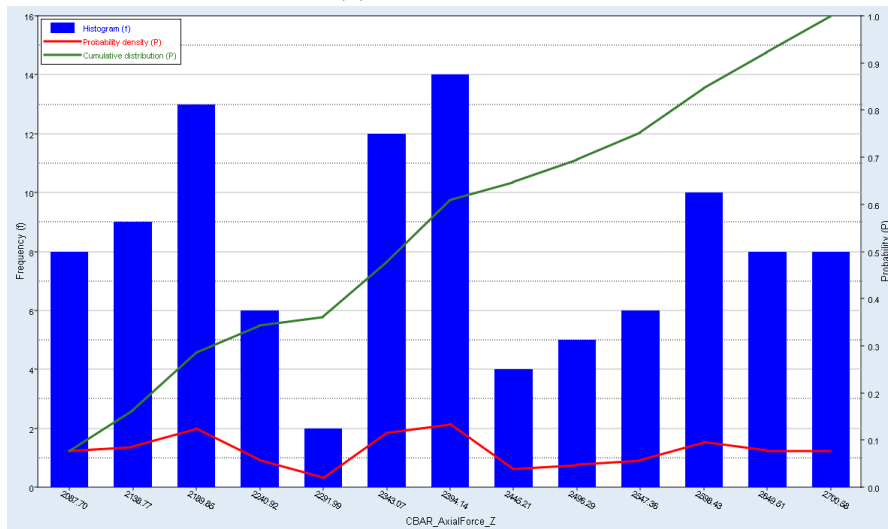


(c) Pareto plot.

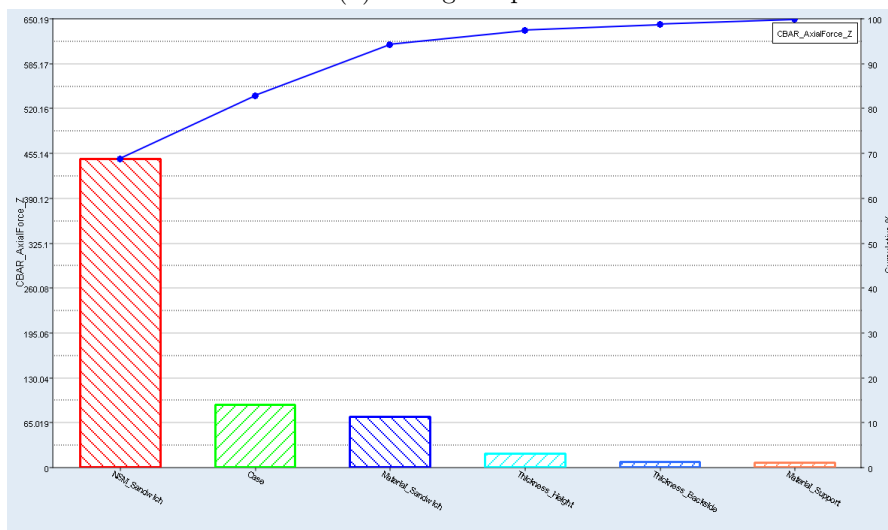
Figure A.5: The plots regarding axial forces in screws in the y -direction for the linear static case.



(a) Evaluation plot.

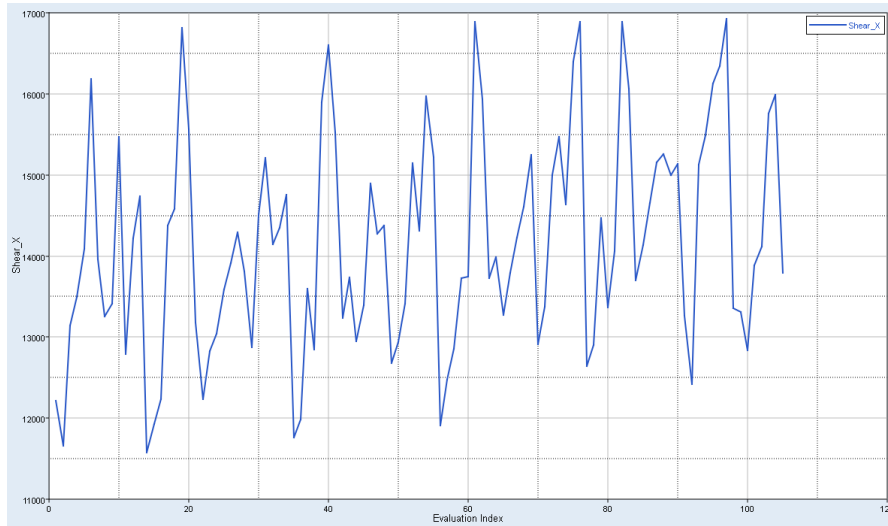


(b) Histogram plot.

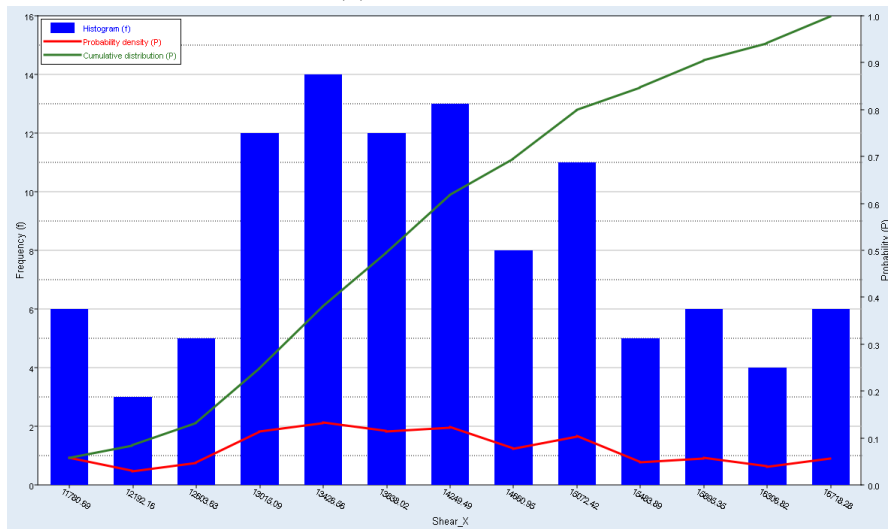


(c) Pareto plot.

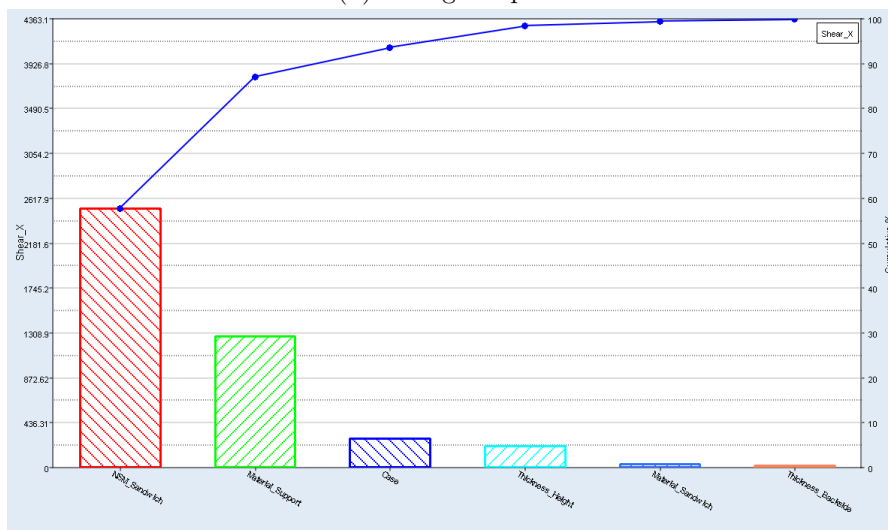
Figure A.6: The plots regarding axial forces in screws in the z -direction for the linear static case.



(a) Evaluation plot.

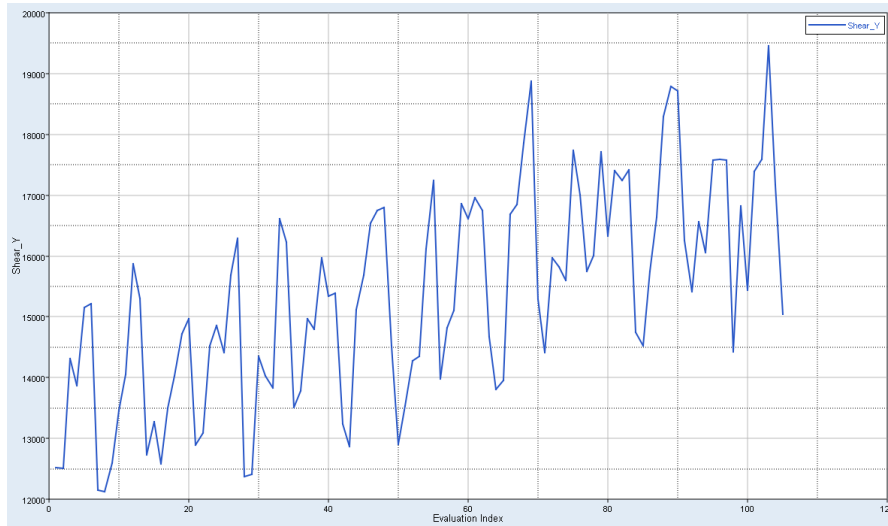


(b) Histogram plot.

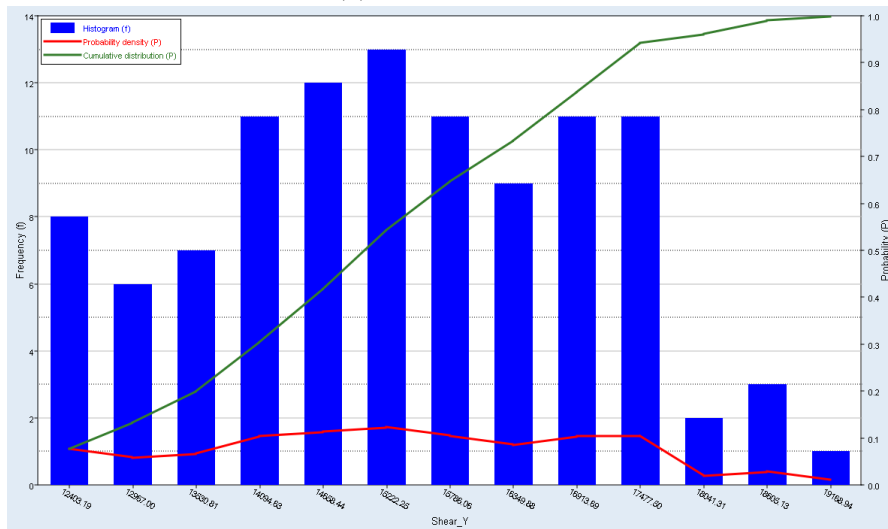


(c) Pareto plot.

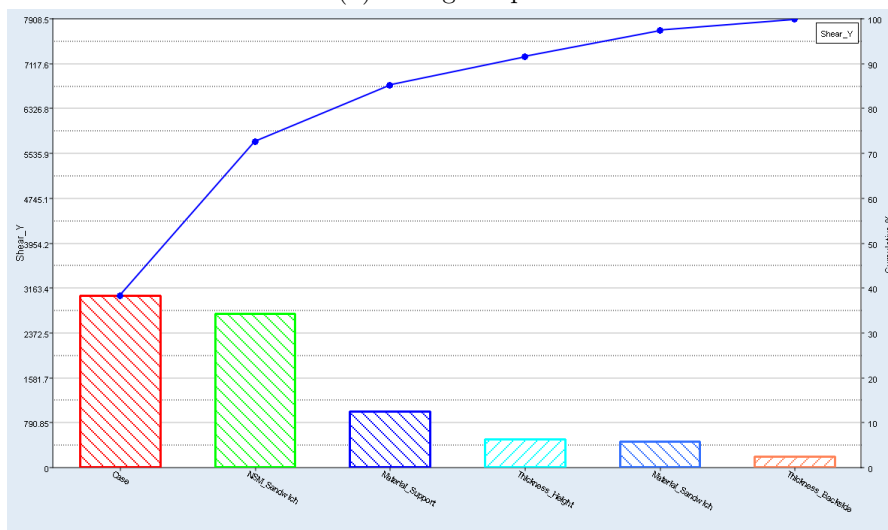
Figure A.7: The plots regarding shear in x -direction for the linear static case.



(a) Evaluation plot.

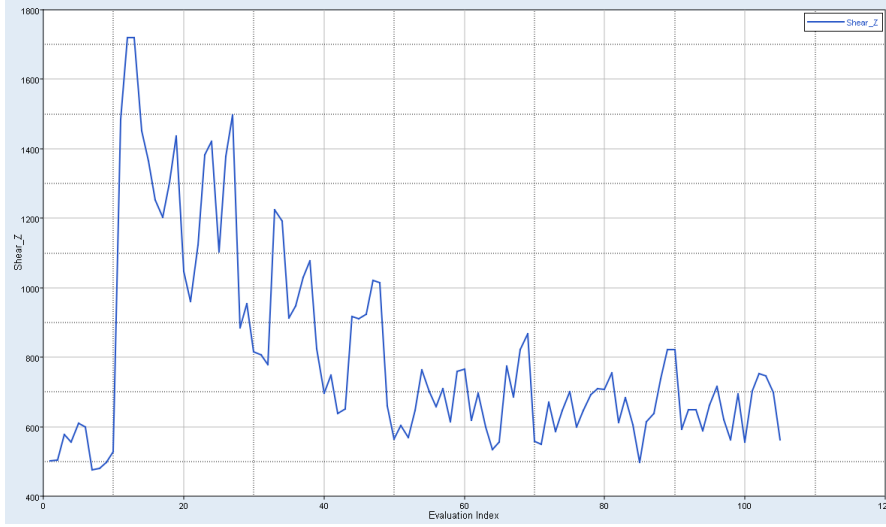


(b) Histogram plot.

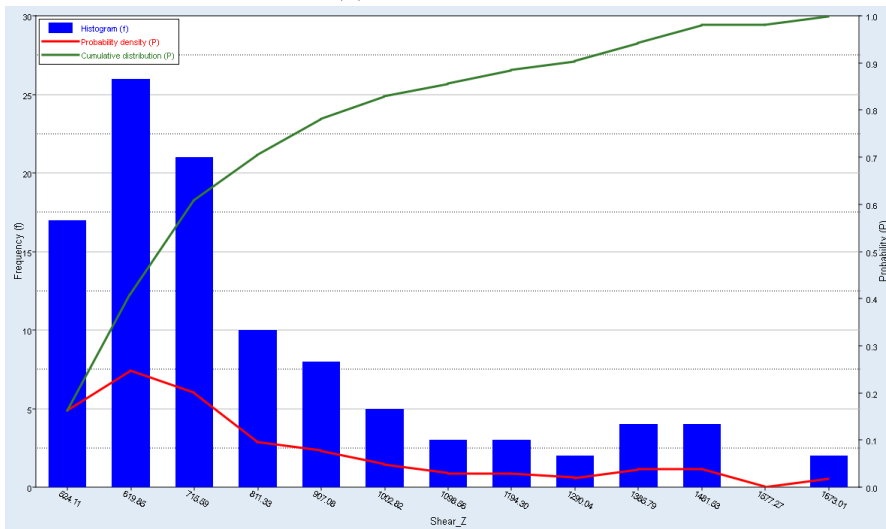


(c) Pareto plot.

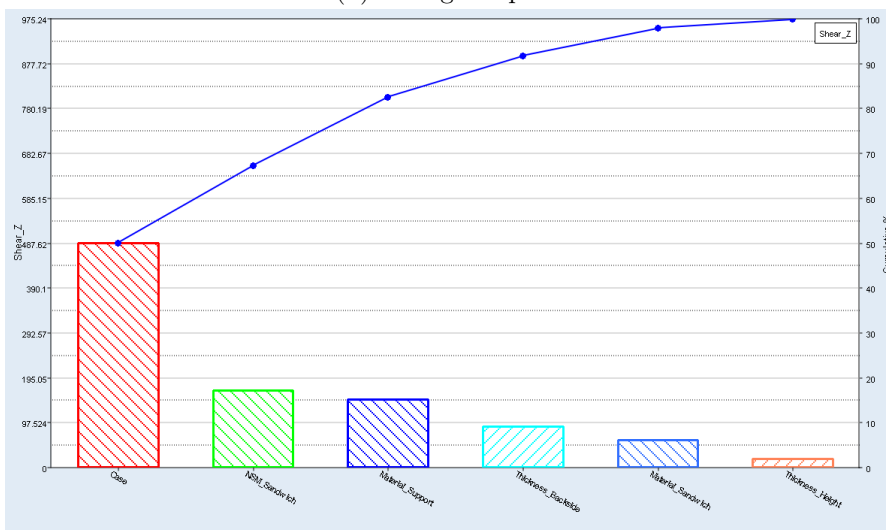
Figure A.8: The plots regarding shear in y -direction for the linear static case.



(a) Evaluation plot.

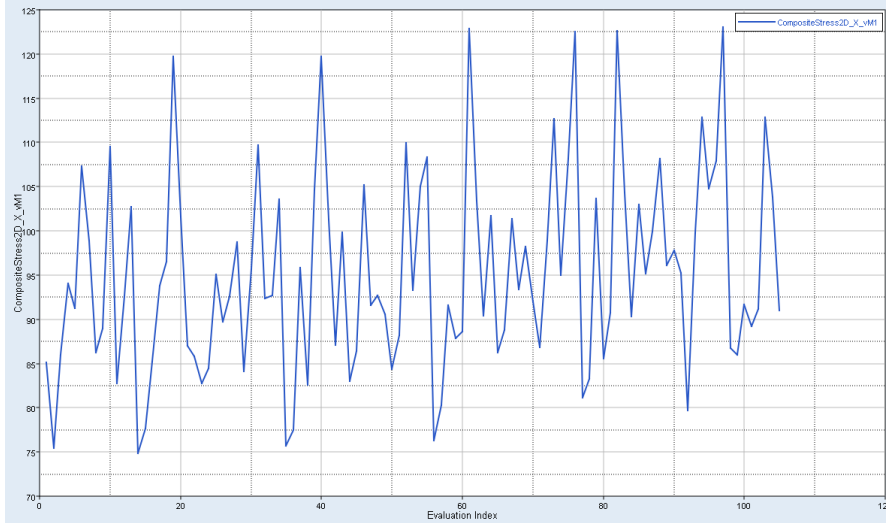


(b) Histogram plot.

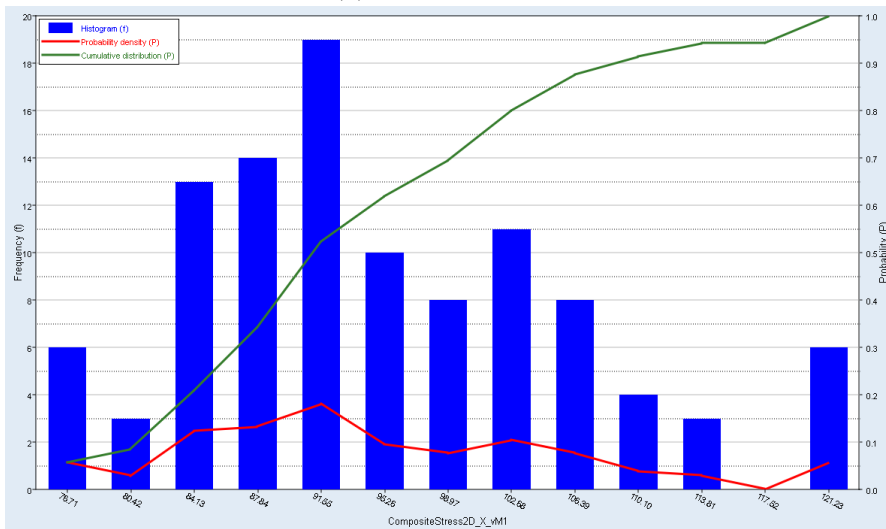


(c) Pareto plot.

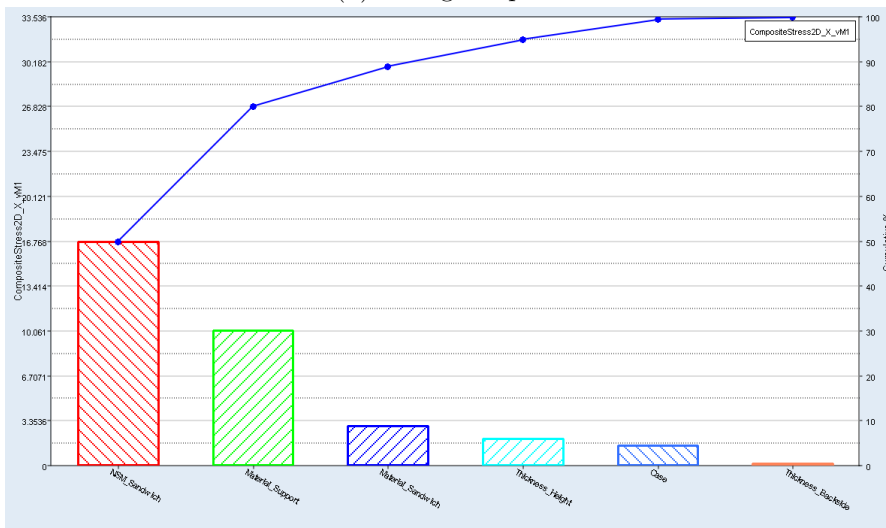
Figure A.9: The plots regarding shear in z -direction for the linear static case.



(a) Evaluation plot.

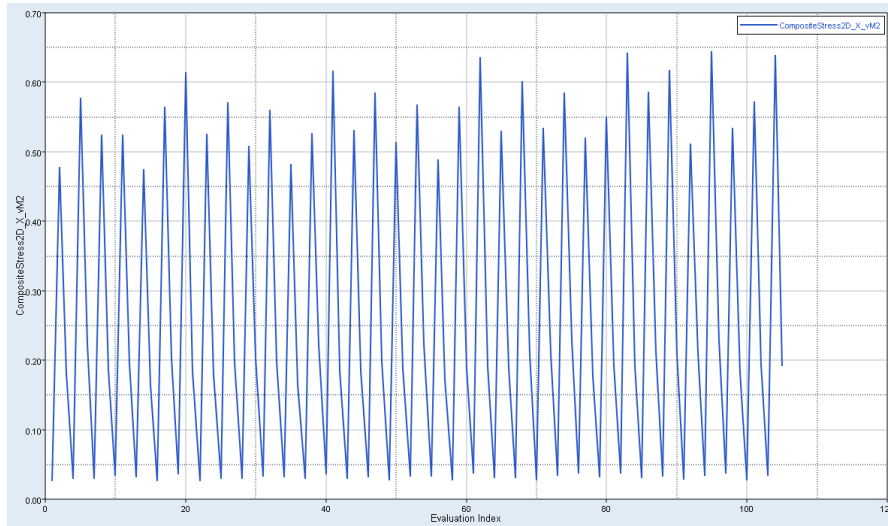


(b) Histogram plot.

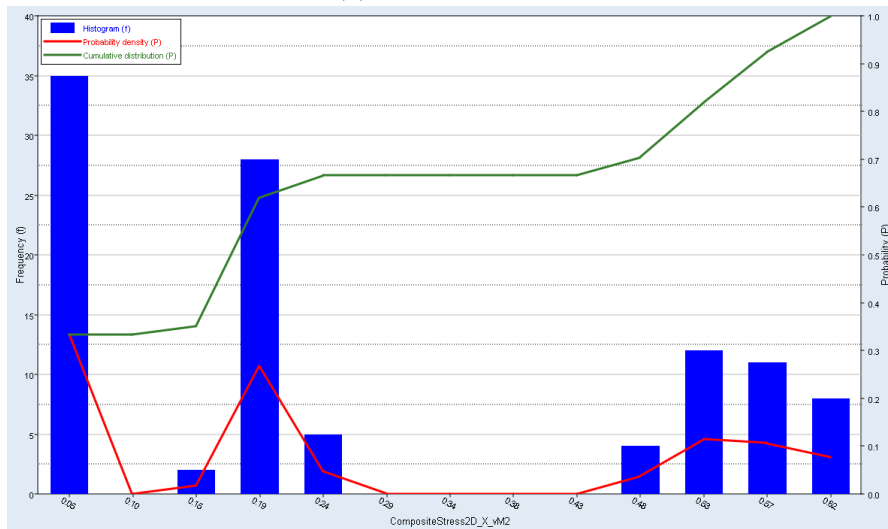


(c) Pareto plot.

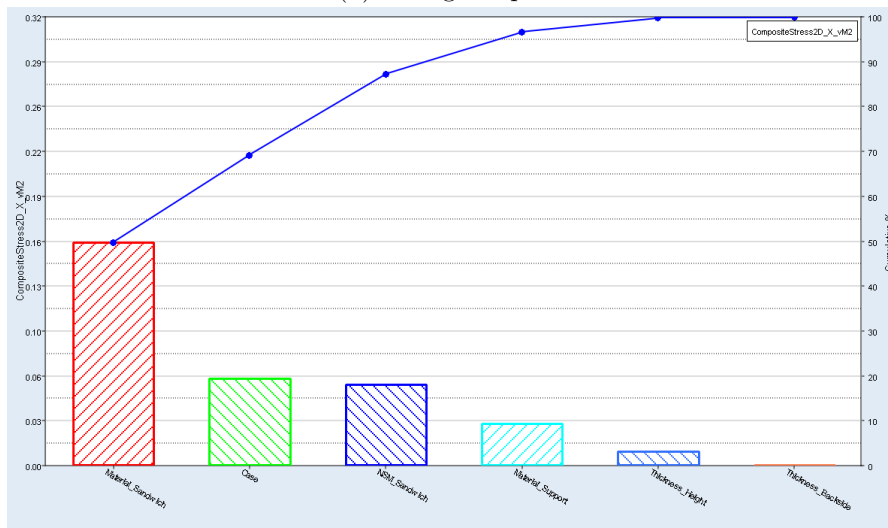
Figure A.10: The plots regarding composite stress (von Mises) in x -direction in ply 1 for the linear static case.



(a) Evaluation plot.

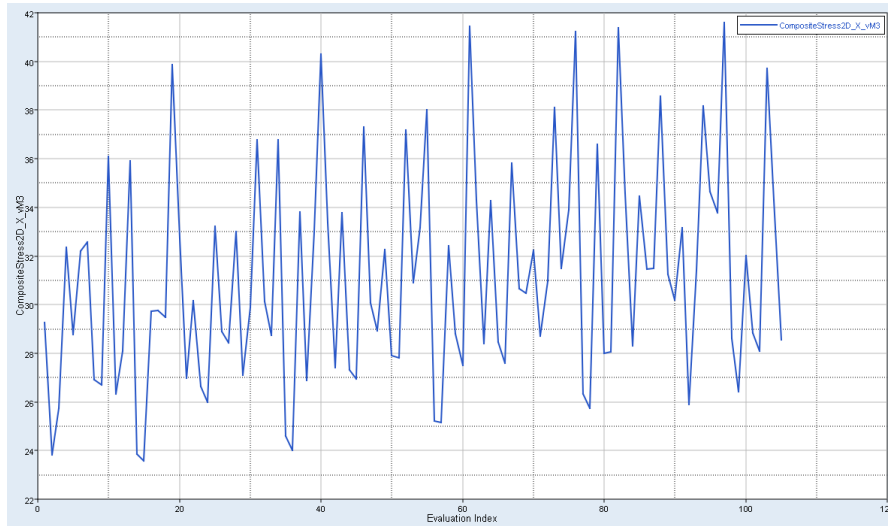


(b) Histogram plot.

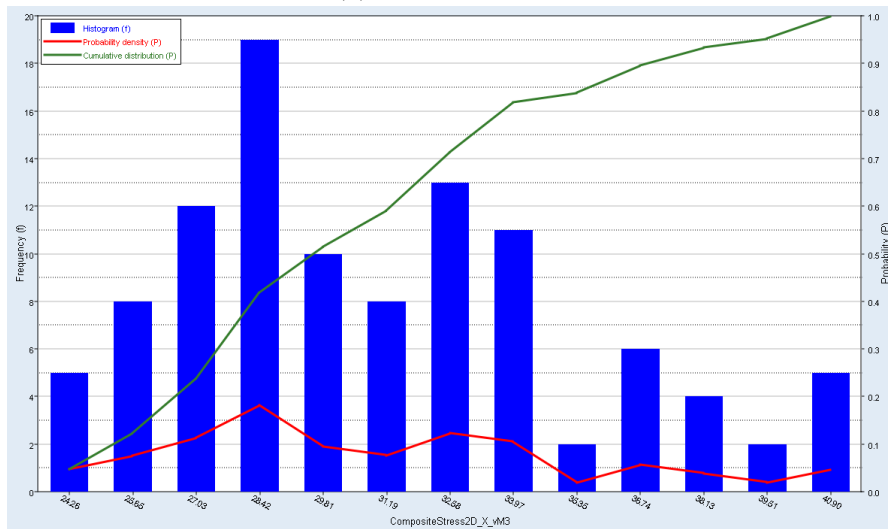


(c) Pareto plot.

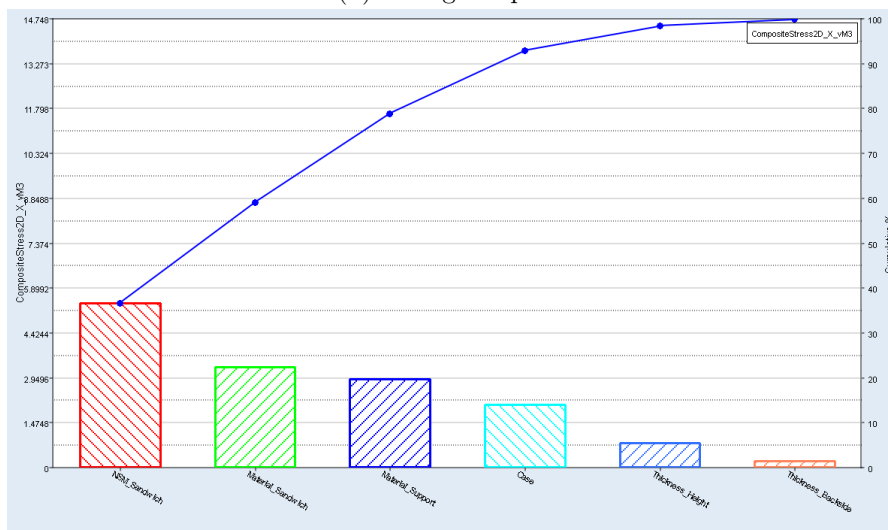
Figure A.11: The plots regarding composite stress (von Mises) in x -direction in ply 2 for the linear static case.



(a) Evaluation plot.

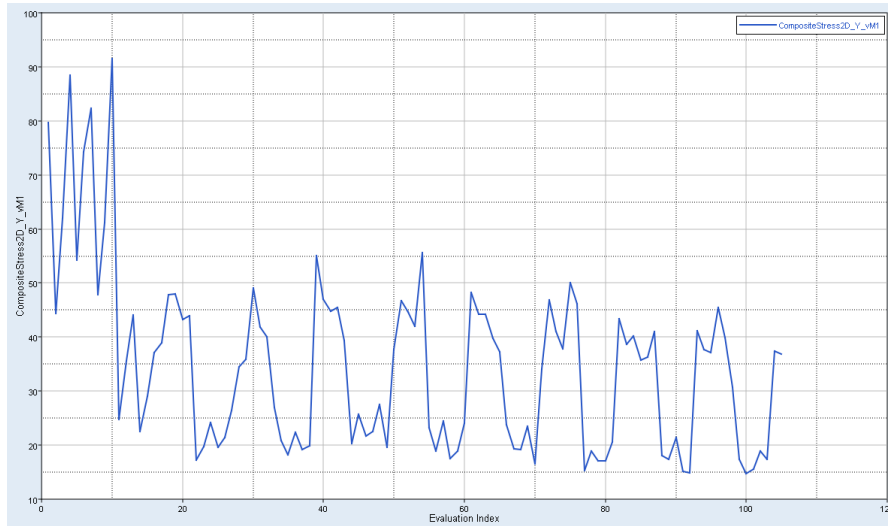


(b) Histogram plot.

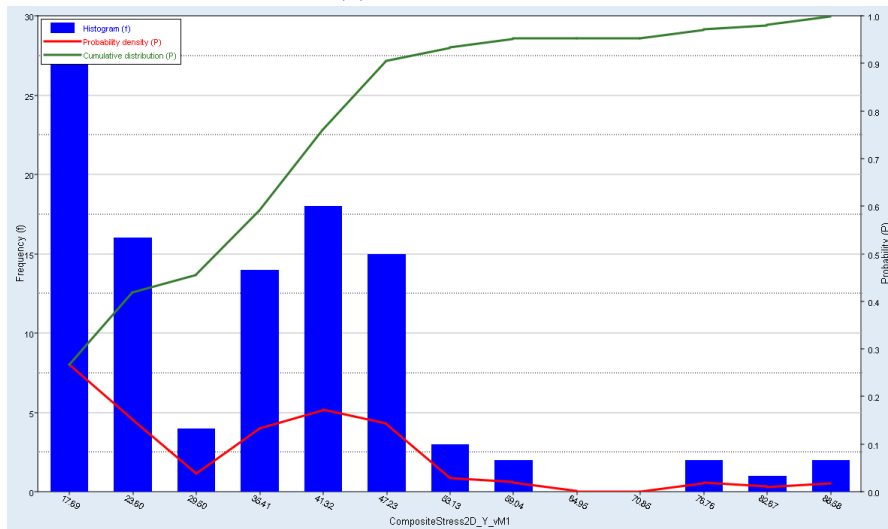


(c) Pareto plot.

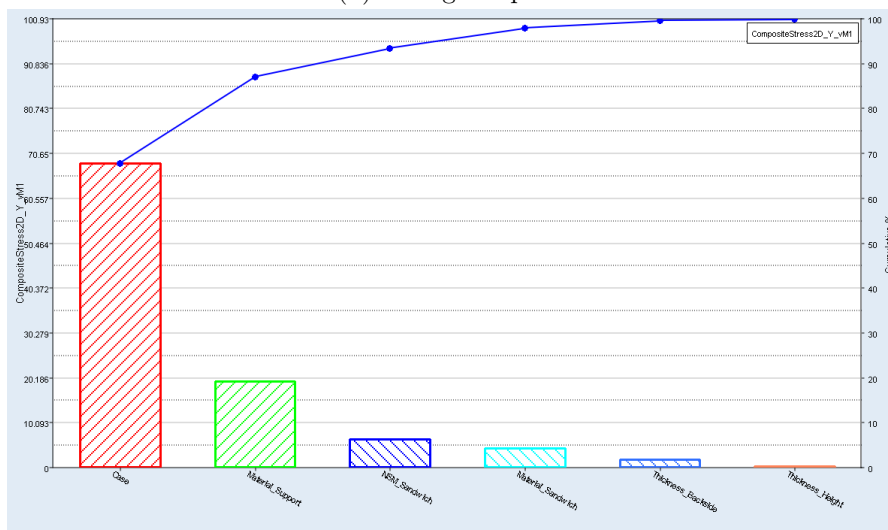
Figure A.12: The plots regarding composite stress (von Mises) in x -direction in ply 3 for the linear static case.



(a) Evaluation plot.

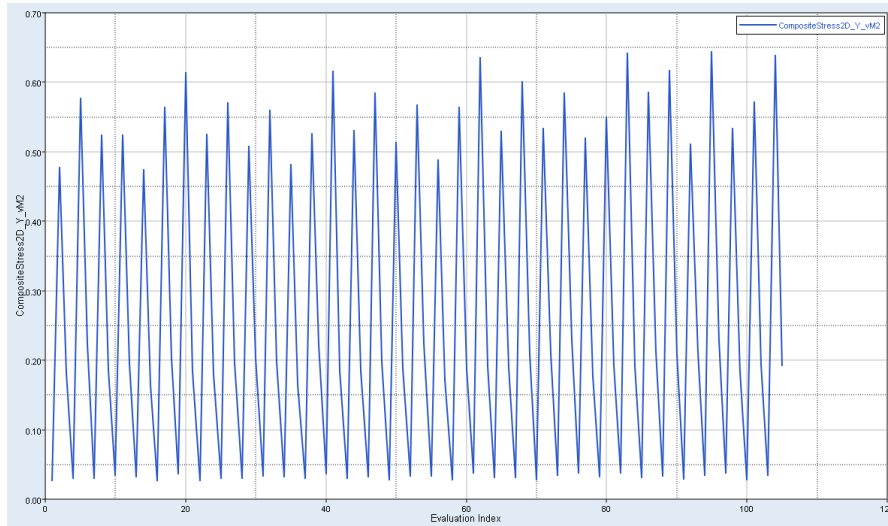


(b) Histogram plot.

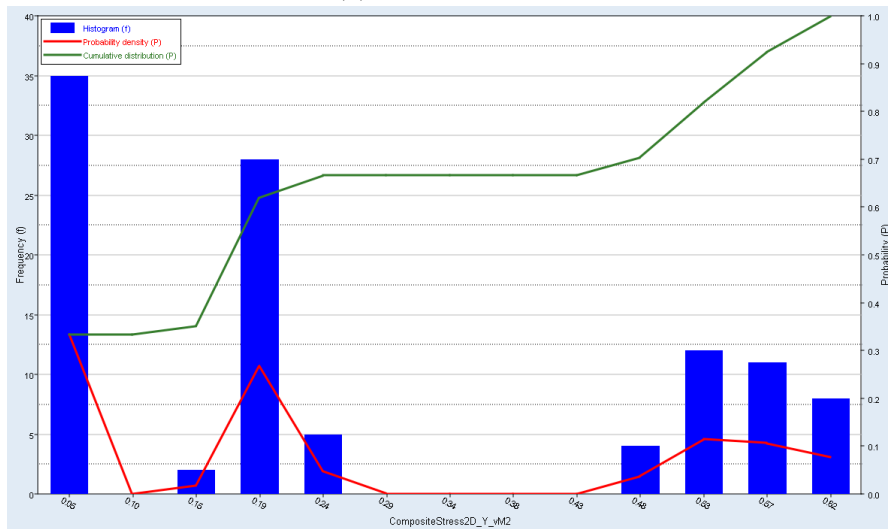


(c) Pareto plot.

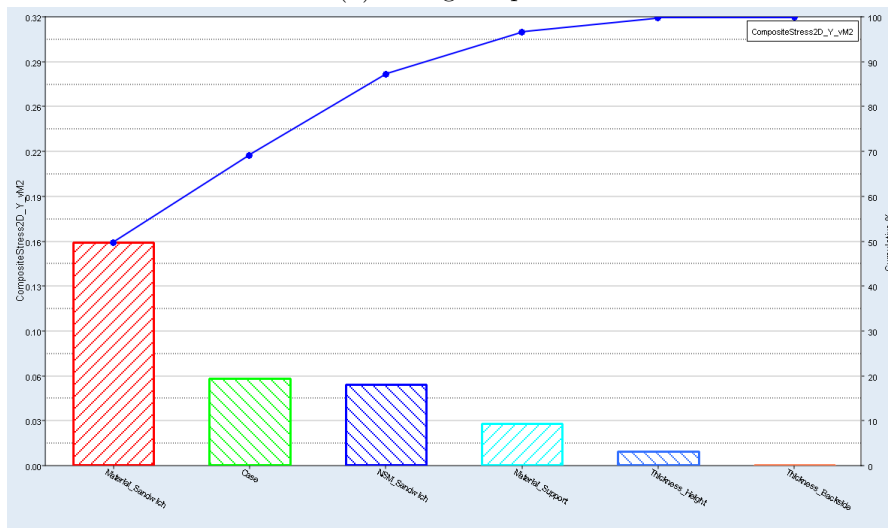
Figure A.13: The plots regarding composite stress (von Mises) in y -direction in ply 1 for the linear static case.



(a) Evaluation plot.

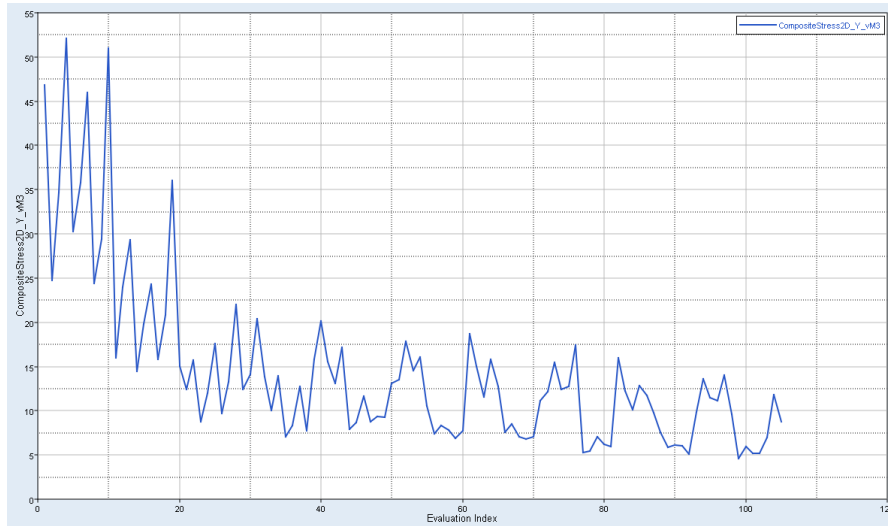


(b) Histogram plot.

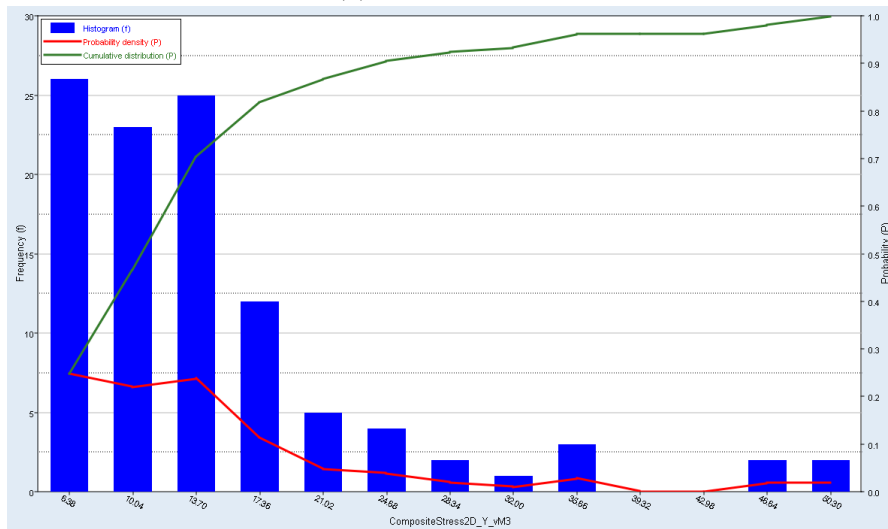


(c) Pareto plot.

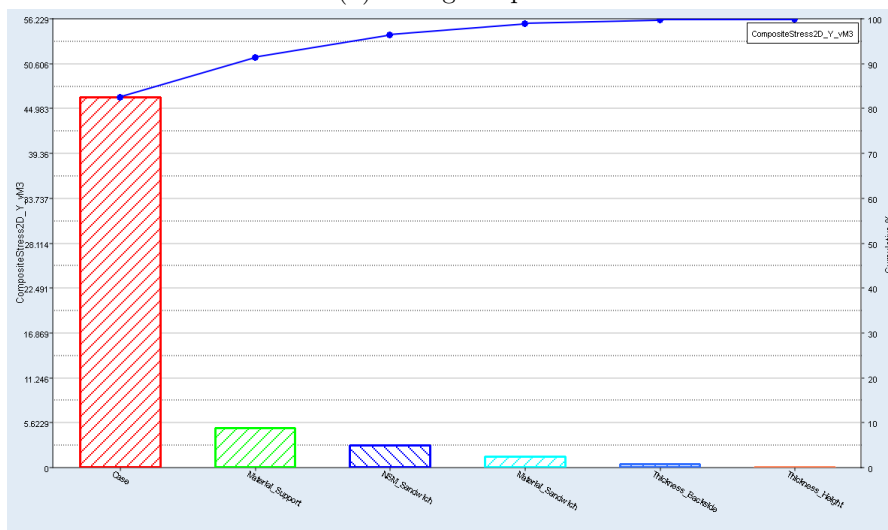
Figure A.14: The plots regarding composite stress (von Mises) in y -direction in ply 2 for the linear static case.



(a) Evaluation plot.

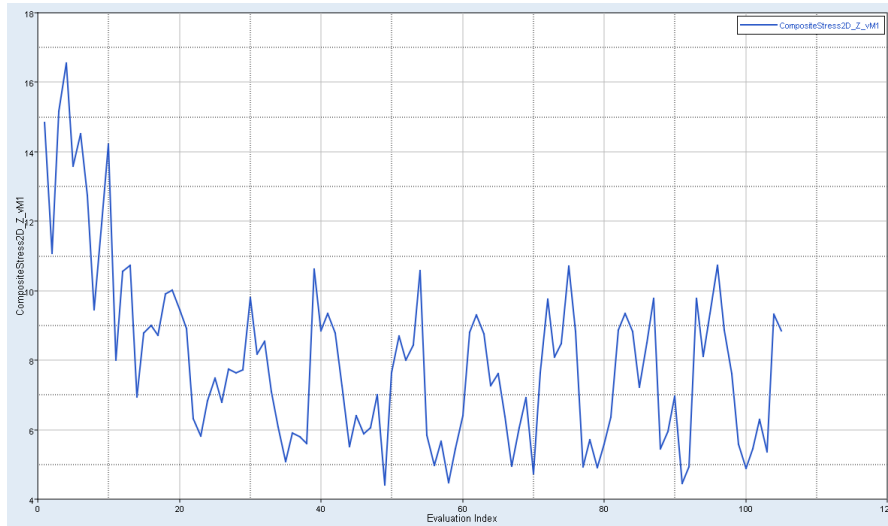


(b) Histogram plot.

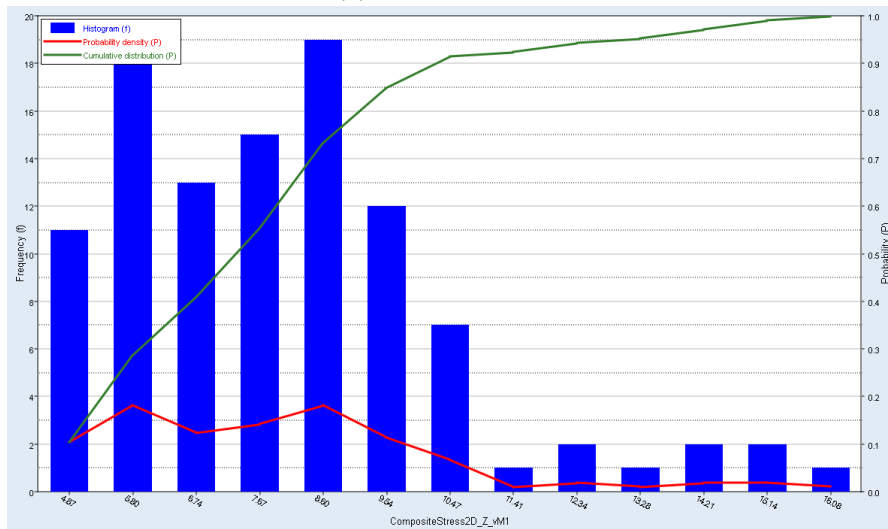


(c) Pareto plot.

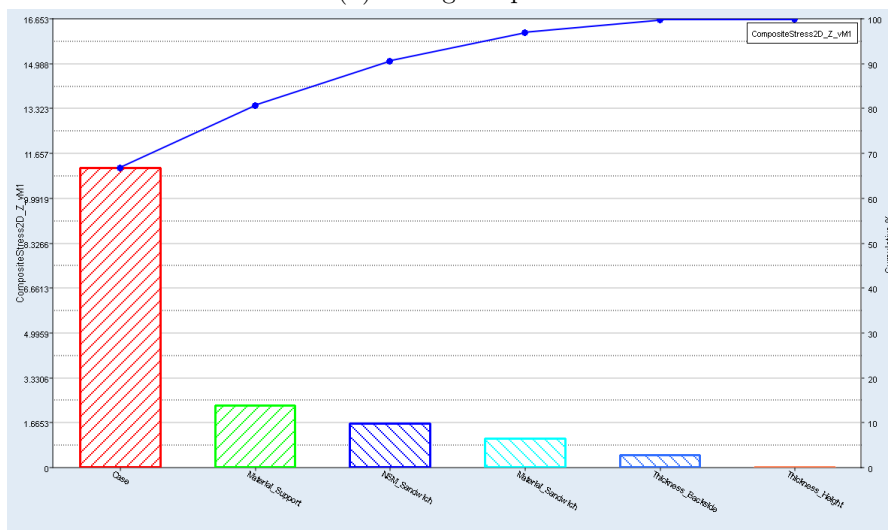
Figure A.15: The plots regarding composite stress (von Mises) in y -direction in ply 3 for the linear static case.



(a) Evaluation plot.

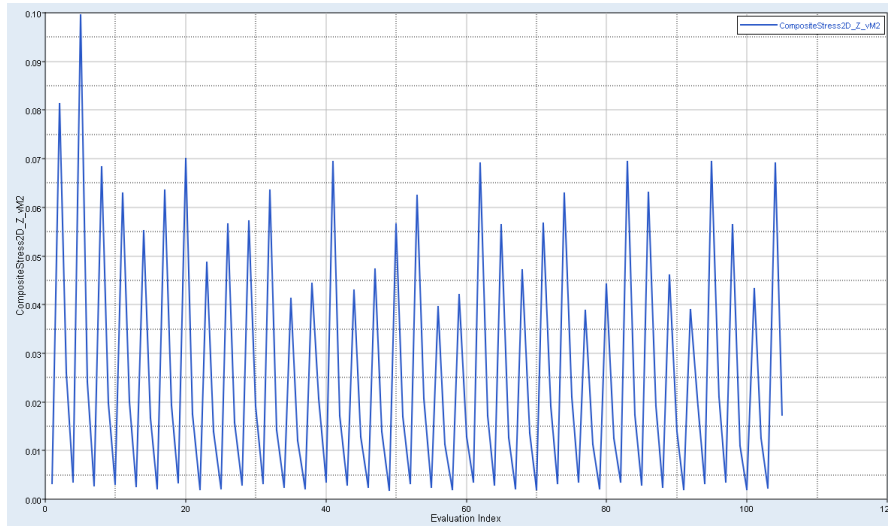


(b) Histogram plot.



(c) Pareto plot.

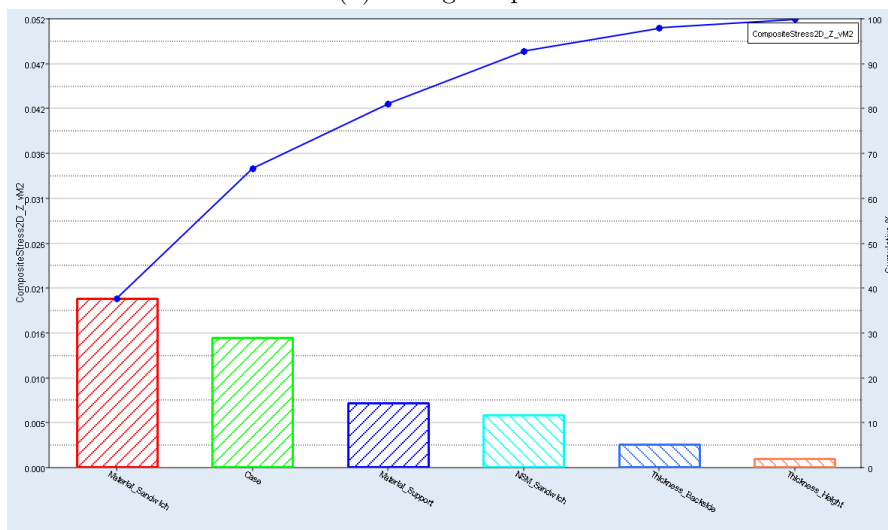
Figure A.16: The plots regarding composite stress (von Mises) in z -direction in ply 1 for the linear static case.



(a) Evaluation plot.

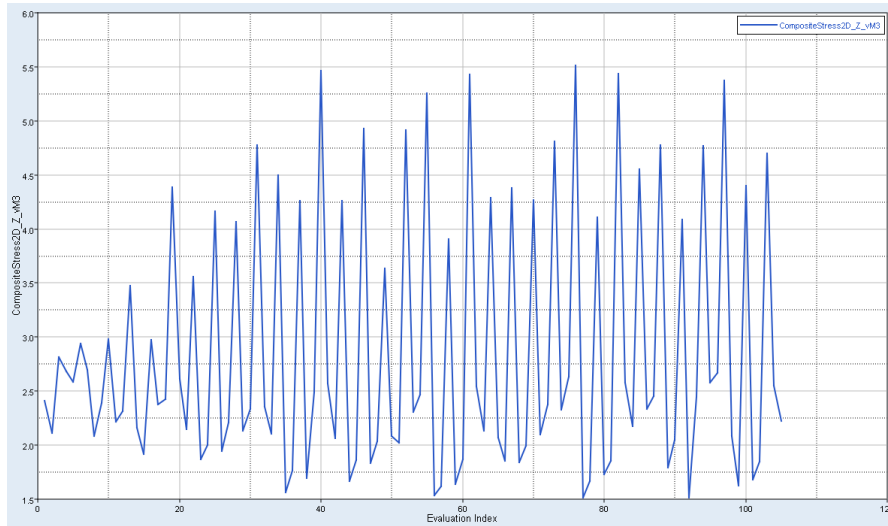


(b) Histogram plot.

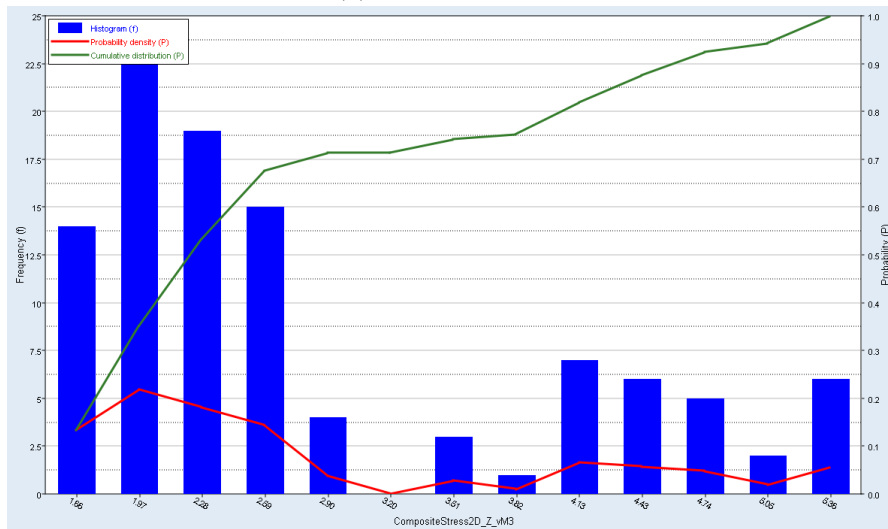


(c) Pareto plot.

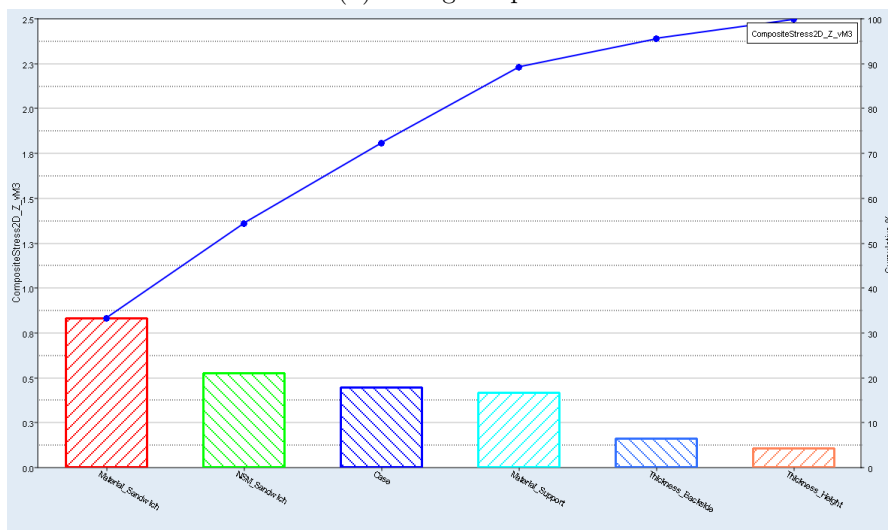
Figure A.17: The plots regarding composite stress (von Mises) in z -direction in ply 2 for the linear static case.



(a) Evaluation plot.

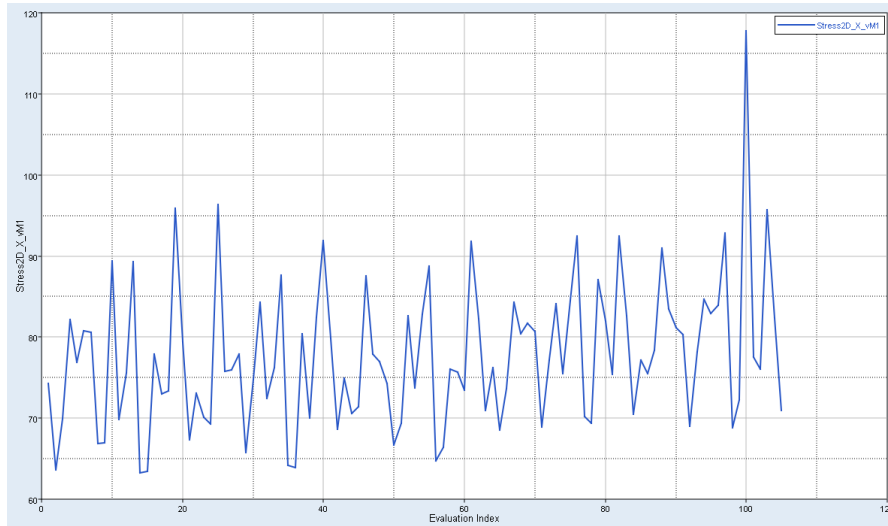


(b) Histogram plot.

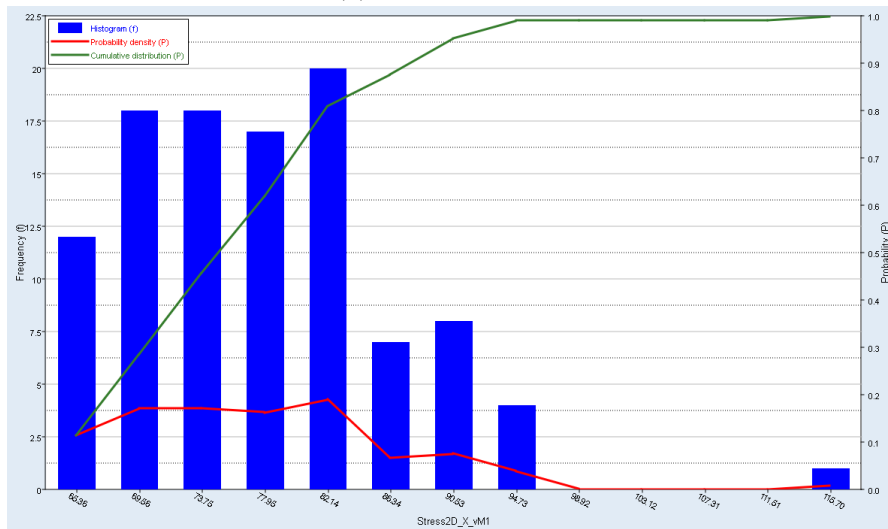


(c) Pareto plot.

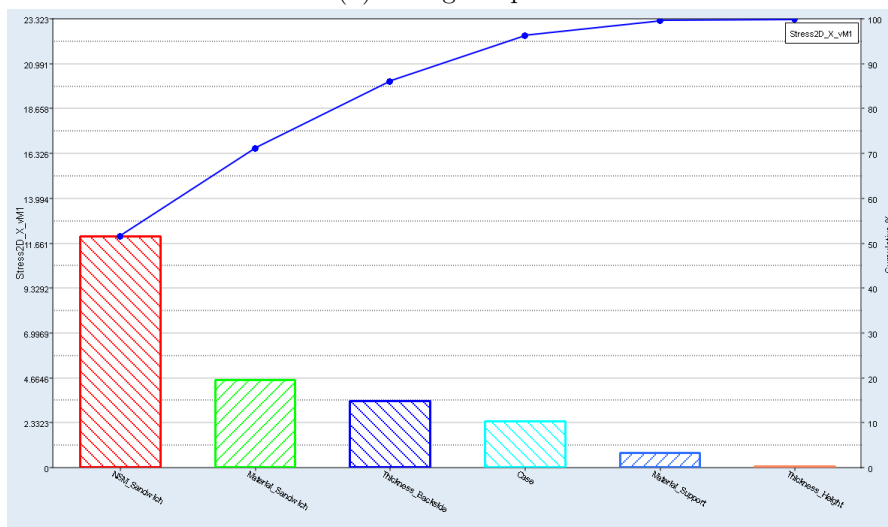
Figure A.18: The plots regarding composite stress (von Mises) in z -direction in ply 3 for the linear static case.



(a) Evaluation plot.

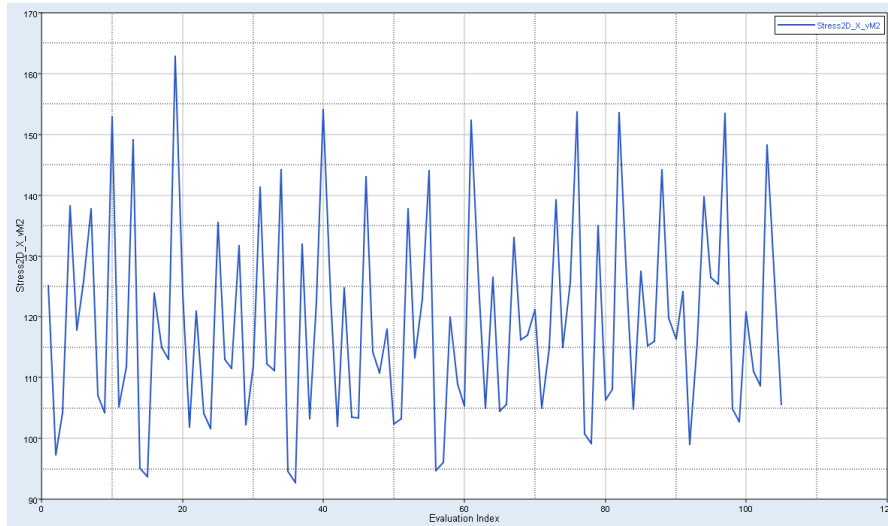


(b) Histogram plot.

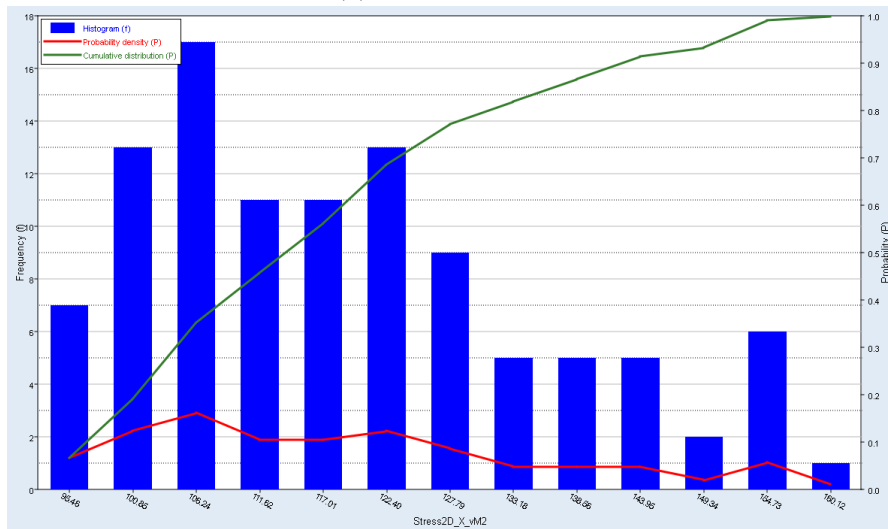


(c) Pareto plot.

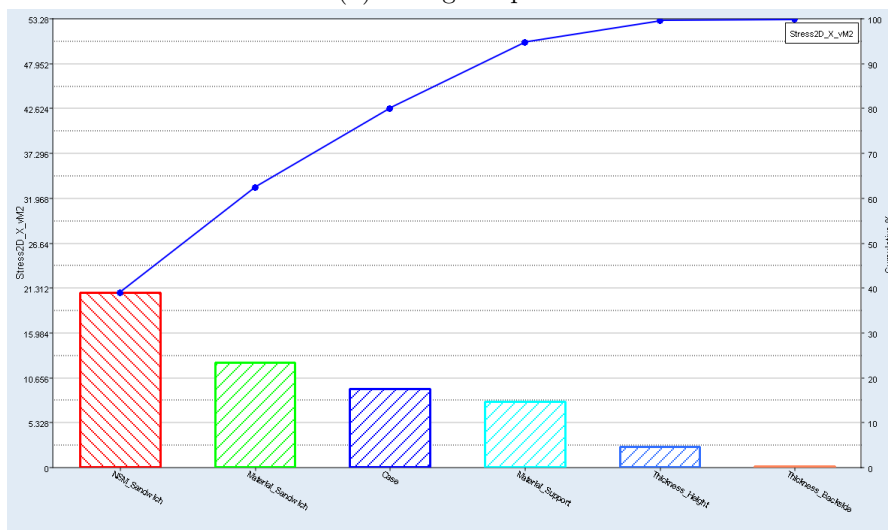
Figure A.19: The plots regarding stress von Mises in x -direction for z_1 for the linear static case.



(a) Evaluation plot.

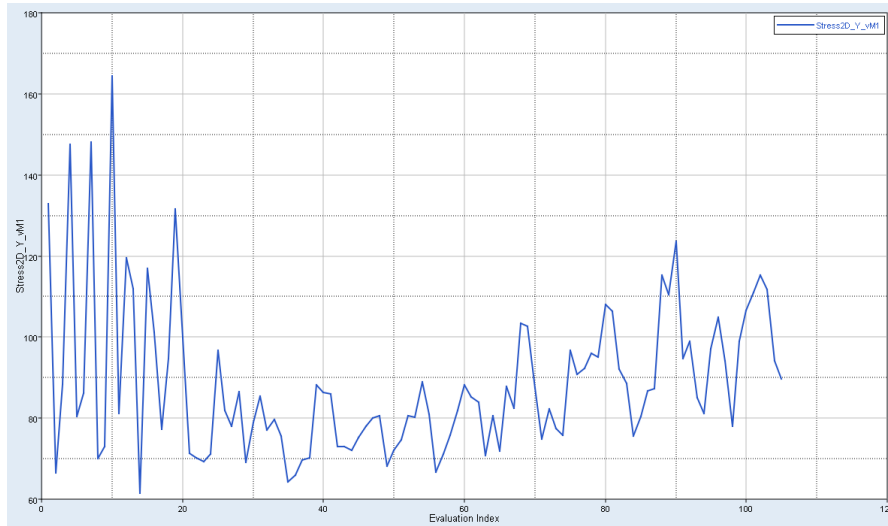


(b) Histogram plot.

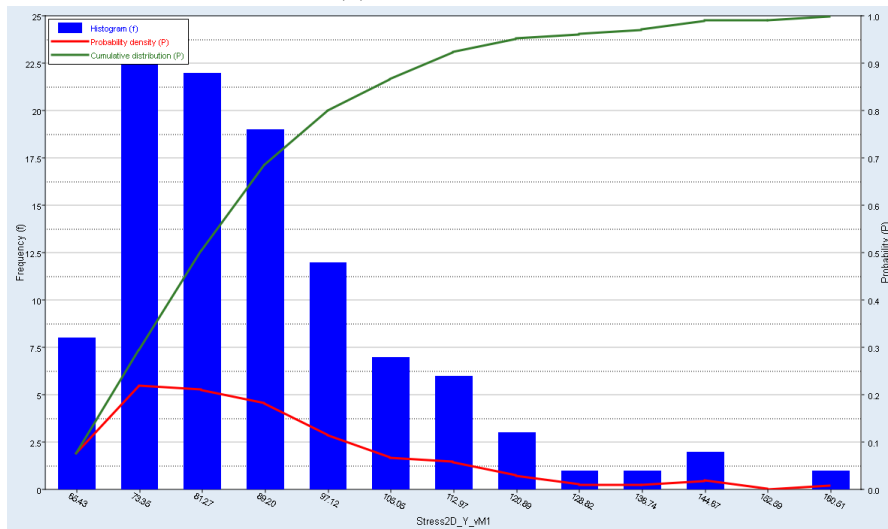


(c) Pareto plot.

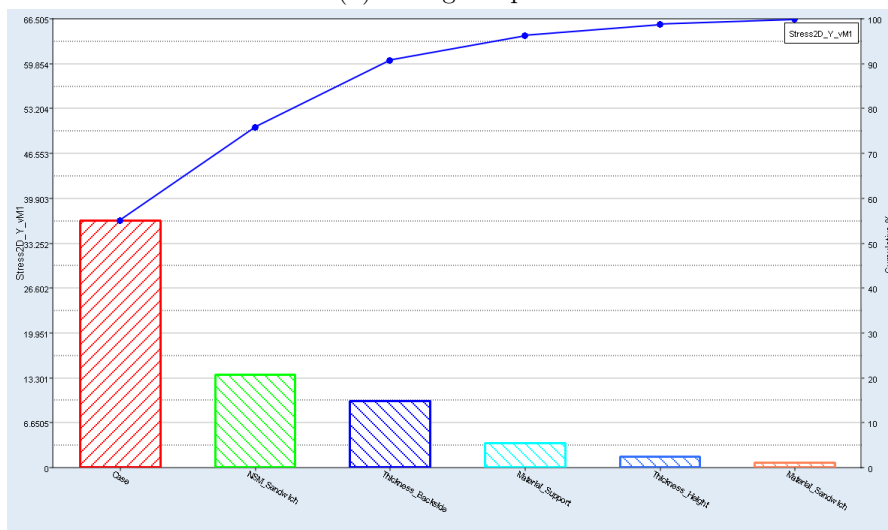
Figure A.20: The plots regarding stress von Mises in x -direction for z_2 for the linear static case.



(a) Evaluation plot.

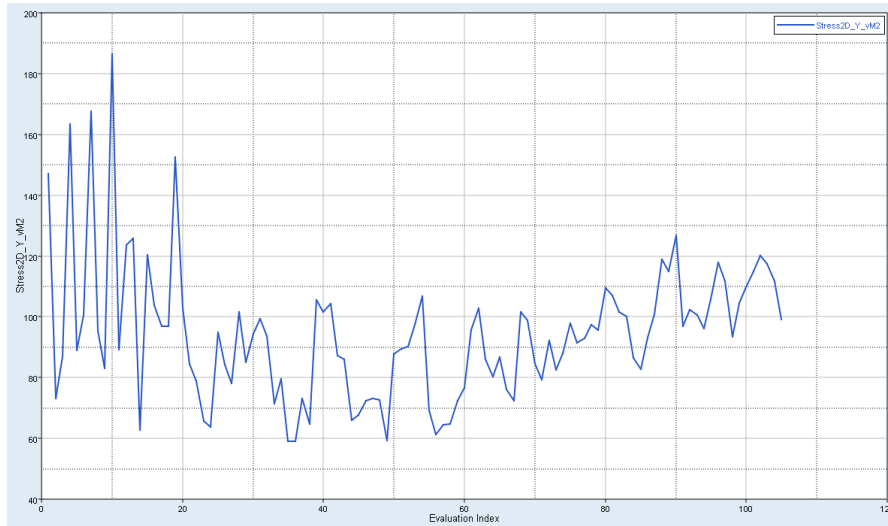


(b) Histogram plot.

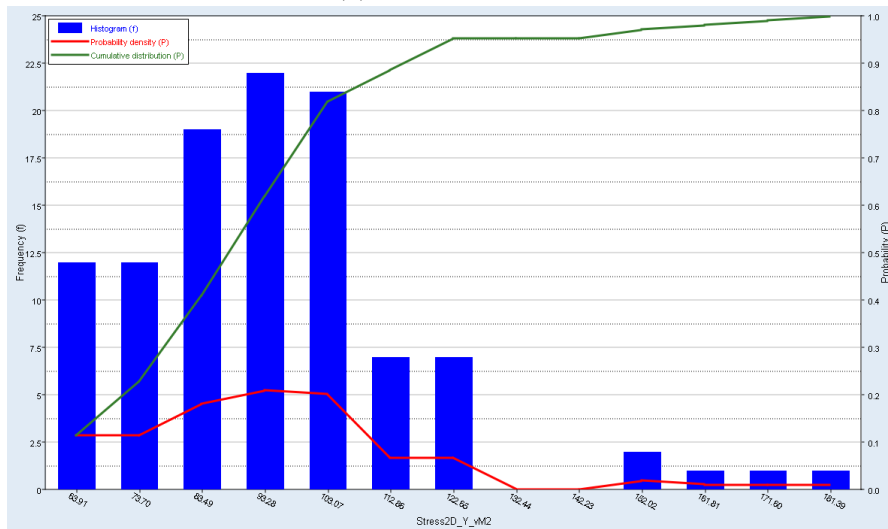


(c) Pareto plot.

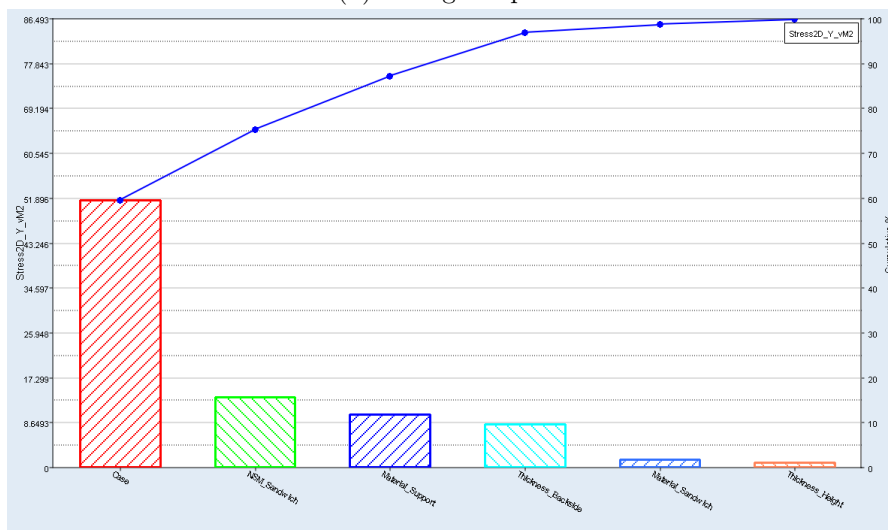
Figure A.21: The plots regarding stress von Mises in y -direction for z_1 for the linear static case.



(a) Evaluation plot.

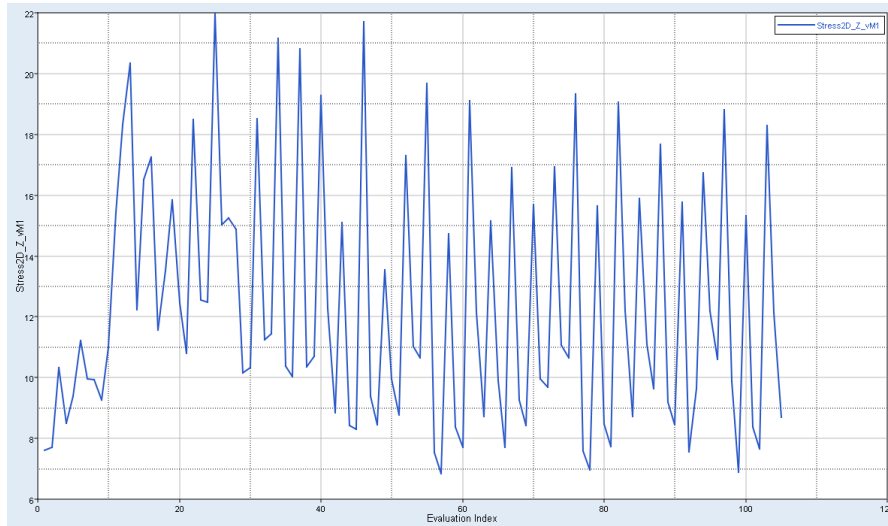


(b) Histogram plot.

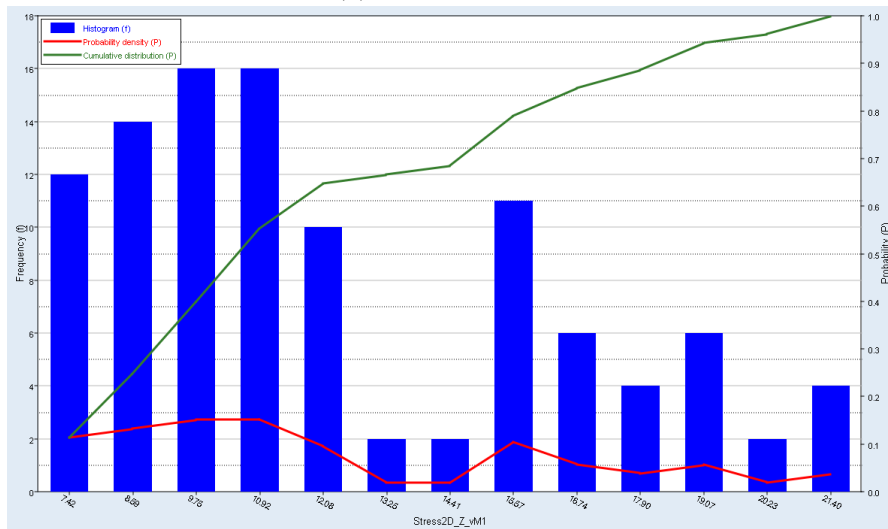


(c) Pareto plot.

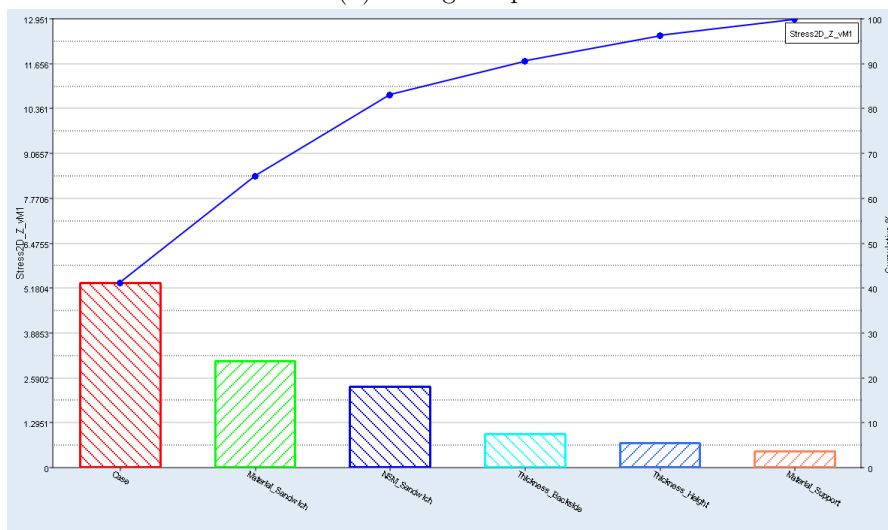
Figure A.22: The plots regarding stress von Mises in y -direction for z_2 for the linear static case.



(a) Evaluation plot.

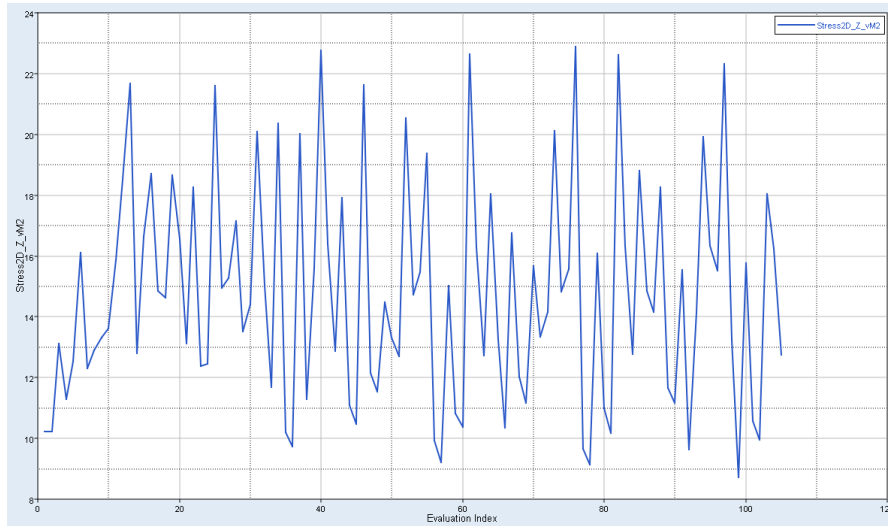


(b) Histogram plot.

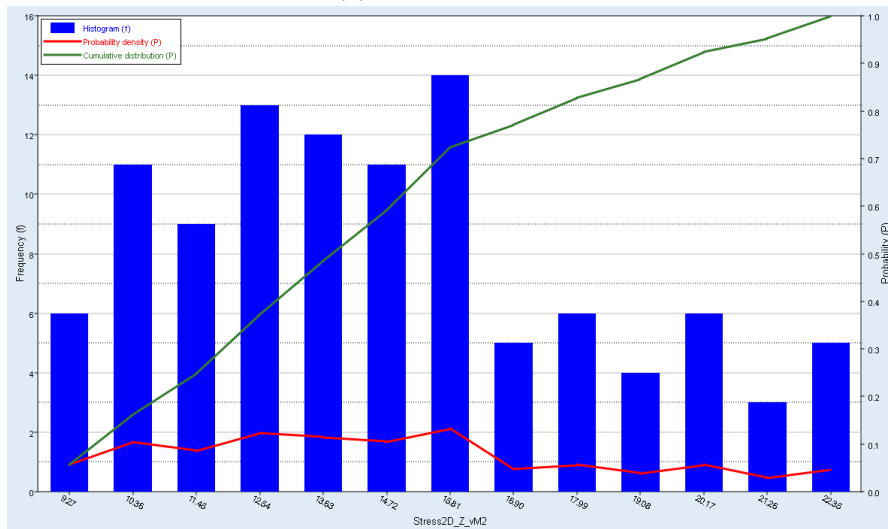


(c) Pareto plot.

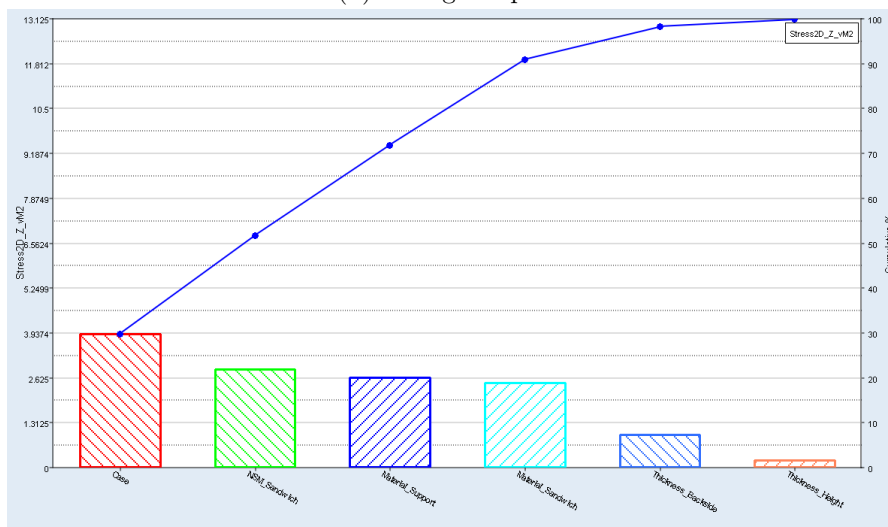
Figure A.23: The plots regarding stress von Mises in z -direction for z_1 for the linear static case.



(a) Evaluation plot.



(b) Histogram plot.



(c) Pareto plot.

Figure A.24: The plots regarding stress von Mises in z -direction for z_2 for the linear static case.

A.2 Natural Frequency analysis

The five first modes for evaluation 36 and 35 can be seen below.

A.2.1 Evaluation 36

Table A.1: Natural frequencies for the 10 first modes for evaluation 36.

Mode	Frequency [Hz]
1	9.336
2	9.396
3	14.14
4	19.77
5	22.73
6	29.88
7	35.62
8	36.19
9	39.68
10	42.11

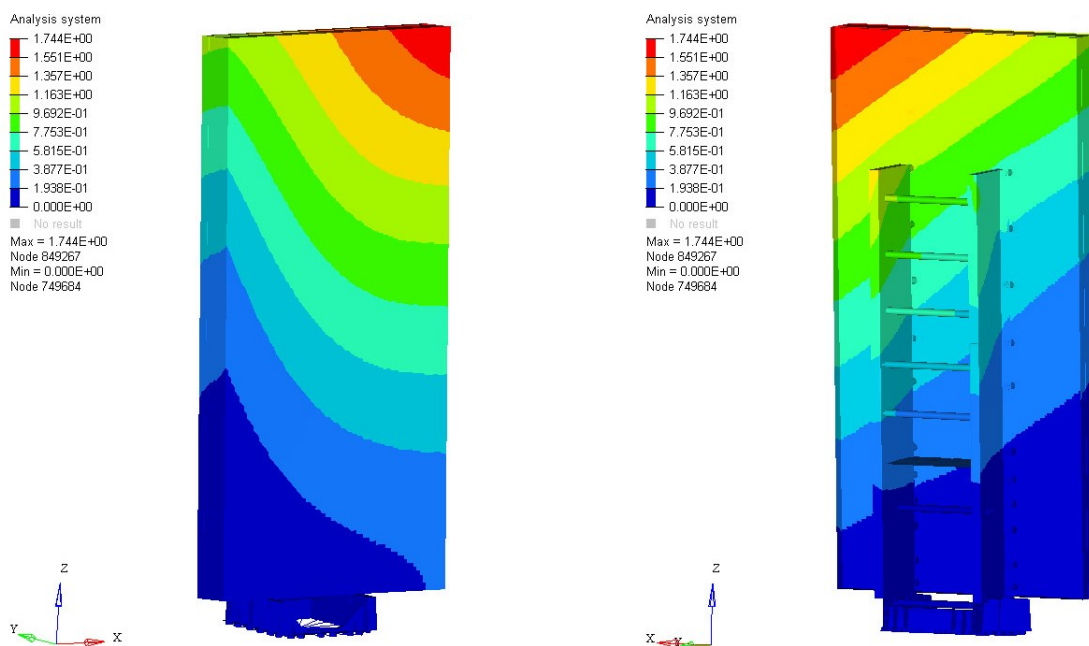
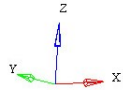
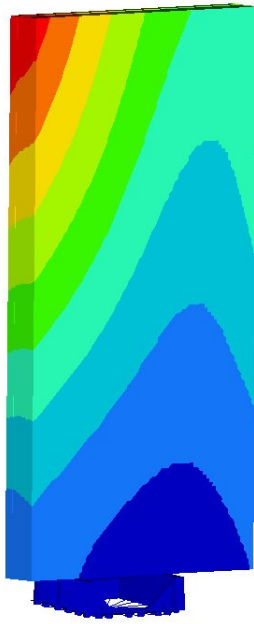


Figure A.25: Evaluation 36, mode 1. Frequency = 9.336 Hz

Analysis system
 1.665E+00
 1.480E+00
 1.295E+00
 1.110E+00
 9.252E-01
 7.402E-01
 5.551E-01
 3.701E-01
 1.850E-01
 0.000E+00
 No result
 Max = 1.665E+00
 Node 649187
 Min = 0.000E+00
 Node 749684



Analysis system
 1.665E+00
 1.480E+00
 1.295E+00
 1.110E+00
 9.252E-01
 7.402E-01
 5.551E-01
 3.701E-01
 1.850E-01
 0.000E+00
 No result
 Max = 1.665E+00
 Node 649187
 Min = 0.000E+00
 Node 749684

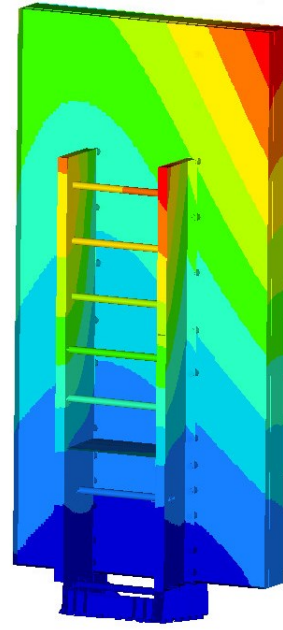
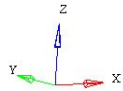
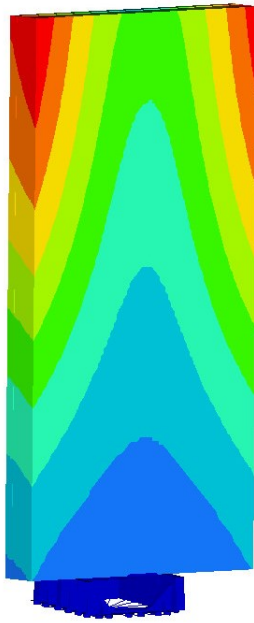


Figure A.26: Evaluation 36, mode 2. Frequency = 9.396 Hz

Analysis system
 1.801E+00
 1.601E+00
 1.401E+00
 1.201E+00
 1.001E+00
 8.006E-01
 6.004E-01
 4.003E-01
 2.001E-01
 0.000E+00
 No result
 Max = 1.801E+00
 Node 849186
 Min = 0.000E+00
 Node 749684



Analysis system
 1.801E+00
 1.601E+00
 1.401E+00
 1.201E+00
 1.001E+00
 8.006E-01
 6.004E-01
 4.003E-01
 2.001E-01
 0.000E+00
 No result
 Max = 1.801E+00
 Node 849186
 Min = 0.000E+00
 Node 749684

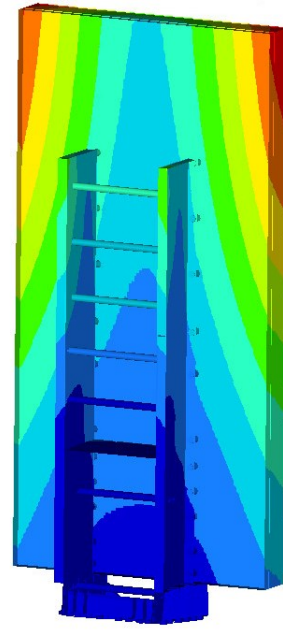


Figure A.27: Evaluation 36, mode 3. Frequency = 14.14 Hz

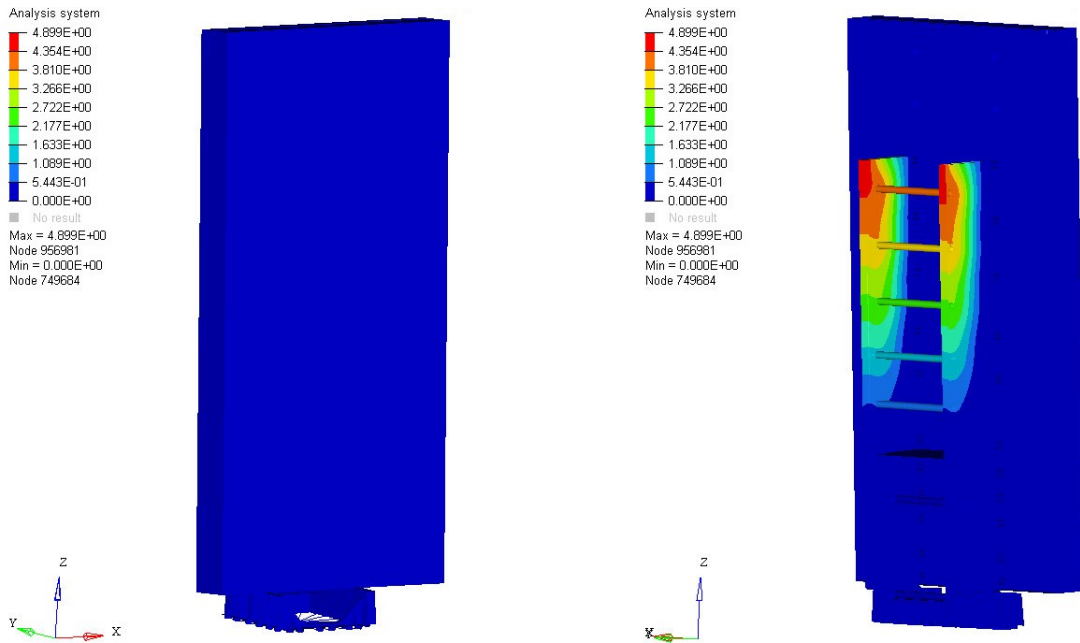


Figure A.28: Evaluation 36, mode 4. Frequency = 19.77 Hz

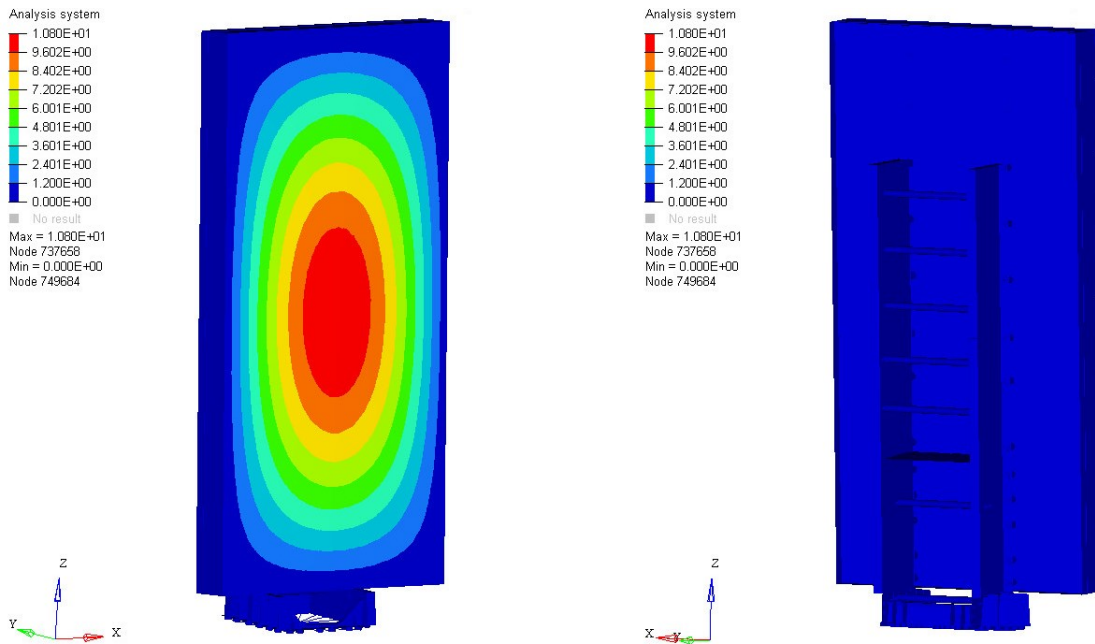


Figure A.29: Evaluation 36, mode 5. Frequency = 22.73 Hz

A.2.2 Evaluation 35

Table A.2: Natural frequencies for the 10 first modes for evaluation 35.

Mode	Frequency [Hz]
1	9.283
2	9.409
3	14.22
4	22.75
5	27.50
6	30.88
7	35.66
8	37.07
9	40.12
10	44.19

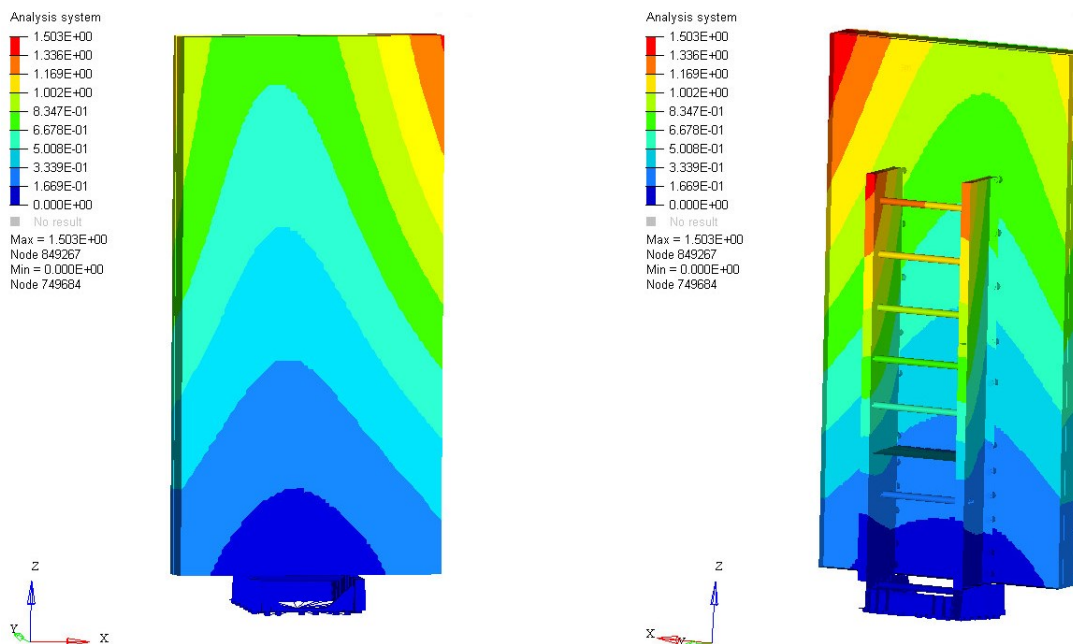


Figure A.30: Evaluation 35, mode 1. Frequency = 9.283 Hz

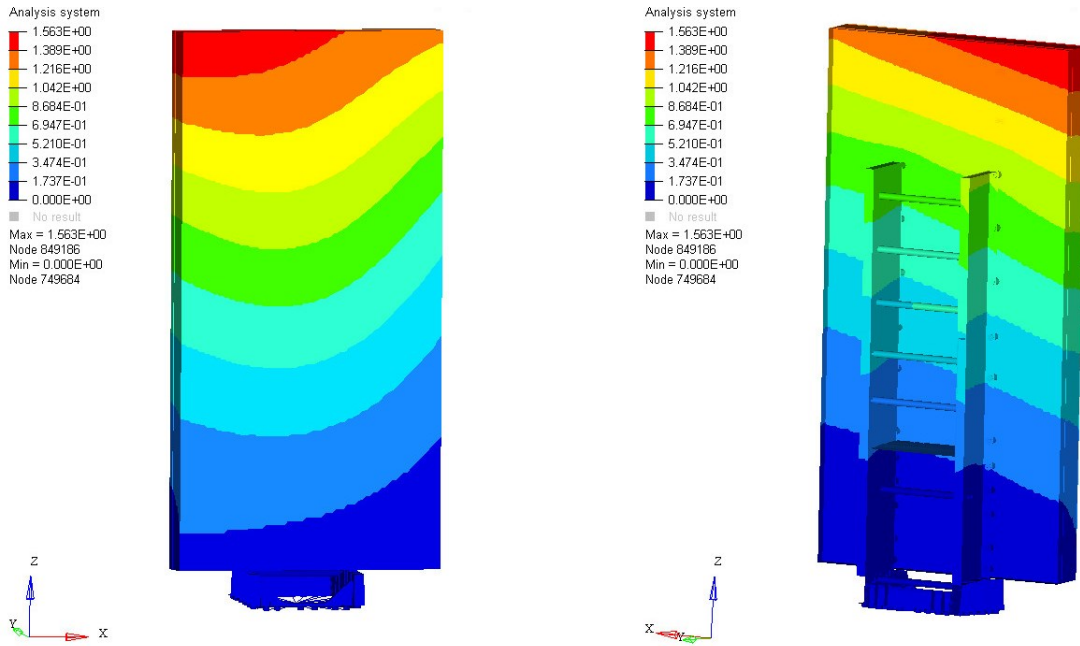


Figure A.31: Evaluation 35, mode 2. Frequency = 9.409 Hz

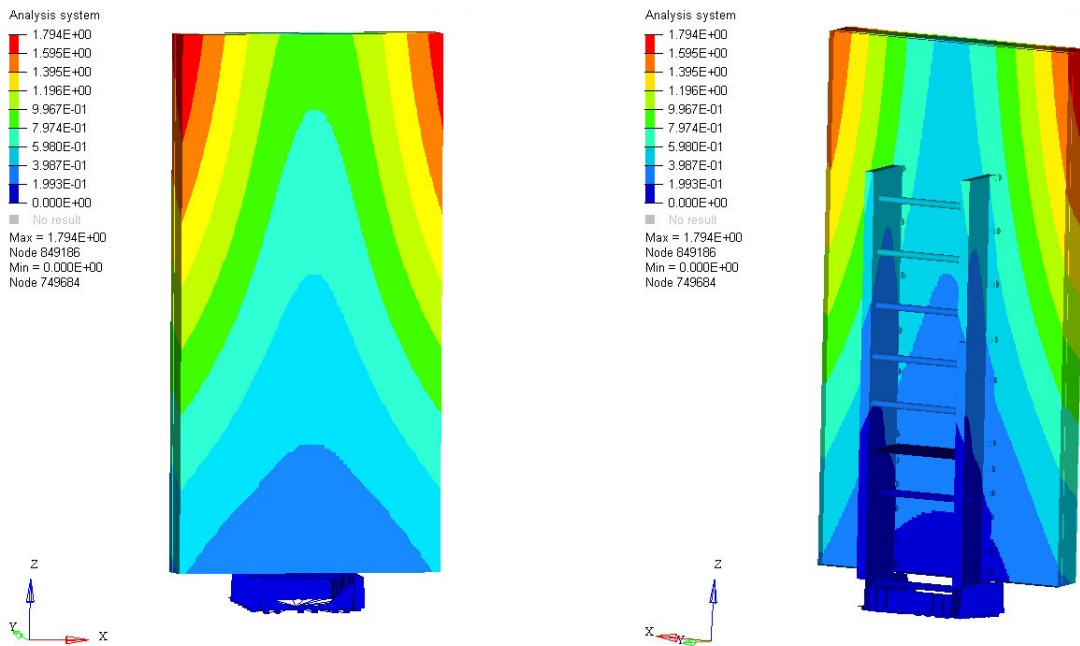


Figure A.32: Evaluation 35, mode 3. Frequency = 14.22 Hz

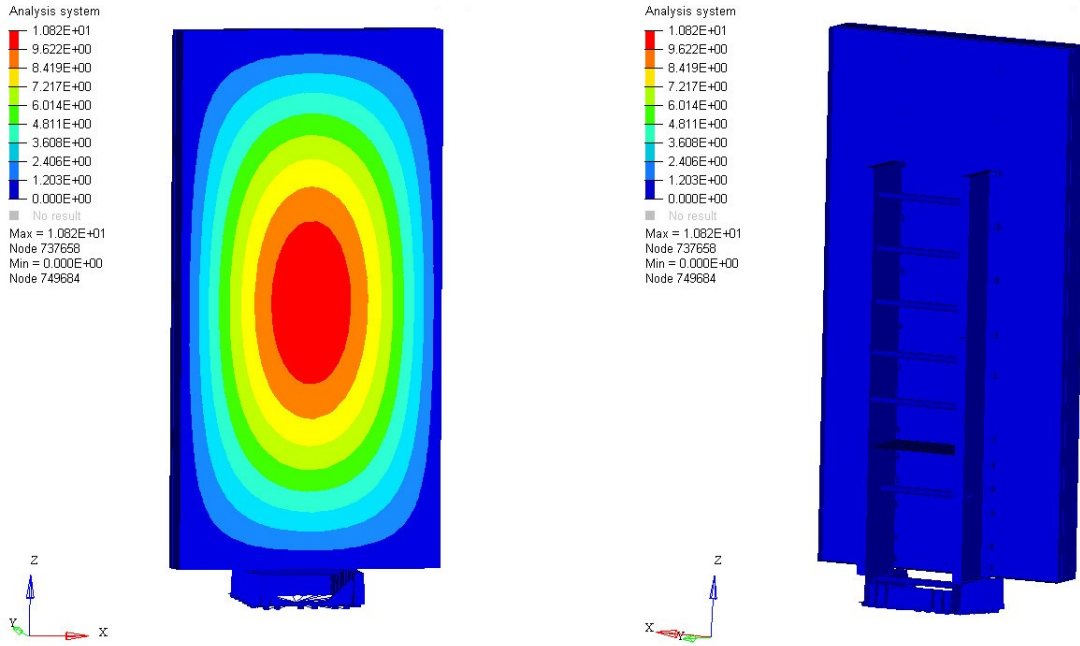


Figure A.33: Evaluation 35, mode 4. Frequency = 22.75 Hz

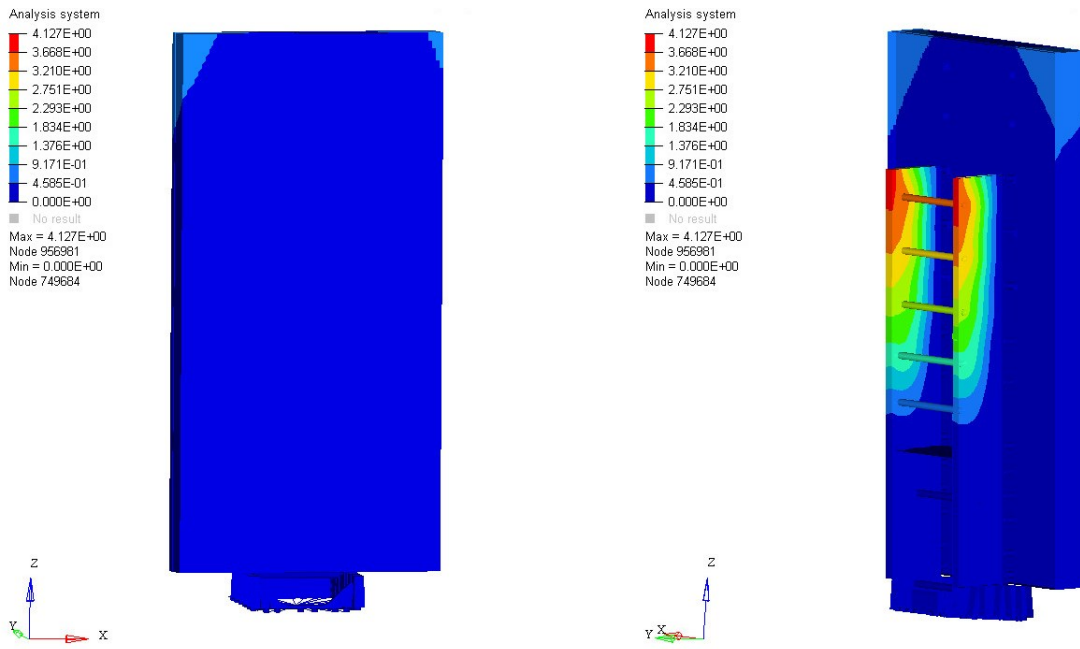


Figure A.34: Evaluation 35, mode 5. Frequency = 27.50 Hz